

UNIVERSITY OF ASTON IN BIRMINGHAM

"THE EFFECT OF ELEVATED TEMPERATURES AND
SPEED UPON THE WEAR OF MILD STEEL"

Thesis submitted for the Degree

of

Doctor of Philosophy

by

Peter M. Dunckley, B.Sc.

Physics Department

October, 1977

21 AUG 1978

219564

620.1717 DUN

SUMMARY.

"The Effect of Elevated Temperatures and Speed upon the Wear of Mild Steel"
Peter Michael Dunckley
Doctor of Philosophy
1977

This thesis describes an elevated temperature wear test rig specially designed to study the friction, wear and heat flow between specimens as a function of load, speed and externally - induced ambient temperatures. The pin and disc specimens used for these experiments were made from EN8 steel.

The variations of wear rate with load revealed wear rate transitions similar to those reported by Welsh (1964). The shape of the 'wear rate versus load' graphs were strongly dependant upon the externally - induced ambient specimen temperatures. It is shown that similar transitions and shapes could also be obtained by increasing the sliding speeds. The division of heat at the specimen interface was measured for selected experiments in which no external heating was supplied to the specimen. Using a surface model, a computer analysis of both the heat flow and the wear rate was carried out to find out how these results could be fitted to an oxidational wear theory and provide realistic estimates of surface temperatures during sliding.

A critical analysis of this method and the difficulty encountered in fitting the computer analysis to an oxidational wear theory has been carried out. Physical and metallographic techniques were applied to worn specimen surfaces and wear debris.

Wear / Friction / Steel / Oxidation / Temperature

To Evelyn, Bill and Sue

ACKNOWLEDGMENTS

I would like to ~~express~~ my gratitude to everyone I have involved in this project. In particular Dr.T.F.J.Quinn for his patient guidance and discussion. To Professor S.E.Hunt in whose department the project was carried out. I would also like to thank Mr. C.J.S.Chapman, Mr.F.Lane and everyone in the departmental workshops for their invaluable help in the construction and design of the wear test machine. I wish to acknowledge the help provided by the B.I.S.R.A. Corporate Laboratories of British Steel, the Science Research Council, and the University of Aston in providing funds and facilities to enable this research to be carried out.

CONTENTS

<u>Section No.</u>	<u>Page</u>
SUMMARY	i
DEDICATION	ii
ACKNOWLEDGMENTS	iii
CONTENTS	iv
LIST OF SYMBOLS	v
LIST OF FIGURES	vi
 <u>CHAPTER 1. INTRODUCTION</u>	
1.1. Unlubricated Wear	1
1.2. General Wear Pattern	5
1.3. Thermal Aspects of Sliding	10
1.4. Wear Theories	14
1.5. Outline of Research carried out in this investigation	20
 <u>CHAPTER 2. THE WEAR TEST MACHINE AND EXPERIMENTAL</u>	
<u>DETAILS</u>	
2.1. The Wear Test Machine	23
2.2. Main Shaft	23
2.3. The Loading Shaft	25
2.4. Specimen Pin Holder	26
2.5. The Drive System	29
2.6. Friction Measurement	29
2.7. Wear Rate Measurement	30
2.8. The Heater Assembly	32
2.9. Temperature Measurement	
2.9.1. Bulk Disc Temperature	33
2.9.2. Pin Temperature	33
2.10. Experimental Details	
2.10.1. Specimen Material	33

2.10.2. Temperature Elevation	34
2.10.3. Wear Measurement	34
2.10.4. Physical Examination of Debris and Worn Specimens	34

CHAPTER 3. EXPERIMENTAL RESULTS

3.1. Equilibrium wear rates as a function of load and speed	36
3.2. Average wear rate	38
3.3. Friction results for the 'room' temperature runs	40
3.4. Microhardness tests	47
3.5. Wear rates as a function of temperature and load for a constant speed	50
3.6. Friction curves for elevated temperature runs	53
3.7. Scanning Electron Micrographs of selected Pin and Disc surfaces	53
3.8. Scanning Electron Micrographs of Debris	64
3.9. Optical Micrographs of sections of Debris	64
3.10. X-Ray Results	
3.10.1. Heat Flow experiments	69
3.10.2. General Wear Pattern	70
3.11. Heat Flow experiment results	71

CHAPTER 4. DISCUSSION OF GENERAL WEAR PATTERN RESULTS

4.1. Introduction	75
4.2. The T_1 Transition	75
4.3. The T_2 Transition	76
4.4. The T_3 Transition	78
4.5. Surface temperatures and the General Wear Pattern	79
4.6. Friction measurements	80
4.7. The elevated temperature wear experiments	80

CHAPTER 5. DISCUSSION OF THE HEAT FLOW EXPERIMENTS AND
OXIDATIONAL WEAR THEORIES

5.1. Introduction	81
5.2. A brief description of Quinn's method	82
5.3. Quinn's results	84
5.4. The application of Quinn's method to the present work	86
5.5. The Theoretical Wear rate	86
5.6. The effect of changing various parameters on the values of N and Q	
5.6.1. Physical properties	88
5.6.2. The flow pressure, P_m	88
5.7. The Division of Heat	89
5.8. The critical oxide thickness, ξ , and the distance over which wearing contact is made, d.	91
5.9. The Activation Energy of Oxidation in wear, Q .	93
5.10. The influential temperature, T_C , T_0 or T_S ?	97
5.11. The contact temperature, T_C .	100
5.12. The number of asperities in contact beneath the pin, N.	101

CHAPTER 6. CONCLUSIONS 102

REFERENCES

APPENDIX 1. Flow diagram

APPENDIX 2. Values of experimental parameters used for
evaluating δ_{expt} and T_S

APPENDIX 3. Heat Flow Theory

LIST OF FIGURES

<u>Figure No.</u>		<u>Page</u>
1.1	The variation of wear rate of 60/40 brass with speed and ambient temperature (after ref.11)	6
1.2	A general wear pattern showing all three transitions	7
1.3	Transition load versus sliding speed for flake grey cast iron (after Eyre, ref.(16))	10
1.4	Theoretical models for corrosive wear	19
2.1	General view of elevated temperature pin and disc wear machine	24
2.2	Side view of main shaft showing spring and ball arrangement for "end float" compensation	27
2.3	Cross-sectional diagram of the pin and pin-holder showing heat flow and thermocouple positions	28
2.4	Close-up view of pin and disc and ancillary equipment	31
3.1	Log w plotted against log W. Sliding speeds: 1.0, 0.75, and 1.25 m.s ⁻¹	37
3.2	Log w plotted against log W. Sliding speeds: 2.0 and 4.0 m.s ⁻¹	39
3.3.	Log w (weight-loss method) plotted against log W. Sliding speed: 1.0 m.s ⁻¹	41
3.4	Log w (weight-loss method) plotted against log W. a) Sliding speed: 0.75 m.s ⁻¹ b) Sliding speed: 1.25 m.s ⁻¹	42

- 3.5 Log w (weight-loss method) plotted against log W.
a) Sliding speed: 2.0 m.s^{-1}
b) Sliding speed: 4.0 m.s^{-1} 43
- 3.6 Friction coefficient versus load.
Sliding speeds: 0.75 and 1.0 m.s^{-1} 45
- 3.7 Friction coefficients versus load.
a) Sliding speed: 1.25 m.s^{-1}
b) Sliding speed: 4.0 and 2.0 m.s^{-1} 46
- 3.8(a) Microhardness of pin and disc surfaces versus
applied load. ($V = 0.75 \text{ m.s}^{-1}$) 48
- 3.8(b) Microhardness of pin and disc surfaces versus
applied load ($V = 2.0 \text{ m.s}^{-1}$) 49
- 3.9 Log w plotted against log W for various externally-
induced disc temperatures 52
- 3.10 Log w (weight-loss method) plotted against log W
for various externally-induced disc temperatures 54
- 3.11 Friction coefficient versus load for various
externally-induced disc temperatures 55
- 3.12 Scanning electron micrographs of pre T_1
transition mild wear disc surface. ($W = 500\text{g}$;
 $V = 0.75 \text{ m.s}^{-1}$) 57
- 3.13 Scanning electron micrographs of disc surfaces.
a) and b)
Severe wear. ($W = 3.25 \text{ kg}$; $V = 0.75 \text{ m.s}^{-1}$)
c) pre T_1 transition mild wear ($W = 500 \text{ g}$;
 $V = 0.75 \text{ m.s}^{-1}$) 58
- 3.14 Scanning electron micrographs of disc surface
undergoing T_2 - T_3 transition wear ($W = 7.9 \text{ kg}$;
 $V = 0.75 \text{ m.s}^{-1}$) 59

<u>Figure No.</u>		<u>Page</u>
3.15	Scanning electron micrographs of disc surface undergoing T_3 transitional wear. ($W = 15.3$ kg; $V = 1.0$ m.s ⁻¹)	61
3.16	Scanning electron micrographs of disc surface from 500°C experiment. ($W = 1.0$ kg; $V = 1.0$ m.s ⁻¹)	62
3.17	Scanning electron micrographs of pin surfaces. a) pre T_1 transition mild wear b) severe wear c) T_2 - T_3 transitional wear d) T_3 transitional wear	63
3.18	Scanning electron micrographs of debris	66
3.19	Scanning electron micrographs of debris	67
3.20	Optical micrographs of sections of debris	68
3.21	Optical micrographs of sections of debris	69
3.22	a) Graph of thermocouple reading (T_g) versus applied load b) Graph of surface temperature (T_a) versus applied load	73
3.23	Graph of pin wear rate (w_{expt}) versus applied load	74
3.24	Graph of frictional force (F) of the pin versus applied load	74
4.1	Graphical results from Quinn(40)	84
4.2	Graphical results from Quinn(40)	85
4.3	Typical asperity contact visualized by Tenwick and Earles	92

LIST OF SYMBOLS

- δ_{expt} = experimentally measured division of heat at the pin-disk interface
- δ_{theory} = theoretically calculated division of heat at the pin-disk interface
- w_{expt} = experimentally measured wear rate of the pin (in units of volume of pin removed per unit sliding distance)
- F = frictional force at the interface between the pin and the disk
- T_s = the temperature of the surface of the pin outside of the real area of contact
- T_c = the temperature of the real area of contact between the pin and the disk
- N = number of sperities in contact beneath the pin
- \bar{m} = thickness of oxide film at the real areas of contact
- a = radius of each of the N circular areas of contact making with the real area of contact
- Θ_m = the temperature at the real areas of contact in excess of surface temperature ($=T_o - T_s$), known as the "flash temperature"
- A_p = Arrhenius constant for parabolic oxidation
- Q_p = oxidational activation energy for parabolic oxidation

- $Z = (K_B / 2R_t h)^{\frac{1}{2}}$
- N_{Nu} = Nusselt number
- N_{Re} = Reynolds number
- U = speed at which air is flowing past the cylindrical surface of the pin
- D = diameter of pin ($=2R_t$)
- K_{air} = thermal conductivity of air
- ρ_a = density of air
- μ = viscosity of air
- W = normal applied load at pin
- H_{total} = total heat per second evolved at the pin-disk interface
 (=UF)
- T_p = the "fictitious" flash temperature at the interface, assuming H_{total} all goes to the pin
- T_d = the "fictitious" flash temperature at the interface, assuming H_{total} all goes to the disk
- ρ_s = density of the disk material (steel)
- c = specific heat of disk material
- L = $(U \cdot a \cdot \rho_s \cdot c) 2K_s$
 = sliding constant depending on L
- P_m = hardness of material used for pin and disk (steel)
- d = distance over which each individual contact is made
- w_{theory} = wear rate predicted by oxidational wear theory
- f = fraction of oxide film which is oxygen

- L_1 = length of pin exposed to the air between the holder and the disk
- T_a = temperature recorded by thermocouple at pin surface just as it emerges from pin holder
- T_b = temperature recorded by thermocouple situated at a distance L_3 along the cylindrical surface of the pin from the thermocouple recording T_a
- L_3 = distance between thermocouples recording T_a and T_b
- T_c = thermocouple reading at the inside diameter of the copper cylinder around the pin and insulator
- H_1 = heat flow per second at the interface between pin and disk
- H_2 = heat flow per second entering the section of the pin where the thermocouple measuring T_a is conducting heat away
- H_3 = heat flow per second leaving the section of the pin where the thermocouple measuring T_a is conducting heat away
- K_s = thermal conductivity of steel
- K_i = thermal conductivity of insulator
- R_a = outer radius of the cylindrical insulating medium
- R_t = radius of the pin
- C = conductance of the thermocouple wire
- M = $(2K_i/K_s R_t^2 \ln(R_a/R_t))^{1/2}$
- h = heat transfer coefficient between cylindrical exposed surface of pin and the air

ρ_o = average density of the oxides formed at the real areas of contact.

R = gas constant

T_E = the bulk disc temperature when external heating was applied

T_R = the bulk disc temperature produced by frictional heat only

CHAPTER 1

INTRODUCTION

1.1 Unlubricated wear

which →
Wear is encountered wherever there is sliding contact and results in loss of material from one or both of the interacting surfaces. There are usually several interacting mechanical, chemical and physical factors involved in the wear process. The detritus may retain the character of the original materials if the process is mainly mechanical or can be changed by a chemical process occurring between the wearing object and its environment. Wear can be useful for example when an engine is run-in but is normally undesirable and is one of the most common causes of plant breakdown and inefficiency. A simple measurement of a dimension can be sufficient to assess wear but the understanding and quantitative prediction of wear is fundamental to the prediction and elimination of mechanical component failure. In the majority of engineering situations there is some sort of lubrication between the rubbing surfaces. However there have been many fundamental investigations of wear between unlubricated surfaces and indeed there are situations where lubrication is impossible or intolerable. It is the unlubricated or dry wear aspects of tribology that are concentrated on in the present work.

→
The effects of wear have always been appreciated but it is only over the last few decades that we have had more sophisticated techniques to unravel the difficulties and complications of the study of wear. Fink (1) in 1930 realised the role of oxidation in the dry wear of steels. Mailander and Dies (2) and Siebel and co-workers (3) studied and attempted to account for the changes in the magnitude and character of the wear of steels with changes in load and speed.

Ragnar Holm (4) suggested an expression for the assessment of the magnitude of wear; he showed that when the wear rate was expressed as the volume removed per unit sliding distance, the severity of the wear rate might be assessed by comparing it with the true area of contact. The above examples represent some of the most notable earlier work in this field.

Surfaces used in engineering practice are not perfectly flat and the load is supported in localised regions where the highest of the protuberances make contact. The material in these regions is deformed by the applied load until the area of contact is sufficient to support it and the true stress on the material is greater than the apparent stress. Wear studies by Burwell and Strang (5) indicated that, in general, the wear rate was proportional to the load and independent of the area of apparent contact. When the load divided by the apparent area approached a value of $\frac{1}{3}$ of the hardness, the wear rate suddenly increased to a high value. Plastic flow increases the apparent area and lowers the shear strength of the peaks.

A comprehensive series of wear tests were carried out by Archard and Hirst (6). They found that for a wide range of mainly metallic materials sliding in unlubricated conditions that each wear test began with a period of changing wear rate until the surface conditions became stabilised, the wear rate then becoming constant and independent of the apparent area of contact. For most of the materials the relation between wear rate and load was close to direct proportionality. They were able to draw a clear distinction between two types or regimes of wear which they named "Severe" and "Mild". Severe (or Adhesive) wear is characterised by intermetallic contact, large scale damage to the surfaces and the production of loose metallic wear particles. In mild wear the surfaces become smooth and are usually protected by surface oxide layers generated during

rubbing, the wear debris consisting of fine particles of the oxide. In severe wear the size of an event can typically have a value of the order of 10^{-4} m. Holm (4) and Bowden Tabor (7), using contact resistance measurements, deduced that the size of the true areas of contact was of the same order. It was inferred that these regions could be subdivided into smaller areas and that mild wear could be confined to these areas, whilst severe wear occurring when the damage grew to include the entire contact region. Dyson and Hirst (8) have confirmed the existence of the subdivided regions and the growth of severe wear from their coalescence has been shown by Cocks (9).

The broad classification of wear into mild and severe was further studied with particular combinations of materials from which detailed mechanisms of wear and the concept of a general wear pattern emerged. In experiments by Kerridge and Lancaster (10) 60/40 brass was rubbed against hardened steel, the brass pin was made radioactive and used to follow the history of the material during the rubbing process. It was found that material transfer was taking place, and that it was a two stage process. This particular combination of materials has been studied in fair detail since its behaviour appears to be typical of severe wear of a soft metal with a harder one and the results are reproducible and the wear rate is proportional to the load.

Lancaster (11) studied the effect of both speed and the ambient temperature of the system on the above combination of materials to investigate the conditions under which the transition from severe to mild wear takes place. Whether mild or severe wear will be exhibited depends mainly on whether or not an oxidised surface skin can build up during rubbing. The extent to which the system remains in mild wear or reverts to severe, or vice-versa, is dependent on load, speed and the ambient temperature. The regions of mild and severe wear are restricted to certain ranges of the controlling variables and the

wear behaviour fits into broad patterns. Welsh (12) in a comprehensive series of experiments with a range of plain carbon steels described these patterns in detail in terms of three main transitions. The concept of the general wear pattern is described in detail in a later section.

Up to this point only two of the three main mechanisms of wear have been discussed, (i) "Adhesive" (or "Severe") and (ii) "Corrosive" (or "Mild" or "Oxidational") wear. A third mechanism is "Abrasive Wear" in which damage occurs to one or both of two sliding surfaces due to the presence of a third abrasive body. The third body could be an abrasive grit or perhaps an abrasive product of the wearing surface. Burwell (13) provides one of a number of the classifications of wear, it outlines five basic mechanisms, those already described along with, cutting or ploughing of a soft material by a harder rough surface, and less common effects such as erosion or surface fatigue. Burwell points out that in any particular instance of wear one may have any of these mechanisms operating either singly or in combination.

An important feature revealed by early studies was that wear rates found with common engineering materials under unlubricated conditions can cover a range of approximately 10^5 while the coefficient of friction covers a range of only 3, and that high values of wear are not necessarily associated with high values of friction. The complex combinations of different wear mechanisms and the wide range of possible wear rates make the task of suggesting an all embracing wear theory a daunting and perhaps impossible task. There are a number of wear theories, normally relating to fairly specific circumstances, all of which start from the concept of the real area of contact. The development of analytical theories of wear stem from the work of Holm (4), Burwell and Strang (5) and Archard (14, 15). Essentially an expression for the wear rate can be given

by equation 1.

$$w = \frac{V}{L} = KA \quad (1)$$

This was the form proposed by Archard, where the wear rate, w , is the volume removed per unit sliding distance, A is the real area of contact and K is the proportion of such contacts producing a wear particle. Archard and Hirst's (6) paper lists values of wear rates, the derived value of K and the hardness. They suggested that K is the important factor in determining the wear rate and also that it can vary over 5 orders of magnitude. If one takes $A = \frac{W}{P}$ from Bowden and Tabor (7), the expression then indicates that w is proportional to W only for circumstances in which K is constant. K can often be changed by different operating conditions and it is more normally found that w is not accurately proportional to W . On the other hand the prediction that w is independent of the apparent area of contact is usually satisfied.

1.2 The general wear pattern

The general wear pattern of a particular combination of materials describes how the type of wear encountered over a wide range of conditions changes from a severe to a mild wear regime. Lancaster (11) has described the general wear pattern for 60/40 brass on hardened steel by varying the load, speed and ambient temperature of a system over a very wide range. It was shown that two opposing processes govern the transition; first the mechanism of severe wear exposes clean metal surfaces and will continue to do so unless affected by some other influence; the second process involves exposure of the surfaces to the atmosphere and the formation of an oxide film. If the film is sufficiently protective the second

process can become dominant and mild wear continues. Mild wear takes place at low speeds, light loads and low temperatures, when there is sufficient time between contacts for a surface film to be established. The formation of this film will be favoured by increasing the rate of oxidation, either by increasing the ambient temperature by external means, or by increasing the frictional heating. Severe wear will take place at intermediate speeds, not so slow that oxidation occurs by virtue of the long periods available, nor so fast that the rate of oxidation increases by frictional heating. If the temperature of the system is increased the range of speeds over which severe wear operates contracts and at a critical temperature, (which depends on the load) severe wear is suppressed. This effect is shown in figure 1.1

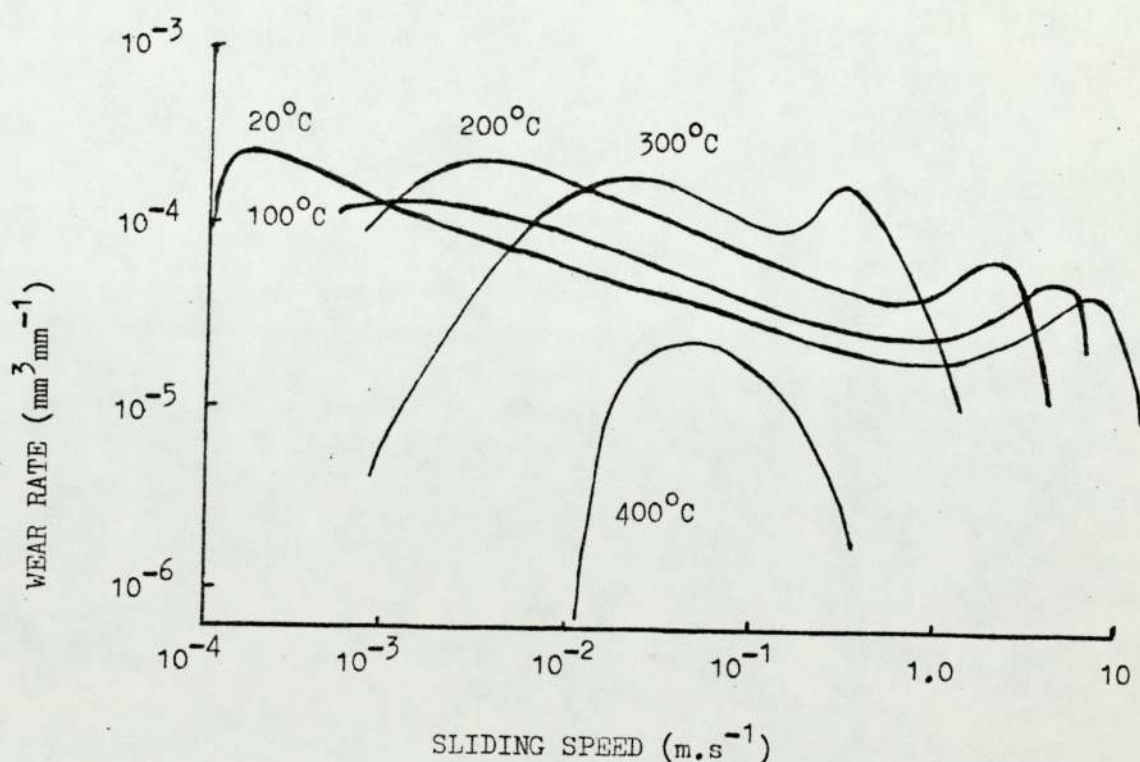


Figure 1.1. The variation of wear rate of 60/40 brass with speed and ambient temperature (after ref.11)

Welsh (12) has carried out a comprehensive study of wear of plain carbon steel pins and rings. When Welsh began his work the existence of only one transition was suspected, that from severe to mild. It was soon realised that further transitions existed which formed a pattern and that the complete pattern is rarely observed as the transition loads can vary widely with changes in sliding conditions. The transitions from one wear process to another occur at well-defined loads, for a given set of conditions, and for soft steels a basic pattern, comprising of three transitions could be found. The transitions are shown in Figure 1.2); T_1 , is a change from mild to severe wear at light loads; T_2 , a change from severe to mild at higher loads; T_3 , a relatively small change in the mild wear at loads above T_2 , where the wear rates of the pin and rings diverged.

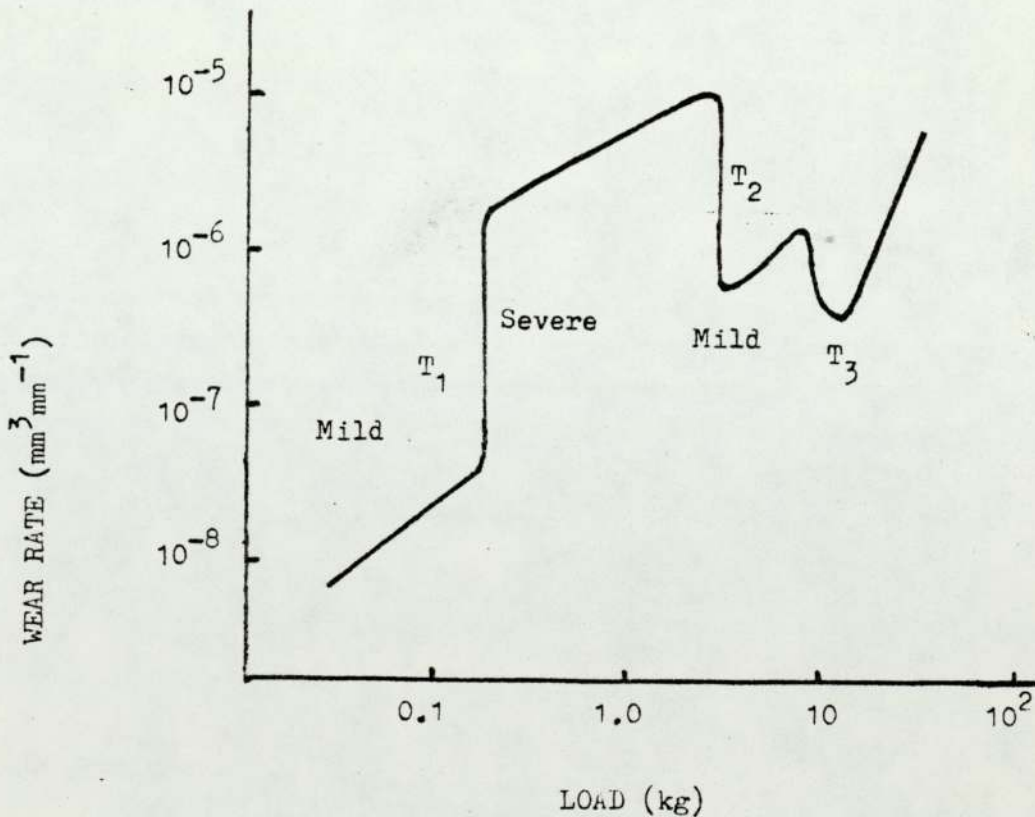


Figure 1.2. A general wear pattern showing all three transitions.

An increase in sliding speed lowers all the transition loads; an increase in hardness elevates T_1 and lowers T_2 and T_3 , and at some critical value, which varies with the composition of the steel, T_1 and T_2 merge together.

It was found by metallography and microhardness tests that, above the T_2 transition, the surface layers of the specimens were hardened by a pseudo-martensitic phase transformation. To examine this region, specimens which had run at loads greater than T_2 and attained an equilibrium oxide film, were treated in two ways. For some specimens the oxide film was removed by etching and then replaced by a new film, established by heating to one of a range of temperatures. For others, the oxide film was left intact, but the hardened surface layers were softened to different values by heat treatment in pure argon. From these and other experiments it was found that above T_2 both hardening and an oxide film were necessary for the continuation of the mild wear regime. At these loads mild wear continued in the presence of an oxide film, once a critical hardness had been achieved. Welsh indicated that phase hardening can occur under conditions where the flash temperatures are insufficient, in terms of normal metallurgical behaviour, to cause hardening, and remarks that the low carbon steels harden more intensively during rubbing than is possible using normal heat treatment. Welsh determined two critical hardnesses using the tempering and etching experiments, the first being that value which was required to support an oxide film and lay between 340 and 425 V.p.n. Since in their softest state, the hardness of all steels is less than this value, severe wear was inevitable during the early stages of rubbing. The second critical hardness was that minimum value required for mild wear without the intervention of an oxide film and fell between the limits 553 to 775 V.p.n.

In the mild wear range below T_1 the requisite surface hardness

is provided mainly by strain hardening and T_1 is the load where the combined rates of oxidation and strain hardening are no longer able to prevail over the increasing opposition of the severe wear process. At T_2 the higher frictional heating, due to increased loads, produces a new and more intensive form of hardening, associated with the second critical hardness. Mild wear is then restored, primarily when the frequency at which phase-hardened regions are formed is sufficiently high with in these circumstances, oxidation playing a secondary role. At T_3 permanent phase-hardening occurs and the probable flash temperature exceeds the eutectoid temperature of 725C, which is the minimum temperature normally required to initiate the transformation. The divergence of the wear rates of the pin and the ring was ascribed to the inherent thermal asymmetry of the system, the different temperatures below the wearing surfaces giving rise to a softer pin than ring and that transfer of material may take place. Also, different types of oxide may be encountered in which one surface may become abrasive.

Welsh concludes that oxidation can only inhibit severe wear if the substrate hardness exceeds a critical value, and hardness itself is only effective if a second higher value is achieved, and that on the basis of hardening and oxidation it is possible to provide consistent explanations for the main facets of the general wear pattern.

It becomes apparent that it is impossible to assess the behaviour of a material in wear from the results confined within a narrow range of conditions. A true comparison of the behaviour of different materials can only be gained if the overall pattern of wear for each material is available. No strikingly different patterns have been proposed and it may be that the main differences between the wear of different materials lies in the extent to which the

patterns are relatively displaced, with respect to the controlling variables, rather than in differences in the form of the patterns themselves. Actual wear rates will not normally have much relevance for specific engineering applications. It is the effect of load and speed on the transition loads which can be useful. Graphs such as figure 1.3 could be used in design to indicate regions of load and speed where severe wear is likely to take place.

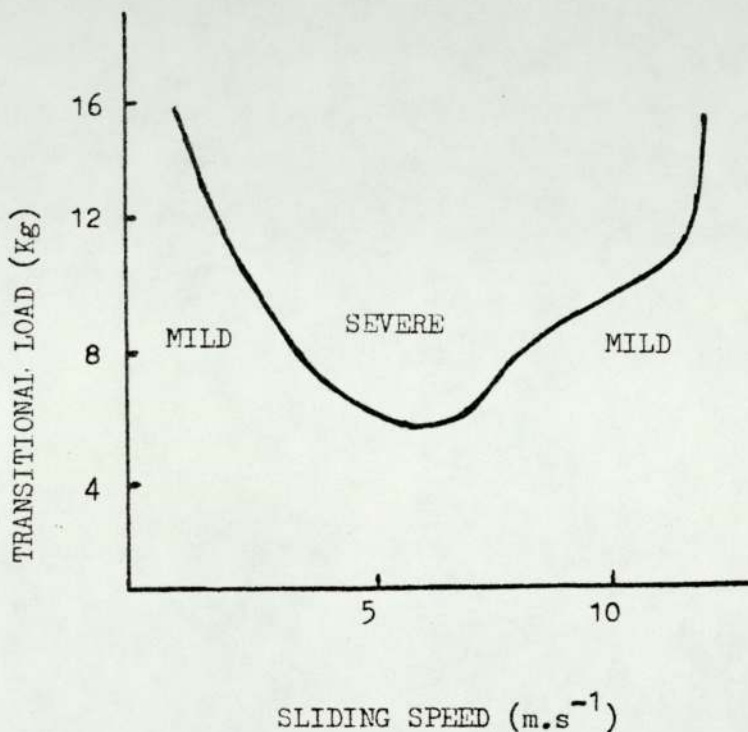


Figure 1.3 Transition load versus sliding speed for flake grey cast iron (after Eyre, ref. (16))

1.3 Thermal aspects of sliding

One of the most important unknowns is the study of wear and lubrication is the temperature of the rubbing surfaces. Temperature affects the physical and chemical behaviour of the rubbing solids as well as the lubricant. There is still much to be learnt about the magnitude and distribution of the surface temperatures generated by friction in real systems. A better knowledge of surface

temperature would be invaluable to the understanding of the mechanism and the prediction of the rate at which wear occurs.

Several theoretical studies have been made on surface temperatures generated by friction. In 1937 Blok (17, 18) investigated the problems of both stationary and moving sources of heat, assuming perfectly plane surfaces and that the bodies to which heat is supplied will have infinite heat capacity. The treatment involves relatively complicated mathematics. A theoretical study, somewhat similar to Blok's theory was later made by Jaeger (19), who carried out the calculations in considerable detail. Simpler mathematical treatments of this problem have been made by Holm (20) and Bowden and Tabor (7). Archard (21) has presented a simpler formulation of Blok's theory and also considered contact areas determined from both elastic and plastic deformation. The general procedure involved in these theoretical studies is to calculate the temperatures on the assumption that (a) the heat is generated at the area of true contact, considering a single area of contact as a plane heat source, and that (b) this heat is conducted away into the bulk of the rubbing members. The theory first requires the solution of the equations for the flow of heat into the bodies. The derived surface temperatures are expressed in terms of the rate of supply of heat, the size and speed of the heat source, and the thermal properties of the material. Secondly, the proportion of the total heat flowing into each body is then determined by the criterion that the equations of heat flow for both bodies shall give the same average temperature over the whole contact area.

During sliding the surface asperities are heated by frictional contact with opposing asperities, resulting in a localised sudden rise in temperature above that of the surface, which is called the flash temperature, Θ_F . The dissipation of the frictionally-

generated heat into the bulk of the specimen gives rise to a subsurface or skin temperature, T_S . It is the temperature that would be measured by a surface thermocouple and is the mean temperature of the surface not in contact. The contact temperature, T_C , or total temperature is given by $(T_S + \Theta_F)$.

The importance of the evaluation of these temperatures is illustrated in the work of Archard (21) and Barber (22). Their equations for Θ_F show the relationship between Θ_F and speed, load and friction as well as the relevant physical properties. The relative importance of T_C and T_S is open to question; this was shown by Earles and Powell (23) who showed that if values chosen for physical properties corresponded to the total surface temperature, then the predicted total temperature for a particular steel was inconsistent with experimentally measured temperatures. A more satisfactory assumption was that the physical properties should be taken at the temperature of the material just below the asperities, i.e. T_S . Support for the use of T_S and not the flash temperatures was given by Hirst and Lancaster (24, 25) when explaining the effect of speed on the wear rate of 60/40 brass on tool steel in terms of thermal softening of the brass. Lancaster (11) came to the same conclusion in experiments with the same material combination when investigating the transition from mild to severe wear. Quinn (26, 27) dealing with oxidational (or mild) wear, however, suggests that since the parabolic oxidation rate increases rapidly with temperature, most of the oxidation will take place during contact at T_C . Archard (28) carried out a rough calculation using typical values for T_S and T_C and found that most of the oxidation should take place during the actual contact period, which supports Quinn's view.

The question is further complicated by a number of factors, for instance, the free flow of oxygen to the interface is obstructed in

contact. We must also consider at what stage of the wear process the oxidation takes place, that is, if the interface is of newly-exposed bare metal in an energised state or of previously-formed oxide.

Another possibility is that most of the oxidation takes place shortly after a period of actual contact when the temperature is somewhere between T_C and T_S . This view has been adopted by Tenwick and Earles (29), they suggest that the oxidation temperature, T_O , is around 200C greater than T_S . The effect of the wear mechanism in oxidative wear upon T_O has been discussed recently by Molgaard (30), with particular reference to the oxide thickness and the role of possible oxide transfer in the wearing process.

The amount of experimental data for verifying the theoretical estimates of interface temperatures is relatively small. Various attempts have been made using direct measurements, such as the dynamic thermocouple, Shore (31), Herbert (32) and more recently Furey (33) and also the use of infrared-sensitive photocells, Bowden and Tabor (7), to detect the temperature flashes as a metal surface rubs over glass. These methods, however, tend to be restrictive in the choice of sliding material combinations. The use of embedded thermocouples close to the contact region is unsatisfactory because the thermocouple itself interferes with the flow of heat and would also be insensitive to the peak temperatures. Indirect measurements include the work of Ling (34, 35, 36) and Quinn (37). This thesis is particularly interested in the attempts to deduce surface temperatures from measurements of the heat flow along the rubbing specimens away from the interface. Grosberg, McNamara and Molgaard (38, 39) developed and applied this method to high speed sliding. Quinn (40) uses a similar method to measure the heat flow along a wearing pin, in a pin on disc machine, although the analysis of the results is taken further; this is discussed in detail at a later stage.

1.4 Wear theories

Severe wear

It has been mentioned previously that any explanation of a wear process must take into account that normally more than one mechanism is operating. It is important to understand how each process occurs from work on systems where one particular mechanism is predominant. Since the early wear studies were carried out on surfaces undergoing severe wear it is convenient to discuss the relevant wear theories for this type of wear first. The wear in this regime is inter-metallic with the production of torn surfaces and metallic debris.

Archard assumed that adhesive or welded junctions are formed between solids at the actual contact areas. The junctions are broken with sliding and at some of the events the junctions would be stronger than the surrounding metal and a particle torn out of the surface. The severe wear of 60/40 brass on hardened steel has been investigated in great detail and its mechanism is well established. Kerridge and Lancaster (10), using a radioactive tracer technique, demonstrated the occurrence of metal transfer. During the initial stages no wear particles are produced. A transferred film of brass builds up on the steel surface and when the thickness becomes a steady value, wear particles start to appear. It was found that brass was transferred to the steel surface and eventually appeared as wear particles. There was no back transfer, probably due to the brass particles becoming heavily work hardened at the first transfer and consequently any further interaction resulting in fracture of the softer brass. It was also found that the wear particles produced had diameters which were typically similar in size to the actual contact areas. Rabinowicz (41) has suggested that a transferred particle will be detached if it contains sufficient stored elastic energy to break its adhesive junction on unloading and also that the influential factor

is the ratio the surface energy to hardness. Over a wide range of materials, he has demonstrated an approximate relationship between this ratio and particle size. Further consideration of this concept is made difficult by the lack of surface energy data. Rabinowicz (41) maintains that severe wear is favoured by factors which encourage adhesion such as clean surfaces and chemical and structural similarities. Wear increases if the material couple are mutually soluble, hence the use of unlike material combinations in engineering situations. Many surface diffusion treatments produce increased wear resistance by chemical contamination to give non-adhesive characteristics.

The introduction of K in the wear equation is a significant factor in any analytical theory of wear. In severe wear, K can be taken as a constant and can be interpreted as the probability of an interaction producing a wear particle. Hence $1/K$ is the number of interactions which a given part of the surface can endure before fracture. A typical value of K for severe wear is 10^{-3} , thereby indicating that each part of the surface must be rubbed 10^3 times before a worn particle is produced. This implies that the majority of events, i.e. those which will determine the frictional force, are contacts between asperities which separate without damage. This assumption implies that wear is a microfatigue process, as indicated by Kerridge and Lancaster (42) and also possibly by Quinn (43). K must take into account the shape of the wear particle. Hence, in the derivation of equation (1), the wear particle was assumed to be spherical. If the particle is a flake, as perhaps in the removal of an oxide film, then K must be adapted accordingly. Finkin (44) proposed a new sliding model applicable to adhesive wear which includes the influence of asperity interaction distance. In the model the asperities move against each other for a considerable distance, l ,

in comparison to the length of the junction. By considering the factors which could affect ℓ , i.e. surface topography and structure and expressing them as geometrical discontinuities, he expresses the probability of wear particle formation, which is related to K, as a function of ℓ . Suh (45), has considered a new theory for the wear of metals based on the behaviour of dislocations at the surface, sub-surface crack and void formation; resulting in the formation of thin flake-like sheet debris. An expression for total wear is given which does not depend directly on hardness and also contains a complex expression for K.

Abrasive Wear

Abrasive wear occurs when hard particles penetrate a surface and gouge out material producing a scored or grooved surface. In practice, abrasive wear occurs in a simple two body configuration or a three body configuration, such as in the contamination of two sliding surfaces by wear debris.

In the theory of abrasive wear it is normally assumed that each abrasive particle is in the form of a cone which ploughs out and removes material from the abraded surface. Burwell (13) suggested that abrasive wear occurs most readily when the abrasive particles are sharp rather than rounded and when the abrasive material is significantly harder than the abraded material. The physical conditions under which a spherical indenter might remove material have been investigated by Kragelskii (46), he produced an expression for the wear rate, equation (2)

$$w = K \left(\frac{2 \cot \theta}{\pi H} \right) W \quad (2)$$

where θ is the half angle of the cone which is the abrasive particle. The main problem is to arrive at a suitable value of θ and then to

deduce values of K. The assumptions of the theory have been examined in tests with single indentors, notably by Krushov and Babichev (47) and by Sedricks and Mulhearn (48, 49). The extent to which the results of such large scale tests are applicable is open to question. Some justification, however, for this procedure has been provided by Mulhearn and Samuels (50).

The prediction of abrasive wear in practical situations is complex, requiring such factors as the relative hardness of each component, the degree of work hardening and change of phase which may occur.

Mild Wear

For a wide range of materials, thin oxide layers on the surfaces are sufficient to prevent intermetallic contact and hence reduce friction and wear. In sliding this oxide is removed by adhesive, abrasive or fatigue mechanisms. In most theories, the general assumption is that practically all of the material which is transformed by attrition to debris has previously undergone oxidation. Under equilibrium conditions the oxidation rate is then equal to the attrition rate.

In the previous section the importance of temperature in the study of sliding wear has been discussed. In oxidational wear, this is particularly true. Oxidation rates are extremely temperature-dependent and the beneficial properties of surface films, and the factors involved in their breakdown and removal, are also temperature-dependent. There are a number of theories which have been proposed, none of which have been generally accepted. Some theories differ by approach, others by interpretations of various parameters. Since this type of wear is of particular interest in the present work and detailed discussion is given later, only a brief outline of the

relevant work and factors involved is given below. There are two main processes taking place in oxidational wear, (i) Oxide growth and (ii) Oxide removal and it is suitable to present the outline in terms of these processes.

Oxide Growth

Oxidational growth rates obey various rate laws, the most commonly adopted are the parabolic and logarithmic laws. That is, the rate of increase in layer thickness decreases as the thickness itself increases, since it becomes harder for oxygen to reach the unoxidised material. Sliding surfaces are at unknown temperatures, pressures and environments and the availability of relevant oxidational data makes the quantitative prediction of oxidation difficult. Data can only be drawn from static experiments with bulk samples notably Kubaschewski and Hopkins (51) and Caplan and Cohen (52). Since data from sliding experiments vary widely and can be apparatus-dependent, their general application is open to conjecture.

Since the whole of the apparent area of contact will be activated to some extent, the question of whether the majority of oxide is grown on the wearing asperities during actual contact or at some other period, arises. If the latter viewpoint is taken as in the work of Clark et al (53), Lancaster (11) and Yoshimoto and Tzukizoe (54) one might assume that the temperature at which oxidation takes place corresponds to the mean surface temperature, T_s . On the other hand Quinn (27) takes the view that oxidation takes place during the contact period and at the total contact temperature, T_c , since this can be relatively high the oxidation rate will accelerate accordingly.

The oxide formed during the unlubricated sliding of steel is a variable composite of the three oxides of iron. The actual composition of the oxide depends on the temperature of sliding. This

was used by Quinn (55) in an attempt to estimate sliding temperatures by comparing oxide composition with known oxidation data.

The effect of oxide composition on the wear of steels was investigated by Good and Godfrey (56) and by Johnson, Godfrey and Bisson (57). They found that Fe_3O_4 offered more protection than $\alpha-Fe_2O_3$, resulting in a lower coefficient of friction and wear rate. Clark, Pritchard and Midgely (53) measured the wear rate of hardened steel on hardened steel at various ambient temperatures. The wear rate increased with ambient temperature up to about 200C after which the trend was reversed. The change coincided with a change from $\alpha-Fe_2O_3$ to Fe_3O_4 . The transition temperature at which this effect occurred was elevated by the presence of alloying elements in the steel, the chromium content being particularly critical.

Oxide removal

Tao (58) demonstrated idealised models of two extreme cases which could represent oxidational wear. These are shown in figure 1.4.

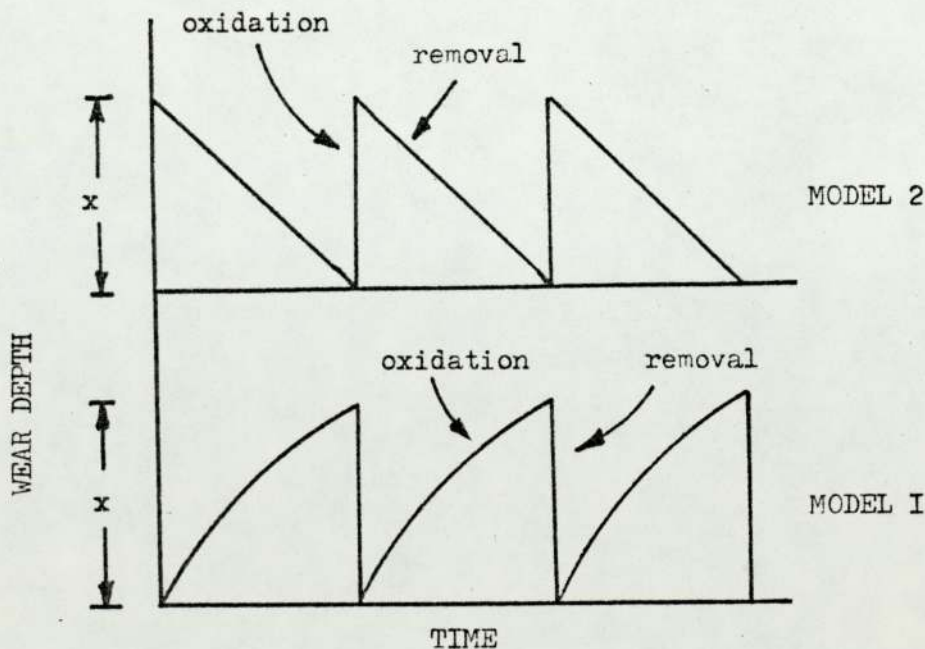


Figure 1.4 Theoretical models for corrosive wear

Model 1 assumes gradual growth of an oxide layer which is removed instantaneously by the rubbing action when a certain thickness x is reached. Model 2 assumes the time for oxide growth is negligibly small in comparison with the time for removing the oxide layer. Comparing experimental data with each model he showed that for his lubricated experiments, using a steel ball-on-cylinder device, that the rate of oxide build-up was much more controlling than the rate of oxide removal, that is favouring model 2; a view generally adopted in the development of oxidational wear theories.

Various mechanisms have been proposed to account for the removal of the oxide film. Yoshimoto and Tsukizoe (54) suggest that the whole film is removed from the contact area at each interaction. Quinn (27) suggests that the oxide thickness is built up over a number of traversals until a critical thickness is reached, it is then removed producing oxide flakes. How these flakes are actually removed from the surface is not clear, the critical oxide thickness may be such that the substrate is no longer able to support it, the electron micrographs of Quinn (43) show signs of cracking and detachment possibly by thermal or contact microfatigue. Archard and Hirst (59) conclude that the final wear mechanism between run-in surfaces is one of abrasion by loose oxide particles.

1.5 Outline of research carried out in this investigation

A limited number of investigations have been made to study the concept of the general wear pattern. Welsh (12) covered most aspects of the wear behaviour of mild steels in a most comprehensive series of experiments. The effect of artificially induced ambient temperatures on the pattern as a whole has not received the same attention. Previous work along these lines normally relates to a range of load or speed which does not incorporate more than one wear regime.

The first aim in the present investigation was to complete a program of wear tests designed to locate and investigate the three transitions comprising the general wear pattern of EN8 steel. These tests were carried out in two parts; firstly, the position of the pattern was established by a series of wear tests at room temperature with increasing loads and at various speeds. Secondly, a series of tests which dealt with the effect of increased ambient disc temperatures on the wear pattern at a given speed. In all the wear tests the wear, friction and relevant temperatures were measured and recorded continuously. Selected wear surfaces and samples of wear debris were investigated using conventional metallographic techniques and scanning electron-microscopy.

Although the author (60) has already carried out some elevated temperature investigations using existing apparatus, it was necessary to construct a new wear testing machine. To investigate the general wear pattern of a material, the machine had to be capable of a wide range of load, speed and ambient temperature. These requirements presented a number of interesting practical problems which took some time to overcome. Details of the machine and the ancillary equipment are described in Chapter 2.

Further work concerned the mild wear regions of the general wear pattern, in particular, the thermal aspects of sliding. Quinn (40) has recently produced a novel technique for the estimation of surface temperatures and the division of heat at the sliding interface. Using a computer analysis of both experimental and theoretical estimates of these and other parameters, a consistent relationship was found between these estimates and the Oxidation Wear Theory. With the aid of this technique attempts were made to estimate the surface temperatures, T_C and T_S for the mild wear regions of the general wear pattern. Previous work concerning the general wear pattern has not included

any emphasis on the role of temperature in the mild wear regions or in the transitional regions. Indications of the approximate temperatures involved have come from observations of metallurgical characteristics such as oxide composition, phase transformations and changes in microstructure of the wearing surface and subsurface.

Estimates of the surface temperatures for certain conditions of load and speed, for the experiments where no external heating was used, together with observation of the shifts in the transition loads due to changes in sliding speed and specimen temperature would provide useful information about the role of temperature in the explanation of the general wear pattern. An attempt to use the computer technique for the estimation of surface temperatures, in the present investigation failed to produce similar results or trends to those obtained by Quinn. The apparent failure of the technique had interesting consequences in the interpretation of oxidational wear in general.

Wear results for the experiments in which speed and ambient temperature were varied are discussed qualitatively in terms of previous work on transitions by Welsh (14). The room temperature results are discussed in terms of previous theories of oxidational wear. Suggestions are proposed for modifying existing theories to account for areas in which improvements are thought necessary. Where relevant, the analysis of specimen surfaces and wear debris is used to support these observations.

CHAPTER 2

THE WEAR TEST MACHINE AND EXPERIMENTAL DETAILS

2.1 The Wear Test Machine

The test equipment built and used for the continuous sliding experiments in this project was the pin and disc machine shown in Figure 2.1. It was designed to fulfil a wide range of applications in wear testing, namely it should be capable of a wide range of loads, speeds, and, in particular it should have the facility to raise the bulk temperature of the disc from Room Temperature to 700 C. Ancillary equipment consisted of devices to measure and record the various desired temperatures, wear rates, friction and speed continuously.

2.2 Main Shaft

Any heater assembly design requires a free surface of the specimen disc to which it can be mounted. It was decided to adopt a slightly irregular configuration, whereby the loading would push away from the main machine and the disc mountings. This necessitated a strong and compact design for the main shaft. A needle roller bearing was chosen for the leading bearing because of its small outside diameter and its capacity to withstand any high side loading. The rear bearing was an angular contact single ball race. This combination resulted in an unacceptable amount of end float which could cause instabilities. To stabilize the assembly, a spring and ball race arrangement (shown in Figure 2.2) was mounted between the main housings. To protect the bearings from overheating (due to conduction of heat from the specimen disc at the higher temperatures), the shaft had to be cooled. This was accomplished by boring the

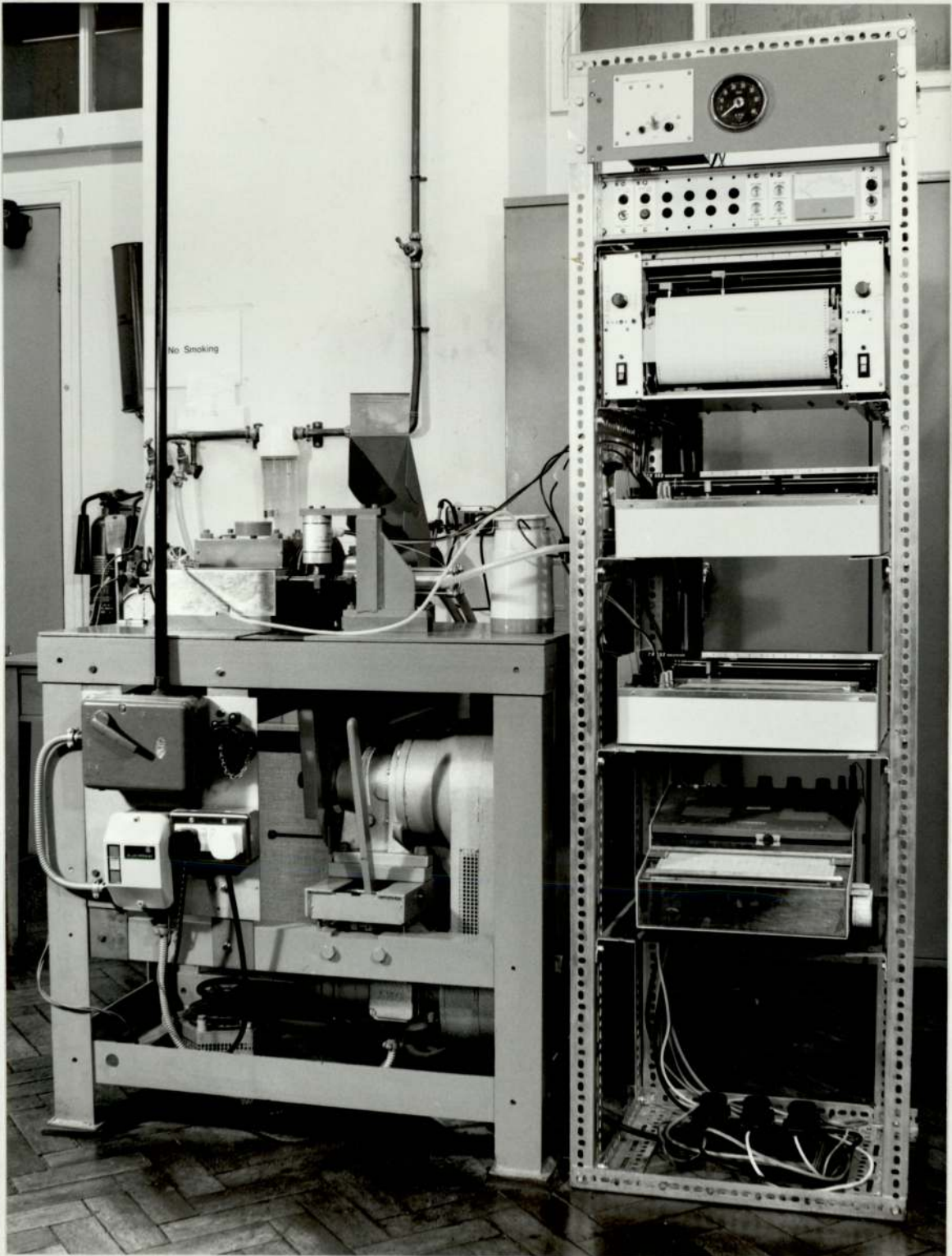


Figure 2. General view of elevated temperature pin and disc wear machine.

shaft and inserting a stainless steel tube mounted in a rotating water coupling so that water could be passed continuously along the shaft whilst rotating. In this way the bearing surfaces were always maintained at temperatures lower than 60 C.

2.3 The Loading Shaft

The shaft was mounted in linear and rotary bearings, in separate housings alongside the main shaft. The pin specimen holder, the wear transducer plate and the friction arm were fixed to this shaft. The shaft can move forward in its bearings when loaded and during the wearing process, and has the freedom to rotate slightly in order to measure the downward frictional forces on the pin.

The load was applied in two ways. Firstly, for loads of 9.8N to 49 ON., a pneumatic system was used. Compressed air, via a regulator, gauge and quick-release valve, powered a piston mounted along the axis of the load shaft. Point contact between the piston and the shaft was made with a ball bearing fixed to the end of the piston rod. The gauge was calibrated by mounting the friction force transducer along the axis and in front of a specimen pin such that point contact could be made with the surface of a specimen pin, and measuring the normal force in Newtons for each of the calibration marks on the standard pressure gauge.

Secondly, for loads below 9.8N., a simple dead weight system was used because it was found difficult to regulate the small pressures required accurately, without installing further small gauges and pistons. With this system loads of 0.5N could be used. Originally it was found that the lowest load which could effectively be used was approximately 5N. The reason for this was friction in the bearing seals and later, in addition, to very fine and hard wear particles contaminating the bearings. To achieve lower loads, the seals were

removed and the entire loading shaft was encased in a metal box so that the normal stroke of the bearings was protected.

The new bearings were given a lighter pre-loading by honing out the inside faces of the outer casing. This resulted in very low friction, the lowest load to pull the relatively heavy shaft, was around 0.2 to 0.3N. Unfortunately the spring in the Linear Voltage Differential Transformer (L.V.D.T.) used to measure the wear rate exerted an extra force of 0.5N-1.5N depending on the extension of the distance probe. The L.V.D.T. spring force had to be taken into consideration for the lowest loads, where it was a significant fraction of the applied load. For low loads, where the wear was 'mild', the wear rate and the linear distance removed was very small so the change in load with extension of the spring could be ignored. If the very low loads were required then the L.V.D.T. could be removed and the wear measured by weight loss.

2.4 Specimen Pin Holder

The pin was held in a heat flow calorimeter arrangement fixed to the loading arm which can be seen in Figure 2.4. The arm was designed so that different pin holders and track radii could be used, if desired. The calorimeter-type holder was used throughout the present work. It enabled the heat flow along the pin to be measured continuously. The design, shown schematically, Figure 2.3 was based strongly upon that used by Grosberg and Molgaard (39).

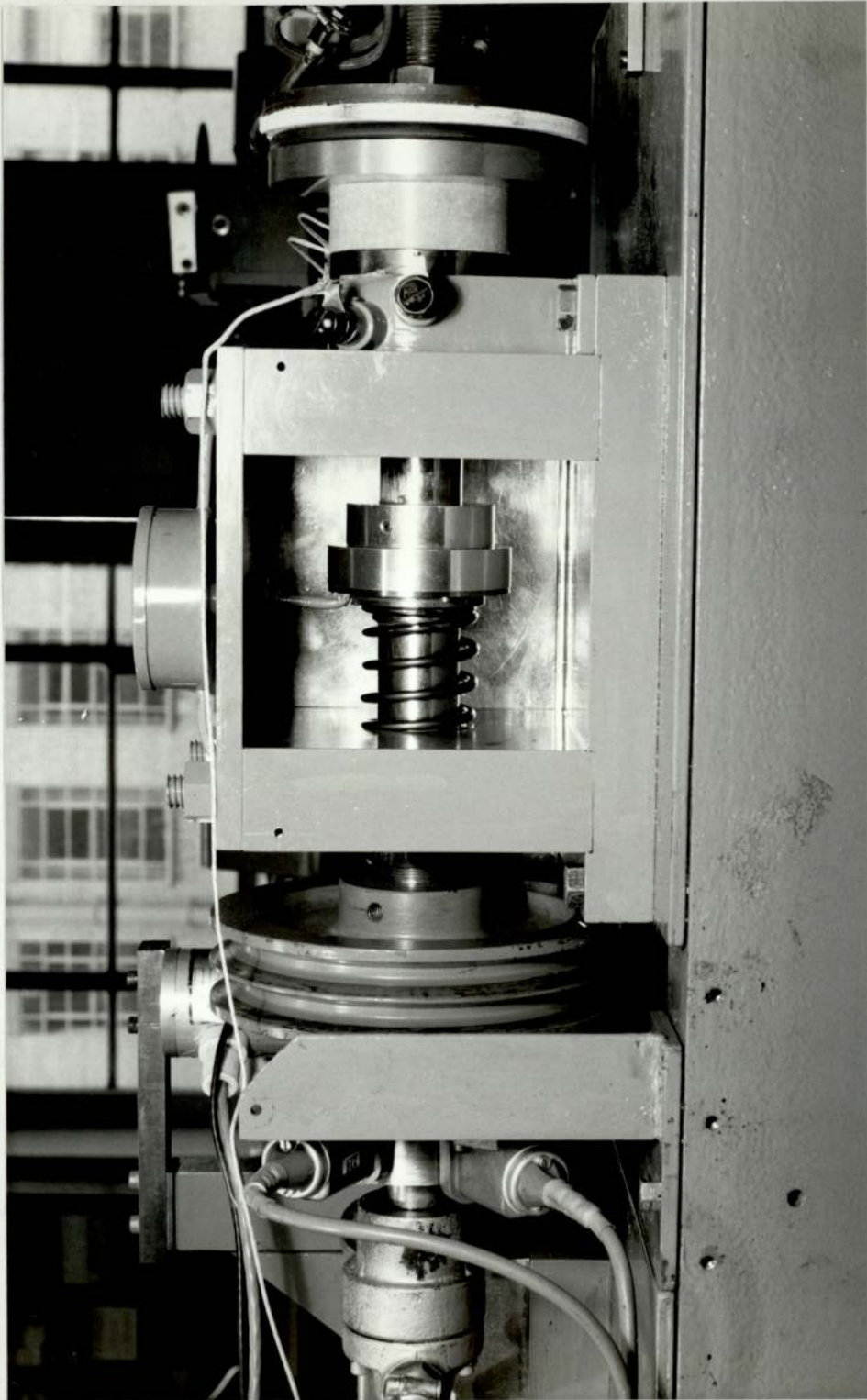


Figure 2.2. Side view of main shaft showing spring and ball race arrangement for "end float" compensation.

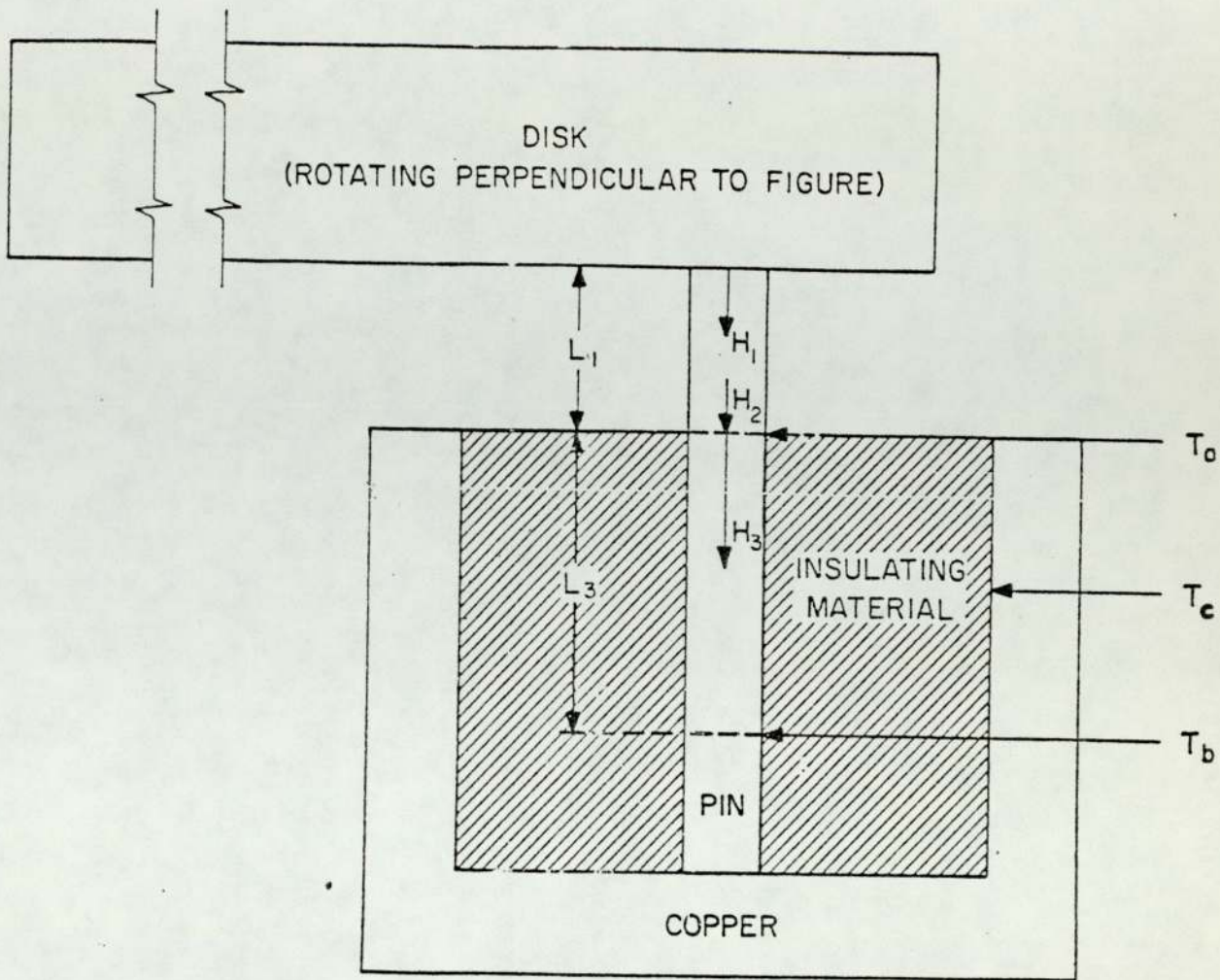


Figure 2.3. Cross-sectional diagram of the pin and pin-holder showing heat flow and thermocouple positions.

2.5 The Drive System

The unit which provided the main drive consisted of a 3-phase, 4 H.P., electric driving motor, a variable speed pulley and a reduction gearbox. This was supplied as a single unit and then modified to have the required orientation within the machine stand. The output speed was infinitely variable between 120 and 720 r.p.m. To increase the range of speeds, pulleys were fitted to the main shaft; this gave a range of 60 - 1440 r.p.m. A constant radius of sliding of 50mm was used throughout, giving a range of linear track speeds of 0.31 to 7.5 m.s^{-1} . The drive unit was mounted in a heavy, angle-iron stand to absorb vibration and sub-mounted on a secondary frame. The latter was pivoted to the main stand so that the motor could be lifted, using a lever system, in order to change the belts and pulleys.

The speed of rotation of the main shaft was measured using a magnetic impulse tachometer. An aluminium ring with 12 steel pole pieces inserted around its periphery was mounted on the main shaft to provide the pulses for the tachometer. One of the pole pieces was made longer than the others so that it would activate another tachometer separately. This provided an external trigger for an oscilloscope upon which the friction trace could be displayed for each revolution.

2.6 Friction measurement

The frictional force of sliding was transmitted to a strain gauge dynamometer which was placed so that it sensed the frictional force in an equal and opposite direction, thereby providing a direct measurement. The friction arm moved forwards as the pin wore, so a miniature ball race was fitted to the dynamometer to act as a rolling line contact. The output of the dynamometer was then fed into a strain gauge amplifier unit; the amplified voltage was recorded by a

chart recorder and by a meter continuously. Friction traces for one revolution of the disc could also be displayed on an oscilloscope if desired. Two dynamometers were used to cover the whole range of possible values from 0 to 1N and from 0 to 50N. It was necessary to introduce some mechanical damping to reduce the effect of bouncing of the friction arm against the dynamometer which occurred at times under severe wear conditions.

2.7 Wear Rate Measurement

The wear was continually measured using a Linear Voltage Differential Transformer (L.V.D.T.), which sensed the forward movement of a plate fixed to the load shaft. The transducer required to be powered by a constant D.C. voltage (from the strain-gauge unit) but needed no amplification. The output was recorded alongside the friction trace on a 2-pen chart recorder. By altering the sensitivities and chart speeds of the recorder, it was possible to resolve small variations in the wear and friction simultaneously. The trace gave the rate of decrease in the length of the pin which, when multiplied by the cross-sectional area, is the volume removed per unit time. When a steady state of wear achieved an approximately straight line trace is obtained, the gradient of which, when divided by the linear track speed, gives the volume removed per unit sliding distance (expressed here in $\text{mm}^3 \cdot \text{mm}^{-1}$). Errors occurred in this method when the area of the pin increased, due to deformation and the production of a collar at the pin tip. This occurred during either particularly severe wear or at the higher elevated disc temperatures. Any effect of this phenomena on the wear rate in terms of the general pattern could be taken into account by comparison with the pattern of wear results obtained by a weight loss method. The average wear rates of both the pin and disc were obtained by weight loss, this will be discussed later.

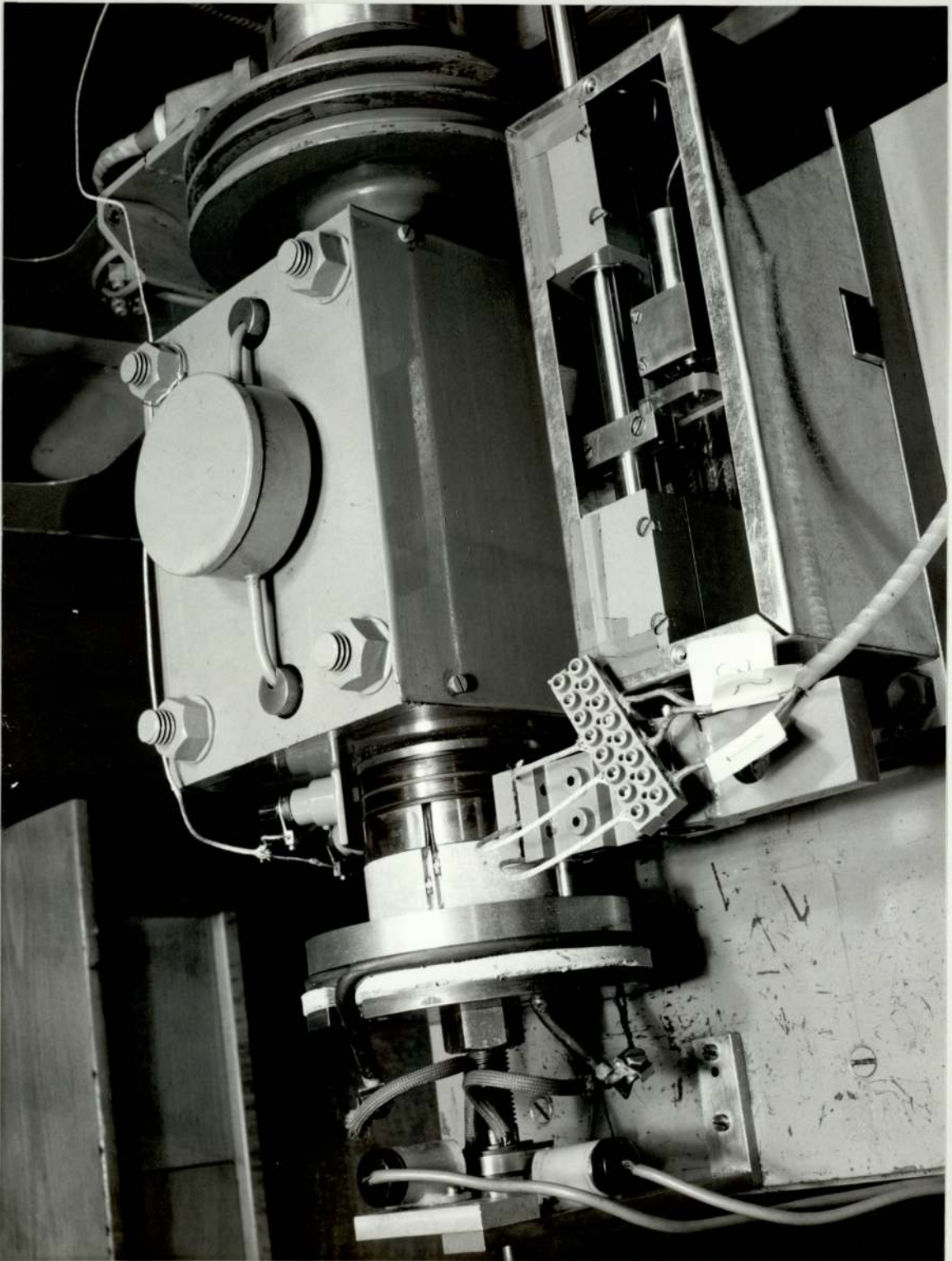


Figure 2.4. Close-up view of pin and disc and ancillary equipment

2.8 The Heater Assembly

A method of raising and maintaining the bulk disc to temperatures of up to 700C was required. Radio-frequency (R-F) heating, using a 4MHz 4kW generator and a copper "pancake" coil designed to couple with the free face of the specimen disc, was tried. On testing, the disc temperature was easily raised to the required high values and had the advantage of not being in contact with the specimen. Some problems of R.F. interference with the measuring equipment were anticipated, particularly with the thermocouple leads. The difficulties, however, were underestimated. Despite the usual precautions of good earthing and elaborate shielding of the work coils, generator, transducers and the instrument rack and the use of electrical filtering, the amount of interference, although reduced, was unacceptable. Long range air-bound interference was still able to affect other equipment in the laboratory.

After many attempts to find an alternative method for heating the specimens, it was eventually decided to use an electrical resistance heater. A domestic cooker ring was fixed to the face of the disc left free for R-F heating and tested statically to determine whether the required temperatures could be obtained. Temperatures of around 650 C were reached with a 1.625W coil. A 2 kW coil was annealed and bent to the required shape and size and fitted flush to the disc. The complete assembly is shown in Figure 2.4. It consists of an insulating annulus, a securing plate and some copper slip rings, all mounted on a shaft screwed into the main shaft. The heater was supplied, via carbon brushes, by a 270V Auto-Transformer. This method provided temperatures up to 720C, which were readily controlled and any temperature could be obtained to $\pm 5C$ when settled conditions were reached in an experimental run. The temperature of the disc decreased with increase in radii and was approximately constant for a given radius over the disc surface.

2.9 Temperature measurement

2.9.1. Bulk disc temperature

A thermocouple was spot welded to the wearing face of the disc at the radius of the asbestos insulating ring and connected to carbon slip rings mounted to the main shaft. Small brass unions were made so that a new thermocouple could be used for each experimental run. It has previously been mentioned that the temperature of the disc increases with decreasing disc radius when the disc is heated externally. To determine the possible difference between the temperature at the actual sliding radius and at the edge of the insulating ring, the steady temperature reached for increasing heater voltage was measured at both positions simultaneously. At a track speed of 1.0m.s^{-1} (the speed used for the externally heated experiments) the temperature was constantly 10C greater at the smaller radius. This was only relevant for the initial setting of the temperature at the start of each experiment.

2.9.2 Pin temperatures

The thermocouples used for the measurement of the heat flow along the pin, T_a , T_o and T_c were spot-welded onto the pin at set distances, as indicated in Figure 2.3, for each experiment. The method by which these temperatures were used in the Heat Flow Analysis is given in Appendix 3.

2.10 Experimental details

2.10.1. Specimen material

The mild steel used for the pin and disc was BS970 EN8 which has the following composition:-

C	Si	Mn	S	P
0.35-0.45	0.05-0.35	0.60-1.00	0.060 max	0.060

The discs were cut from black bars and randomly ground to around 0.2μ inch C.L.A. The pins were taken from cold-rolled rods and turned to a smooth finish. The bulk hardness of the pin and disc material was 210 ± 10 Vpn. The discs dimensions were 0.12 m. diameter and 12.7 mm thick; the pins were 38.1 mm long and 6.35 mm in diameter. The discs and pins were degreased by washing in acetone and petroleum ether prior to use.

2.10.2. Temperature elevation

At the start of each elevated temperature run, the bulk disc temperature was raised to the desired value and maintained for about 15 min. with the pin loaded against the disc. During the early stages of each test the temperature was corrected, if required, by altering the voltage, care being taken to ensure that the temperature did not exceed the desired value by more than 30C. Once a steady wear rate was achieved the bulk temperature needed little or no further adjustment. If, however, transitional behaviour was experienced, changes in temperature of a few degrees were obtained.

2.10.3. Wear measurement

The equilibrium wear rate was found by inspection of the chart trace from the L.V.D.T. as mentioned previously.

The average wear rate of the pin and disc were found by weighing before and after each experimental run. The wear rate was expressed as the weight loss per unit sliding distance ($\text{kg} \cdot \text{m}^{-1}$). Good accuracy could not be obtained for low wear of the disc as the accuracy of the Triple-beam Balance used was only to 10^{-4} kg. The pins were weighed using an electronic chemical balance.

2.10.4. Physical examination of debris and worn specimens

It was not possible to apply all the physical techniques to every sample from each experiment, since a large number of experiments

were conducted. The debris, pin and disc from every experiment were stored and one or two samples were eventually selected from each region of the general wear pattern or from a particular set of experiments.

Debris samples were examined using X-ray diffraction with a cylindrical powder camera. Co K radiation was used throughout. In some cases the debris was very fine and produced diffuse lines so care had to be taken to ensure that the debris was tightly packed.

The surface hardness of the pin and disc surfaces was measured using a microhardness tester. The average of ten measurements of the areas which appeared to have been the contacting areas when the run was stopped was recorded. These hardened regions were surrounded by softer areas and appeared as smooth burnished patches.

Pin and disc surfaces for the same experiment were examined using a scanning electron microscope. Difficulties were encountered in preparing replicas of the disc surface for the extensively damaged severe wear specimens so sections of the disc were cut out to fit into the microscope.

A few samples of debris were examined using the scanning electron microscope. Mounting stubs were ground and polished and a thin film of perspiration was applied to the ground surface before dipping into the debris. The perspiration acted as both an adhesive and an electrical conductor which would not interfere with the examination.

Selected samples of debris were set in opaque plastic and then ground and polished in order to provide sections of the debris which could be examined under optical microscopy.

CHAPTER 3

EXPERIMENTAL RESULTS

3.1 Equilibrium wear rates as a function of load and speed

This section describes the results obtained from a series of wear tests at various sliding speeds, constant initial hardness and with no external heating of the specimen disc. The graphs of the log wear rate against log applied load obtained for sliding speeds of 1.0, 0.75 and 1.25 m.s⁻¹ are shown in Figure 3.1.

V = 1.0 m.s⁻¹

The T₁ transition from mild wear to severe wear was not found at the lowest loads obtainable. Severe wear, with the production of bright metallic debris particles, was experienced until the T₂ transition to mild wear occurred at between 4.3 and 4.7 kg. The wear rate dropped by an order of magnitude and the coefficient of friction fell from 0.55 to 0.38. The debris changed character and consisted of black oxidised particles. At loads above 6.4 kg the wear could still be described as mild but the wear rate increased rapidly with increasing load and at 15.3 kg the wear rate was greater than that for the severe wear at lower loads. The debris at the high wear rates was oxidised but had a metallic character which was not present in the wear immediately following the T₂ transition.

V = 0.75 and 1.25 m.s⁻¹

The reduction in speed to 0.75 m.s⁻¹ produced mild wear at low loads. The oxide produced consisted of fine powder of light brown Fe₂O₃ and took long periods of running-in before mild wear established. Extended runs were necessary before oxide cover was made over the entire wear track. The wear rates in this wear regime were around

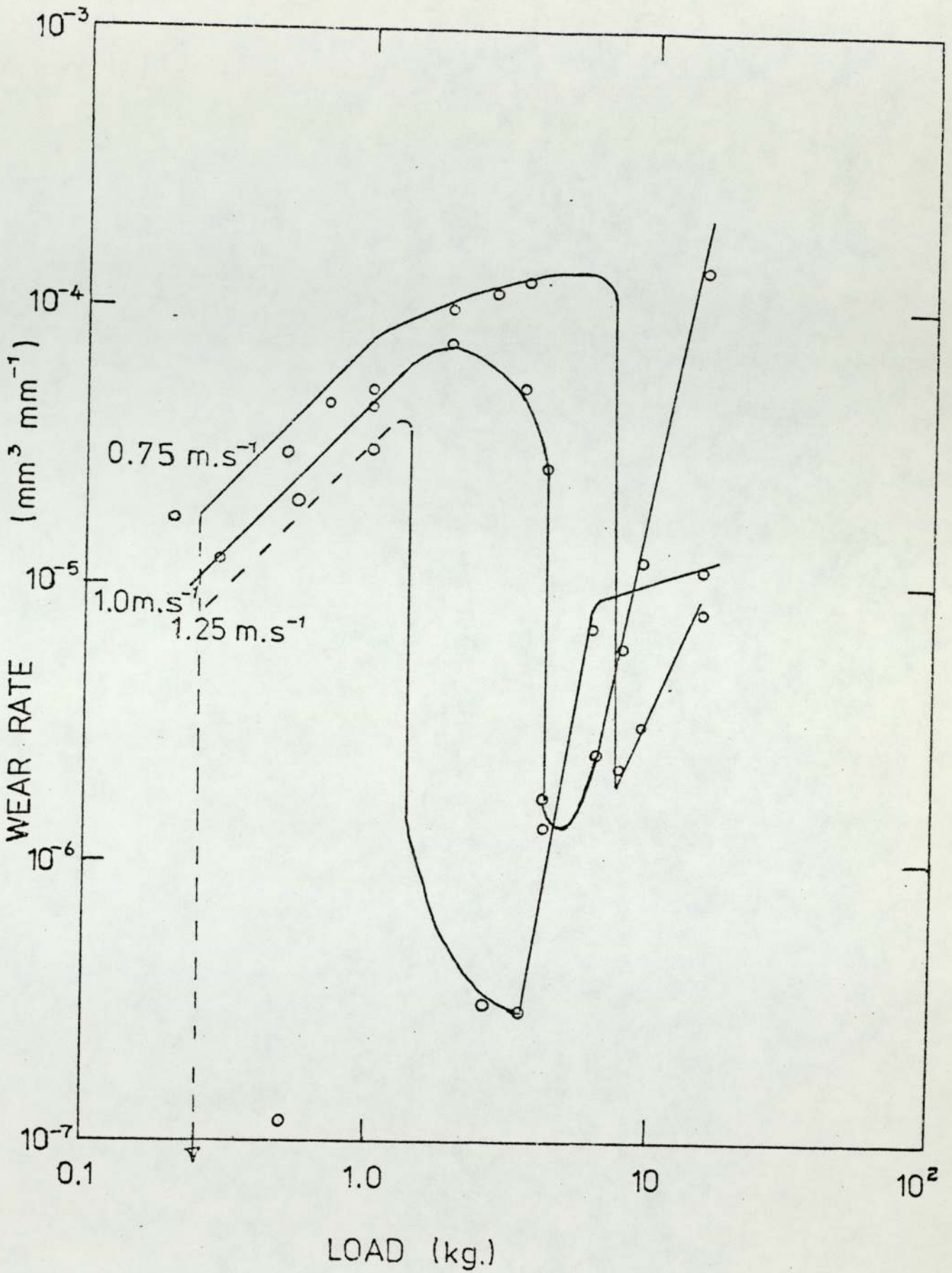


Figure 3.1. Log w plotted against log W . Sliding speeds: 1.0, 0.75 and 1.25 m.s⁻¹.

$2 \times 10^{-9} \text{mm}^3 \text{mm}^{-1}$. The T_1 transition to severe wear could not be given to occur at a specific load and lies between 200 and 300 g. Lack of accuracy in loading at these low loads, as described previously and the nature of the transition itself meant that the wear rates were not reproducible. The effect of reducing the sliding speed from 1.0 to 0.75 m.s^{-1} on the T_2 transition was to increase the transition load by 3 kg. At the increased speed of 1.25 m.s^{-1} the transition load was decreased by a similar amount.

The change to a steeper slope at around 6.4 kg for the 1.0 m.s^{-1} wear rate curve was possibly due to a T_3 -type transition occurring quickly after the T_2 transition. This effect was also found for the 0.75 and 1.25 m.s^{-1} wear curves. A further change in wear rate slope was observed for the 1.25 m.s^{-1} experiments at loads above 6.4 kg where the curve flattens out instead of maintaining the rapid increase in wear rate.

$V = 2.0$ and 4.0 m.s^{-1}

To obtain sliding temperatures significantly higher than those obtained at 1.0 m.s^{-1} , the sliding speed was increased to 2.0 and 4.0 m.s^{-1} . The wear rates obtained are shown in Figure 3.2. At these higher speeds the no transitions were found because the T_2 transition would be expected to occur at loads of less than 100 g. There was an increase in the slope of the wear rate curves for both speeds at around 1.0 kg, the significance of this feature will be discussed in detail at a later stage. The wear was mild with debris similar to the $T_2 - T_3$ wear at lower speeds.

3.2.

Average wear rate

For the experiments at 1.0 m.s^{-1} , the weight loss of the pin was measured and plotted as log wear rate (g.cm^{-1}) against log load, Figure 3.3. The wear pattern was very similar to that given for the

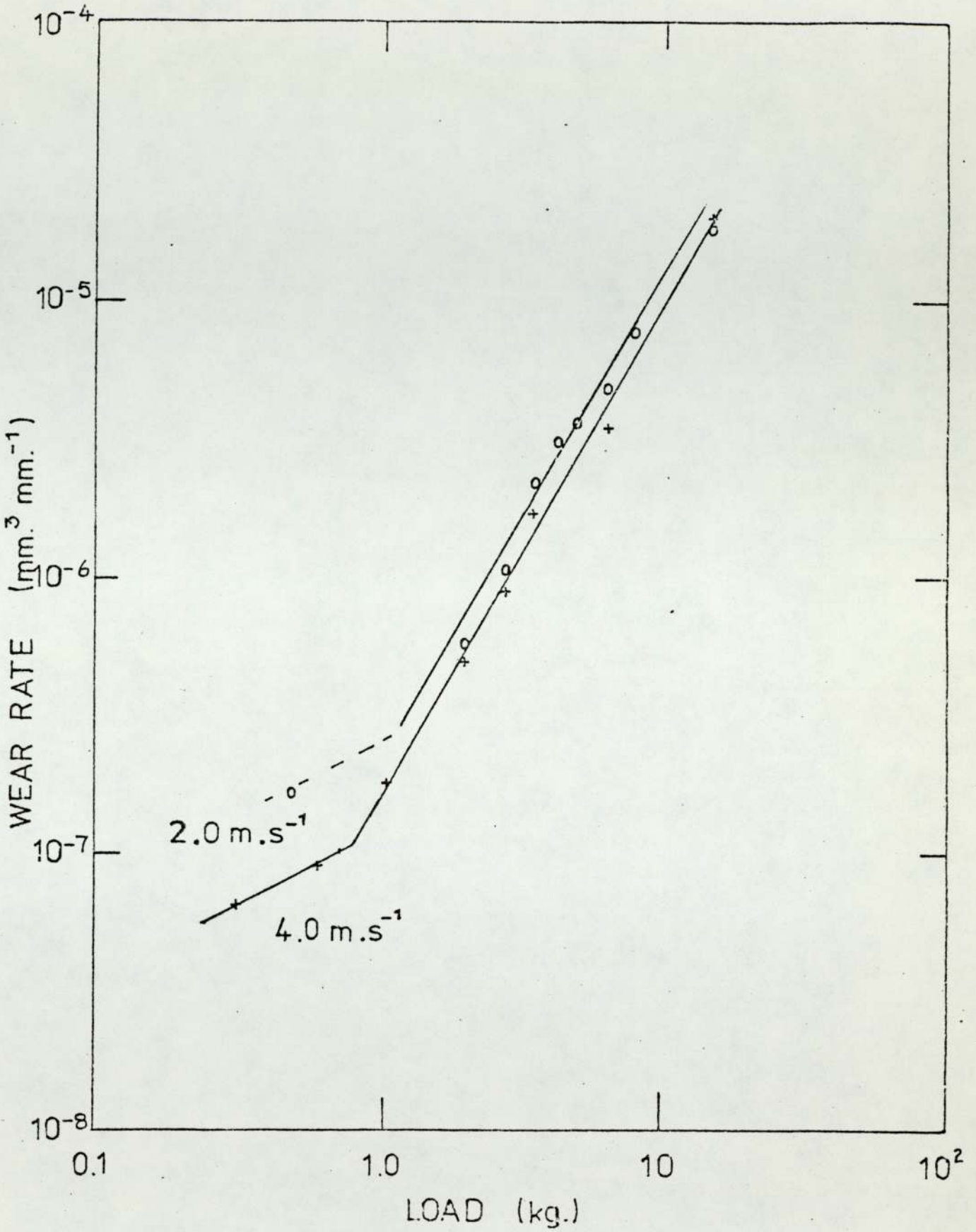


Figure 3.2. Log w plotted against log w. Sliding speeds: 2.0 and 4.0 m.s⁻¹.

plot of equilibrium wear, Figure 3.1. For some of the severe wear tests there was appreciable wearing of the disc and it was decided that the weight loss of the disc should also be measured for all further tests.

The graphs obtained for all other track speeds are given in Figures 3 (4, 5). In each case the pin wear curve exhibits the same form as that shown by the equilibrium wear rate plot. At 0.75 m.s^{-1} (Figure 3(4a)) the disc wear followed that of the pin; for 1.25 and 2.0 m.s^{-1} , the disc wear tended to decrease with increasing wear of the pin. At 4.0 m.s^{-1} (Figure 3(5b)) the disc wear shows a rapid increase at about the same rate as the pin wear.

3.3.

Friction results for the room temperature runs

The frictional force was measured continuously for all the runs in the present work.

In general the friction peaked at the early, run-in stages of each experiment. The high value would reduce to a more or less steady value once a steady or equilibrium wear regime was obtained. If the wear was transitory the friction trace would reflect the changes in wear behaviour.

During severe wear, the trace oscillated about a mean value, when this was observed on an oscilloscope, very high peak values could be seen four or five times the average. These high values could be due to the large metal particles being trapped between the rubbing surfaces before escaping. The relatively high mean values are caused by the metal to metal welding interactions. The sudden release of the entrapped wear particles resulted in some bouncing of the pin on the disc, this however, was not detected in any other wear regime although it is possible that it occurs to a very much smaller degree. The frictional and wear character of a run was also reflected by the mechanical noise of the rubbing.

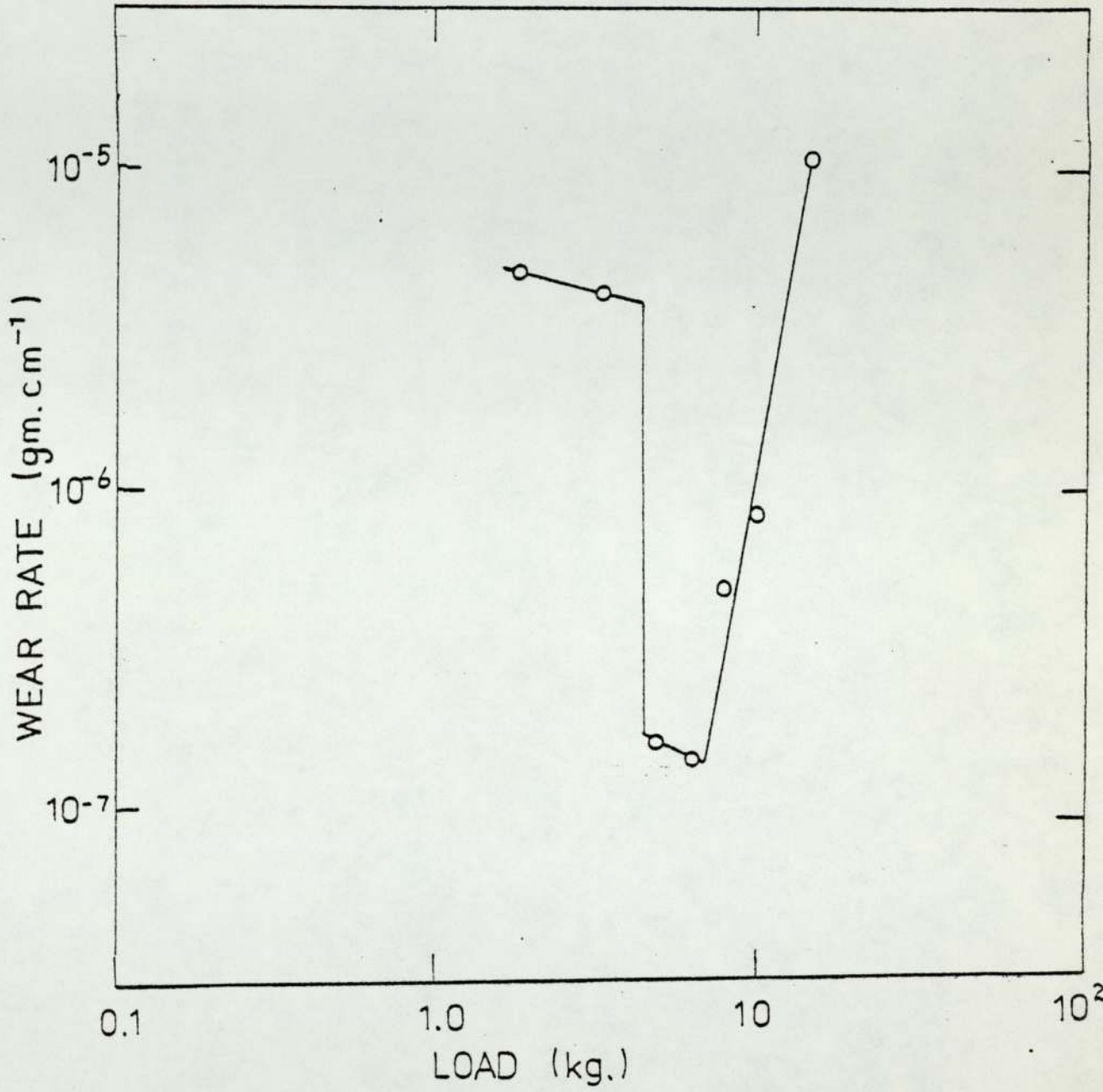
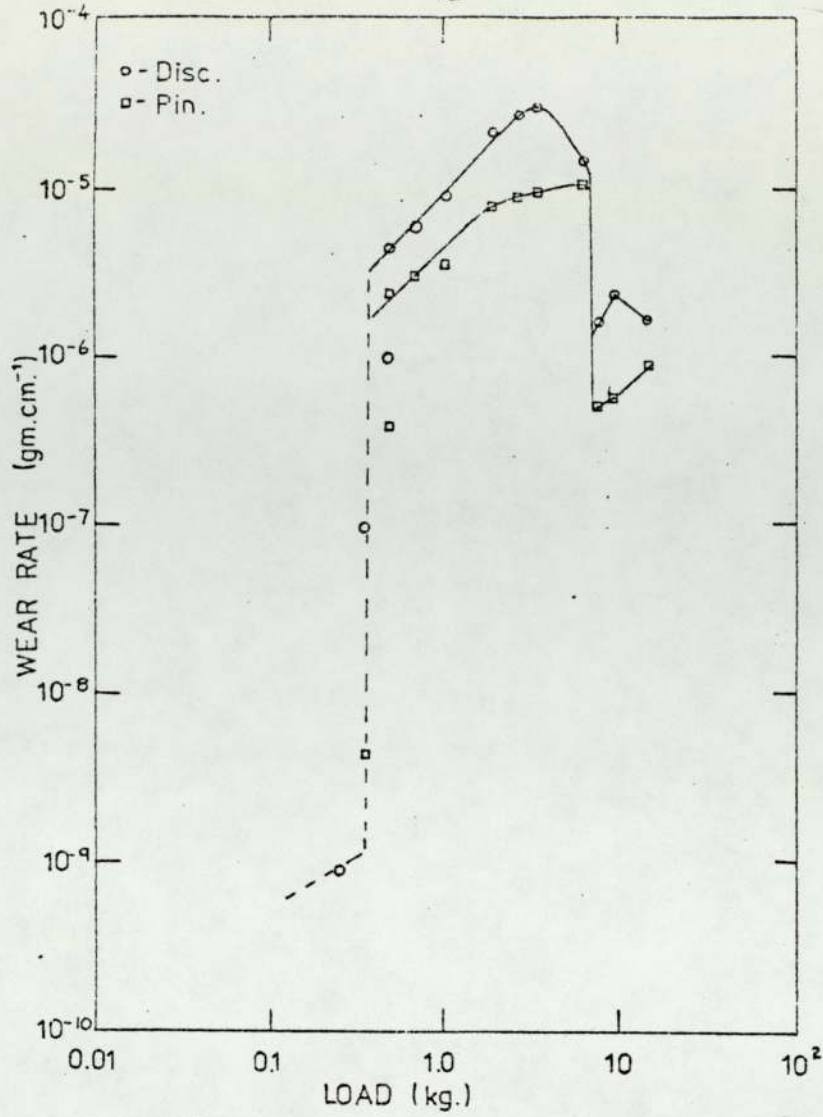
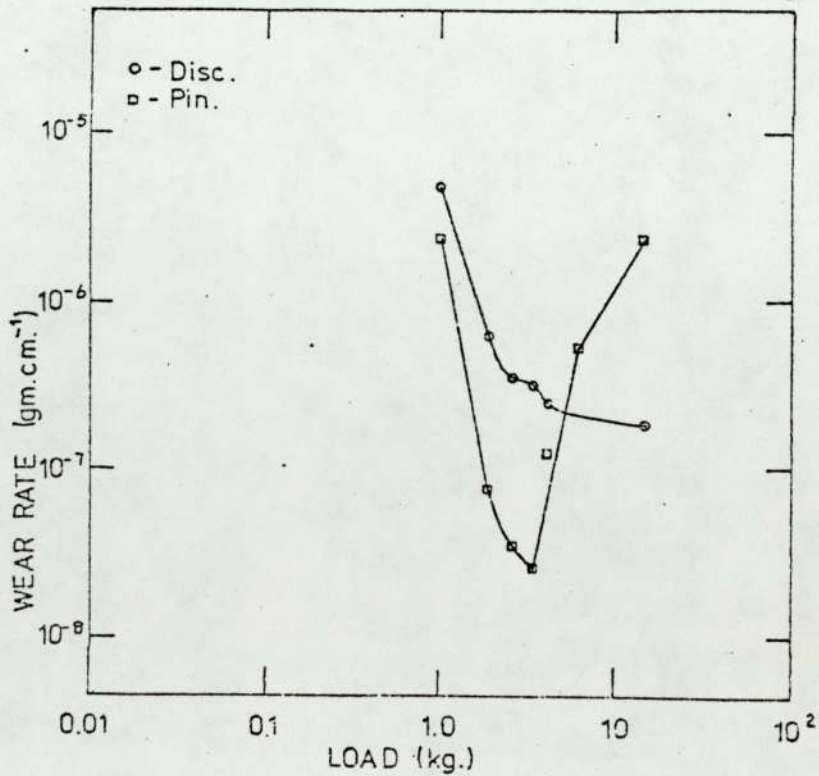


Figure 3.3. Log w (weight-loss method) plotted against log W
Sliding speed : 1.0 m.s

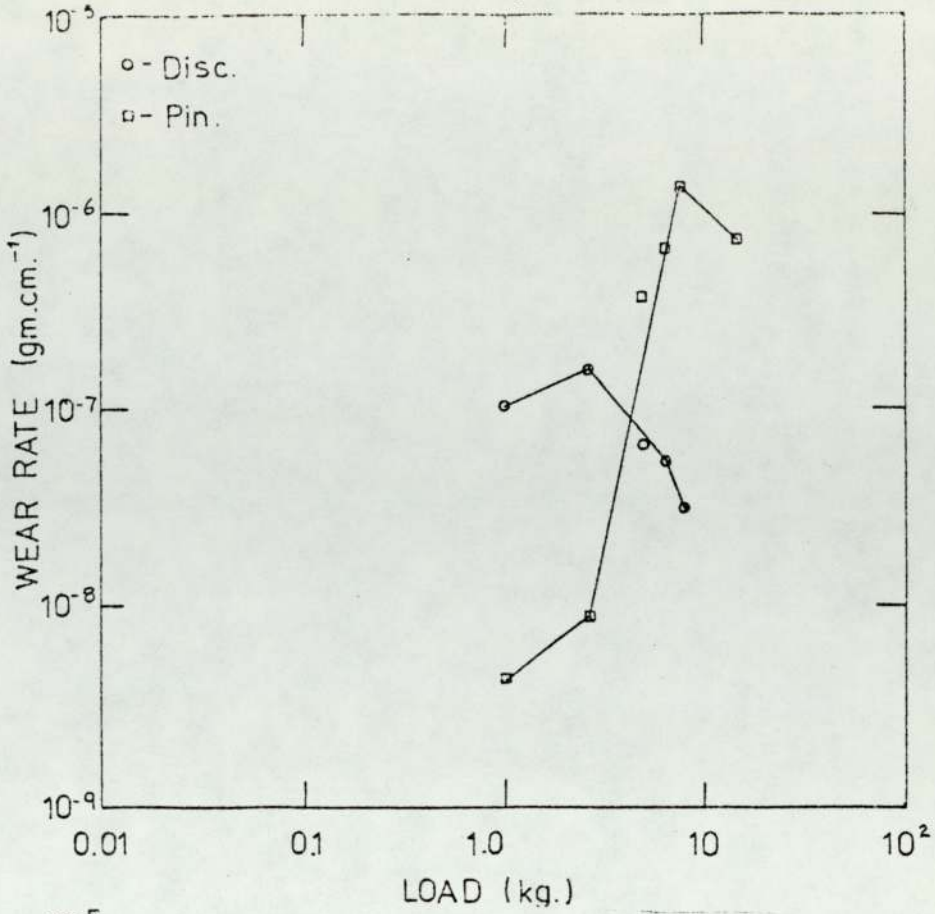


a)

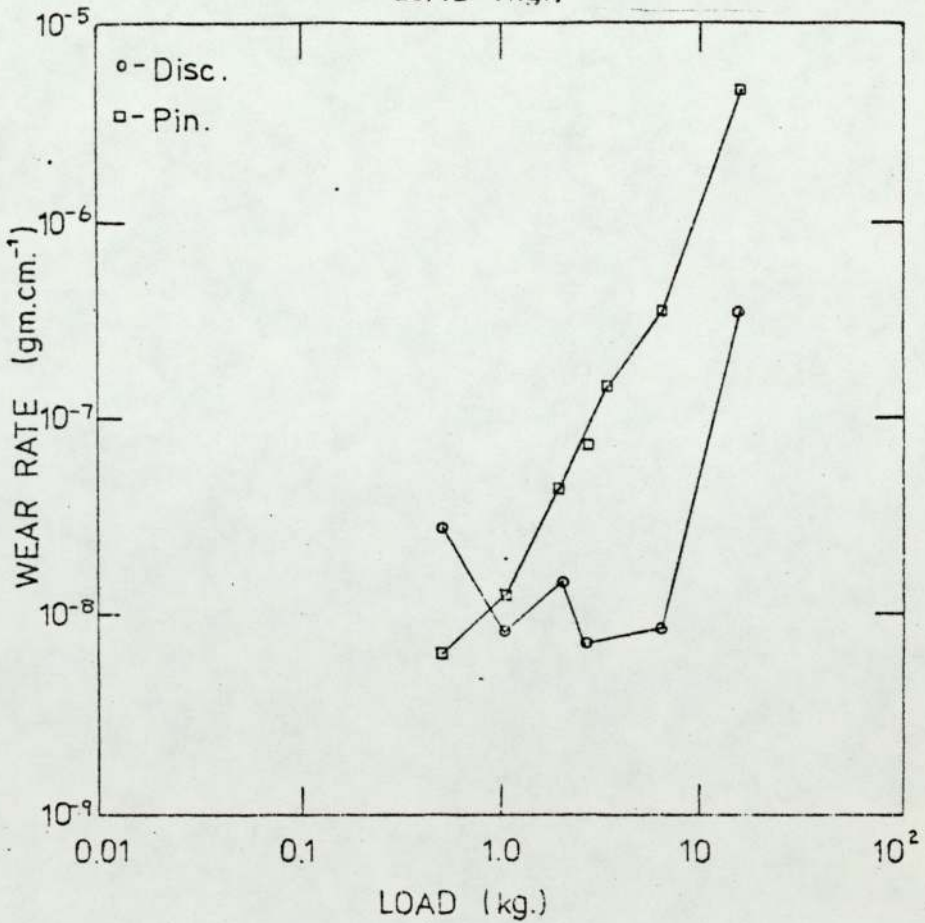


b)

Figure 3.4. $\log w$ (weight-loss method) plotted against $\log W$.
a) Sliding speed: 0.75 m.s^{-1}
b) Sliding speed: 1.25 m.s^{-1}



a)



b)

Figure 3.5. Log w (weight-loss method) plotted against log W.
a) Sliding speed : 2.0 m.s⁻¹
b) Sliding speed : 4.0 m.s⁻¹

The range of values of the coefficient of friction, μ , was between 0.35 and 0.9, for the mean values, although peaks of 1.0 or greater were observed during run-in and severe wear. The graphs of μ against load presented below show a general decrease in μ as the load increases.

$$\underline{V = 1.0, 1.25 \text{ and } 0.75 \text{ m.s}^{-1}}$$

The curves obtained for these speeds are given in Figures 3.6 and 3.7(a) the friction in all cases shows a stepped decrease with load, settling down to approximately constant value between 0.3 and 0.4. It is interesting to note the positions of the transitions occurring at each speed. The T_1 transition only occurs at 0.75 m.s^{-1} , μ , for the mild wear below this transition was approximately 0.4. The friction increases rapidly once the transition to severe, metal to metal interaction is complete. The maximum value seems to occur at the highest wear rate obtained during the region where the wear rate is directly proportional to the load, it then decreases until just prior to the T_2 transition, where μ remains almost constant before decreasing sharply at the transition to the second region of mild wear. The friction falls slightly before levelling out at the T_3 transition, remaining constant for the region where the wear rate increases steeply.

$$\underline{4.0 \text{ and } 2.0 \text{ m.s}^{-1}}$$

The curves obtained at these speeds (Figure 3.7(b)) show a distinct change in the frictional behaviour, since there are no transitions in wear character. Again the friction appears to be independent of the wear rate when it increases within the same wear regime, in this case when the wear is mild, producing the black oxidational debris, typical of the wear after the T_2 transition.

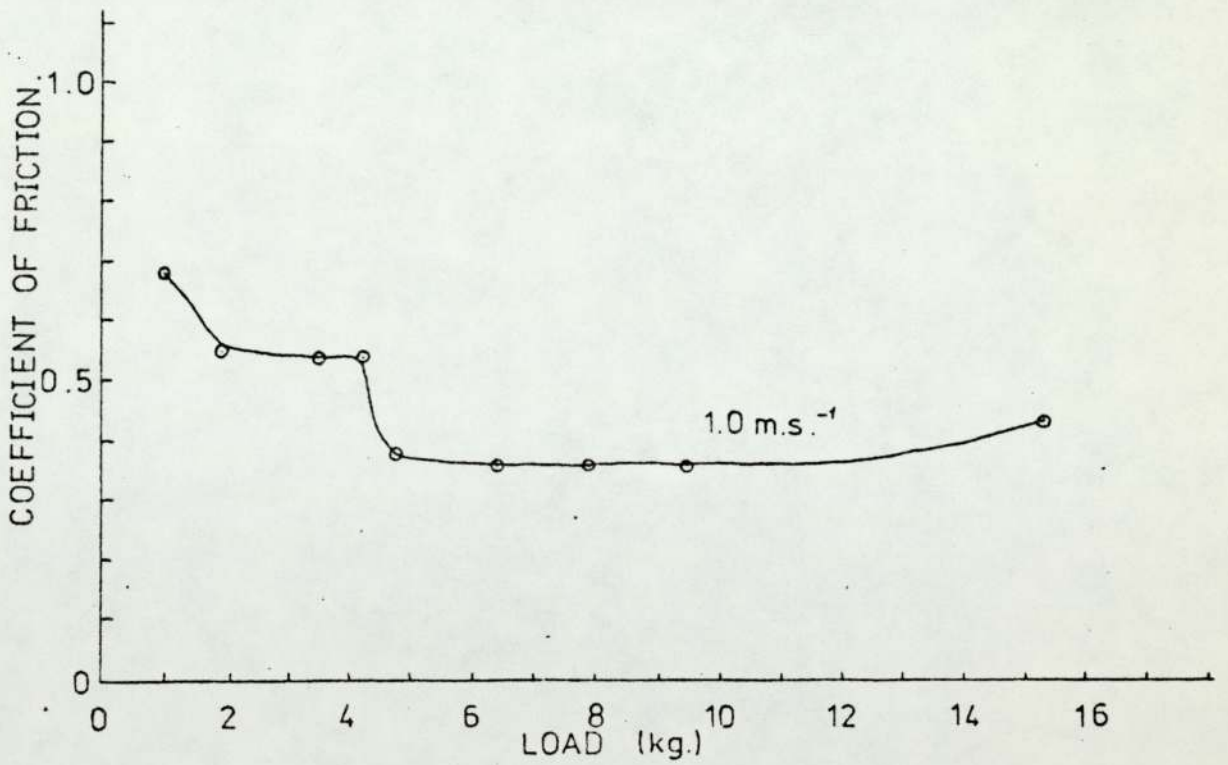
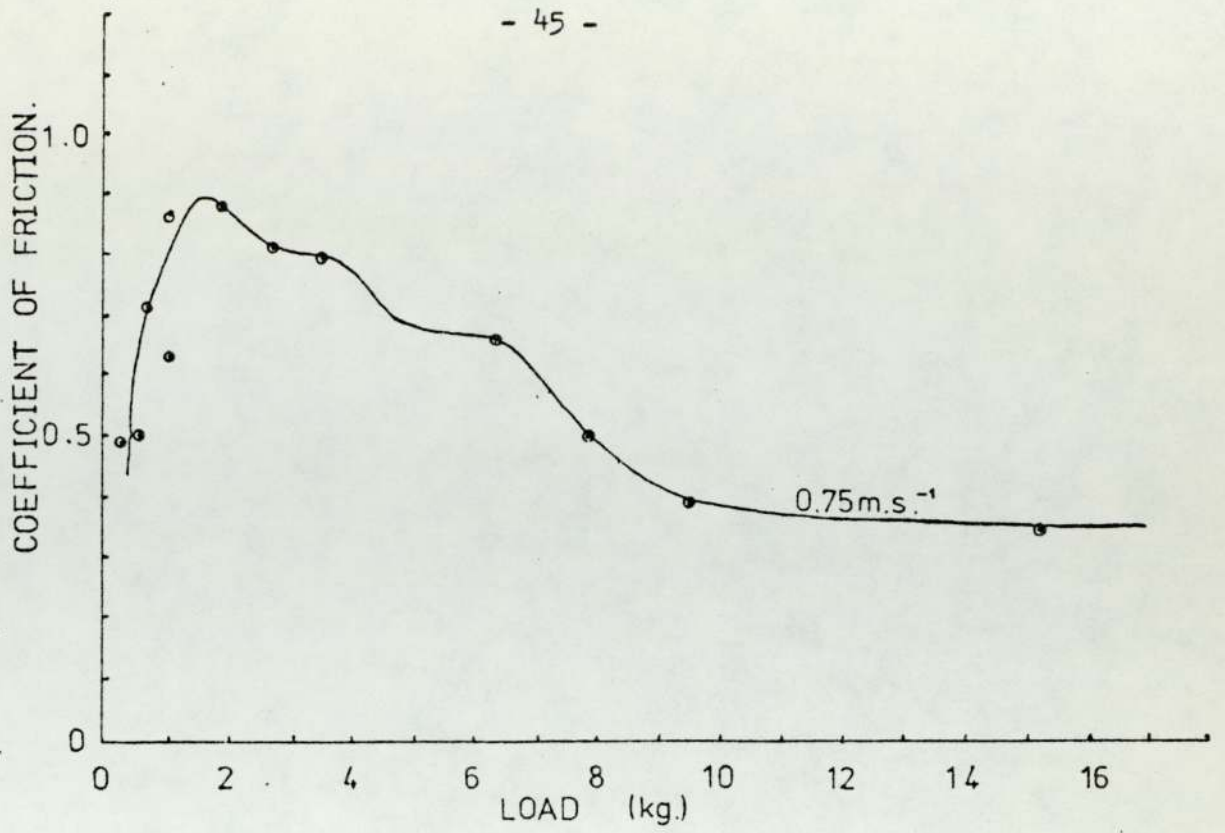


Figure 3.6. Friction coefficient versus load
Sliding speeds : 0.75 and 1.0 m.s.^{-1}

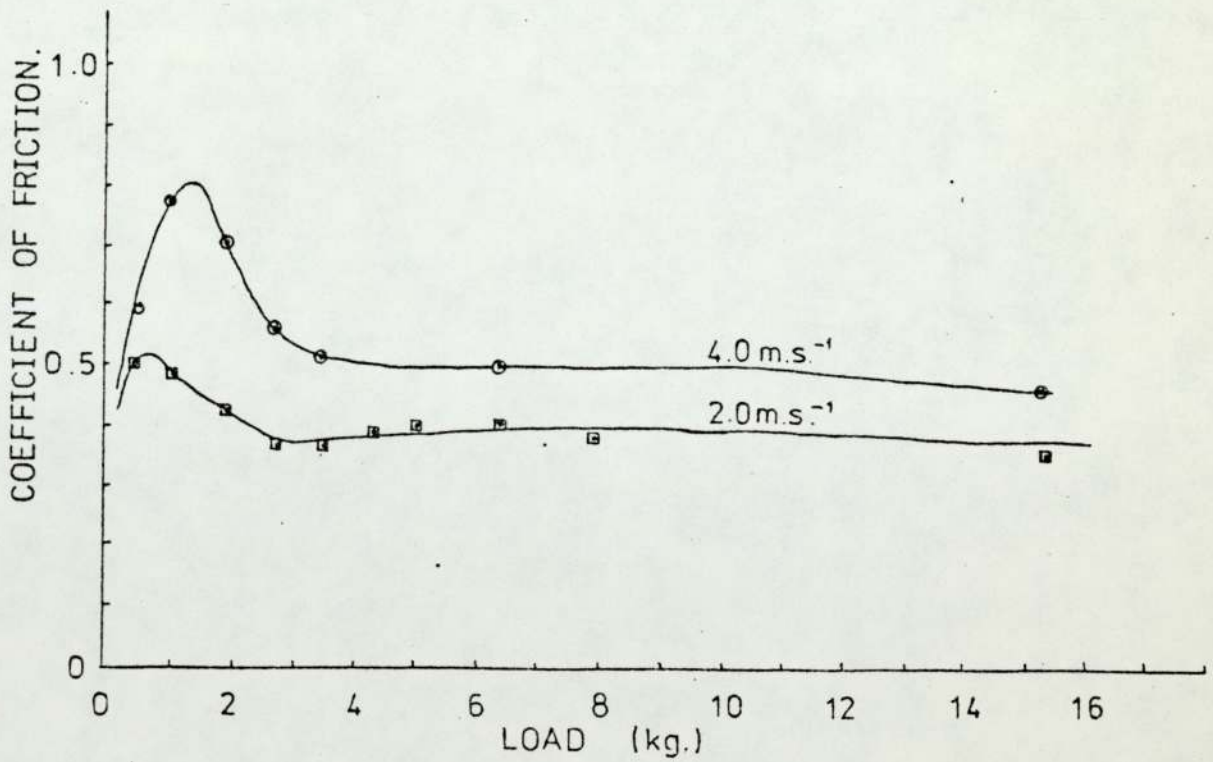
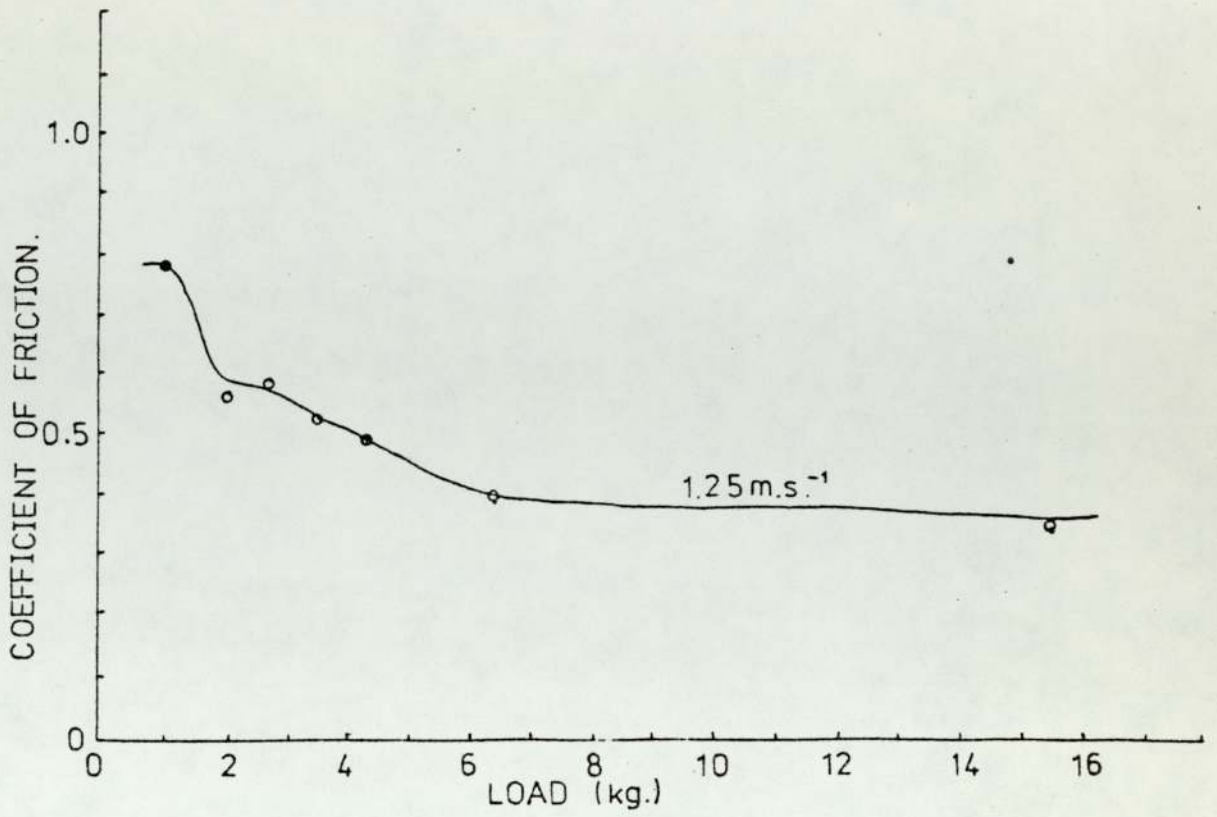


Figure 3.7. Friction coefficient versus load.

a) Sliding speed : 1.25 m.s^{-1}

b) Sliding speed : 4.0 and 2.0 m.s^{-1}

3.4 Microhardness tests

The microhardness of the hardened regions on the pin and disc surfaces was measured for the experiments where the sliding speed was 0.75 and 2.0 m.s⁻¹ the graphs of applied load against hardness for each speed are given on Figure 3.8. Although each point on the graph represents the average of ten readings the accuracy of the results was not satisfactory and the graphs can only be taken to indicate levels and rough trends in the hardness. Changes in surface hardness which may be associated with the transitional behaviour of the wear pattern could not be identified as readily as was desired.

$$\underline{V = 0.75 \text{ m.s}^{-1}}$$

A complete set of readings could not be taken for the discs, the missing values correspond to the experiments in which severe wear took place. The wear tracks became too deeply curved and rough for measurement. The hardness of the unrubbed material was around 200Vpn. Figure 3.8(a) shows a steady increase in hardness with load for the pin surfaces and the positions of the wear transitions. The hardness levels at both transitions coincide with the critical hardness values found by Welsh (i.e. 340 to 425 Vpn for the first critical hardness and 553 to 775 Vpn for the second which is associated with the T₂ transition).

$$\underline{V = 2.0 \text{ m.s}^{-1}}$$

The experiments at this speed were used for the Heat Flow analysis and oxidational experiments and it was important to know how the hardness varied with load. The pin hardness is again lower than the disc, as found with the experiments at V = 0.75, and it appears to follow the shape of the wear rate versus load graph for V = 2.0 m.s⁻¹.

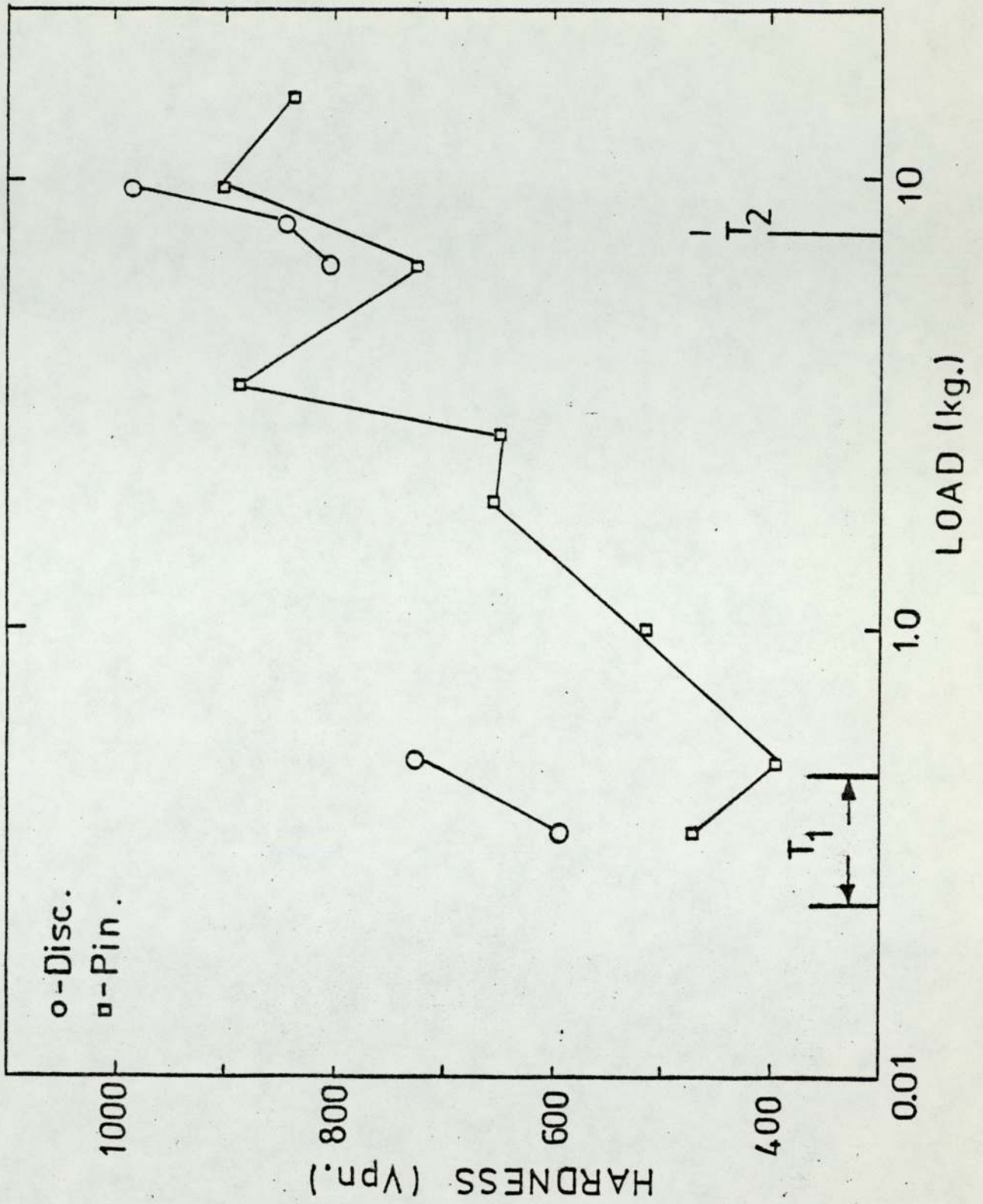


Figure 3.8(a). Micro hardness of pin and disc surfaces versus applied load. ($V = 0.75 \text{ m.s}^{-1}$)

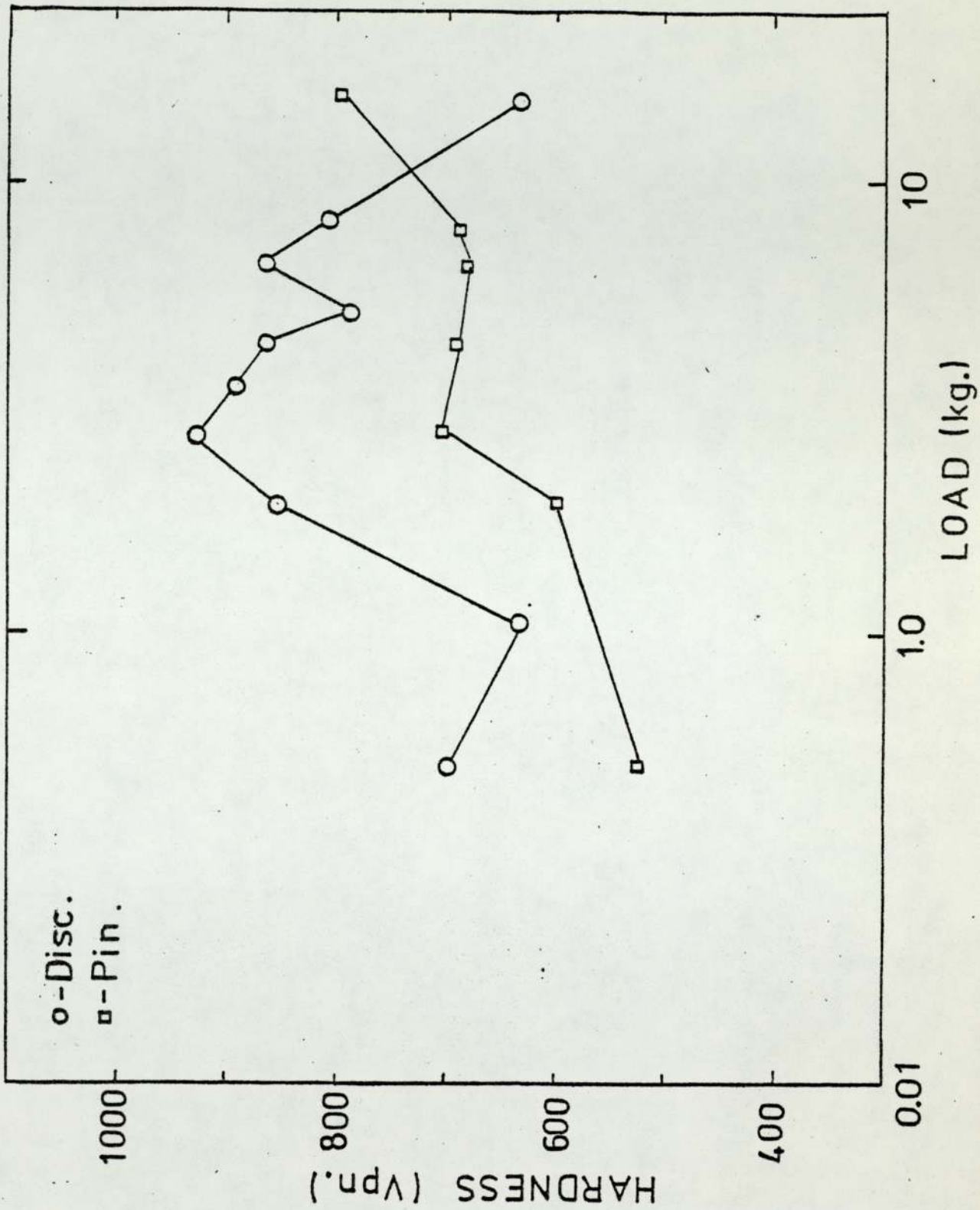


Figure 3.8(b). Micro hardness of pin and disc surfaces versus applied load ($V = 2.0 \text{ m.s}^{-1}$)

Results of the Elevated Ambient Temperature experiments

3.5

Wear rates as a function of temperature and load for a constant speed

The wear curves produced from the wear experiments carried out at a constant sliding speed of 1.0 m.s^{-1} and at bulk disc temperatures up to 500C , are given in Figures 3(8,9). As in the previous series of experiments the wear rates are expressed as both the equilibrium wear rate and the average wear rate found by the weight loss technique.

The experiments which were carried out with no external heating will be referred to as 'room' temperature experiments. The bulk disc temperature produced by frictional heating only is called T_R ; and T_E , the bulk disc temperature when external heating was applied.

$T_E = 100\text{C}$:

The curve has the same overall shape as that obtained for the corresponding 'room' temperature experiments and is displaced to lower loads. The effect on the wear curve, produced by maintaining the bulk disc temperature at this level, is similar to that which was obtained by increasing the sliding speed in the previous experiments. By inspection of Figure 3(1) it would appear that the decrease in transition loads of around 2kg is equivalent to increasing the sliding speed to between 1.0 and 1.25 m.s^{-1} . The relatively small effect of the increased ambient temperature was to be expected since the difference between T_R and T_E was small. The amount of frictional heating produced for a given experiment is dependent upon the frictional force and the sliding speed. For the present experiments only the load and the coefficient of friction, which depends on the wear regime, are important.

By artificially maintaining the bulk disc temperature at T_E for a series of loads; $T_E - T_R$ will not be constant for each load and the effect of the constant bulk disc temperature upon the wear pattern

will be asymmetrical. This effect became more obvious at higher loads and particularly so for the experiments at 15.3 kg where the wear rates were almost equal and little or no external heating was needed to maintain T_E at 100C.

$T_E = 200C:$

The T_2 transition from severe to mild wear was not found at this temperature and presumably displaced to lower loads. The run-in time was shortened, mild wear occurring in less than 5 mins. with the production of fine particles of black oxide typical of post T_2 wear although the wear rate was of the order of the mild wear prior to the T_1 transition ($1.0 \times 10^{-7} \text{ mm}^3 \text{ mm}^{-1}$).

The shape of the wear curves obtained for $T_E = 200, 300$ and $400C$ were similar, showing a general increase in wear rate with load and in each curve there was a region where the wear rate increased only slightly over a 1.5 to 4kg interval.

$T_E = 500C:$

Experiments at this temperature gave very low wear rates at low loads ($5.0 \times 10^{-8} \text{ mm}^3 \text{ mm}^{-1}$); the wear rate increased without any interruption as in the previous temperature.

$T_E = 600C:$

Initial experiments at this temperature showed that even for the lower loads the disc became too soft, resulting in very high wear of the disc surface whilst leaving the pin surface untouched. The disc debris was a very fine powder and was found to be mainly Fe_2O_3 .

The wear rate versus load graphs, where the wear rate is expressed in gm.cm^{-1} for the elevated temperature experiments are given in Figure 3.10. As in the previous room temperature experiments, the average pin wear rate reproduces the same characteristics as those

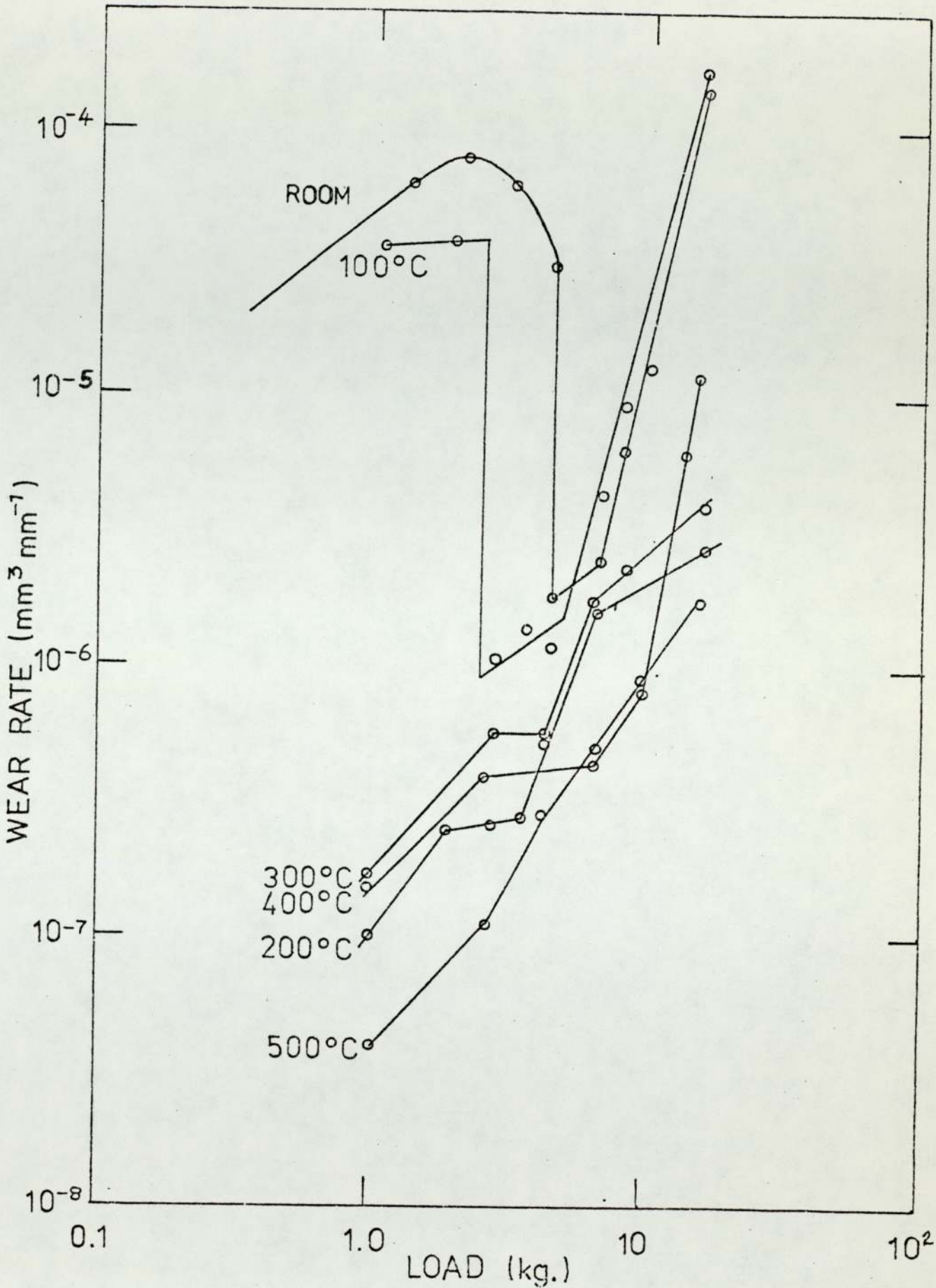


Figure 3.9. $\log w$ plotted against $\log W$ for various externally-induced disc temperatures.

exhibited by the equilibrium wear rate graphs. The only significant difference between the wear behaviour shown in Figure 3.9 and Figure 3.10 was in the position of the $T_E = 2000$ curve of loads up to around 4 kg relative to the 300 and 4000 curves.

3.6

Friction curves for elevated temperature runs

The friction curves for the elevated temperature runs are shown in Figure 3.11 and as expected the friction curve for 1000 was similar to that obtained at room C. The curves for 200, 300, 4000 and in particular at 5000 showed the same form as that obtained for the room temperature experiments of $V = 2.0$ and 4.0 m.s^{-1} where there was no definite transition taking place.

3.7

Scanning Electron Micrographs of Selected Pin and Disc Surfaces

This section presents a selection of Scanning Electron micrographs of worn pin and disc surfaces. Specimens were taken from each wear region of the 'room' temperature experiments and from the 'elevated' temperature runs. The micrographs illustrate various features typical to each region or set of experiments and also the relative scale of damage.

The micrographs shown in Figure 3.12 were taken from a disc surface which had undergone mild wear in the region below the T_1 transition ($W = 500 \text{ g}$; $V = 0.75 \text{ m.s}^{-1}$). The disc surface mostly covered with light brown Fe_2O_3 oxide. (a) shows an area which is typically found on mild wear surfaces, that is, a smooth area from which material has been removed revealing a relatively rough area below the surrounding surface. The thickness of the removed particle appears to be about $1 \mu\text{m}$. (b) is a build-up of material in layers of less than $1 \mu\text{m}$ thickness which could possibly indicate successive growth of thin oxide layers before removal as a particle or flake. The height of the feature in (b) is not clear from the micrograph

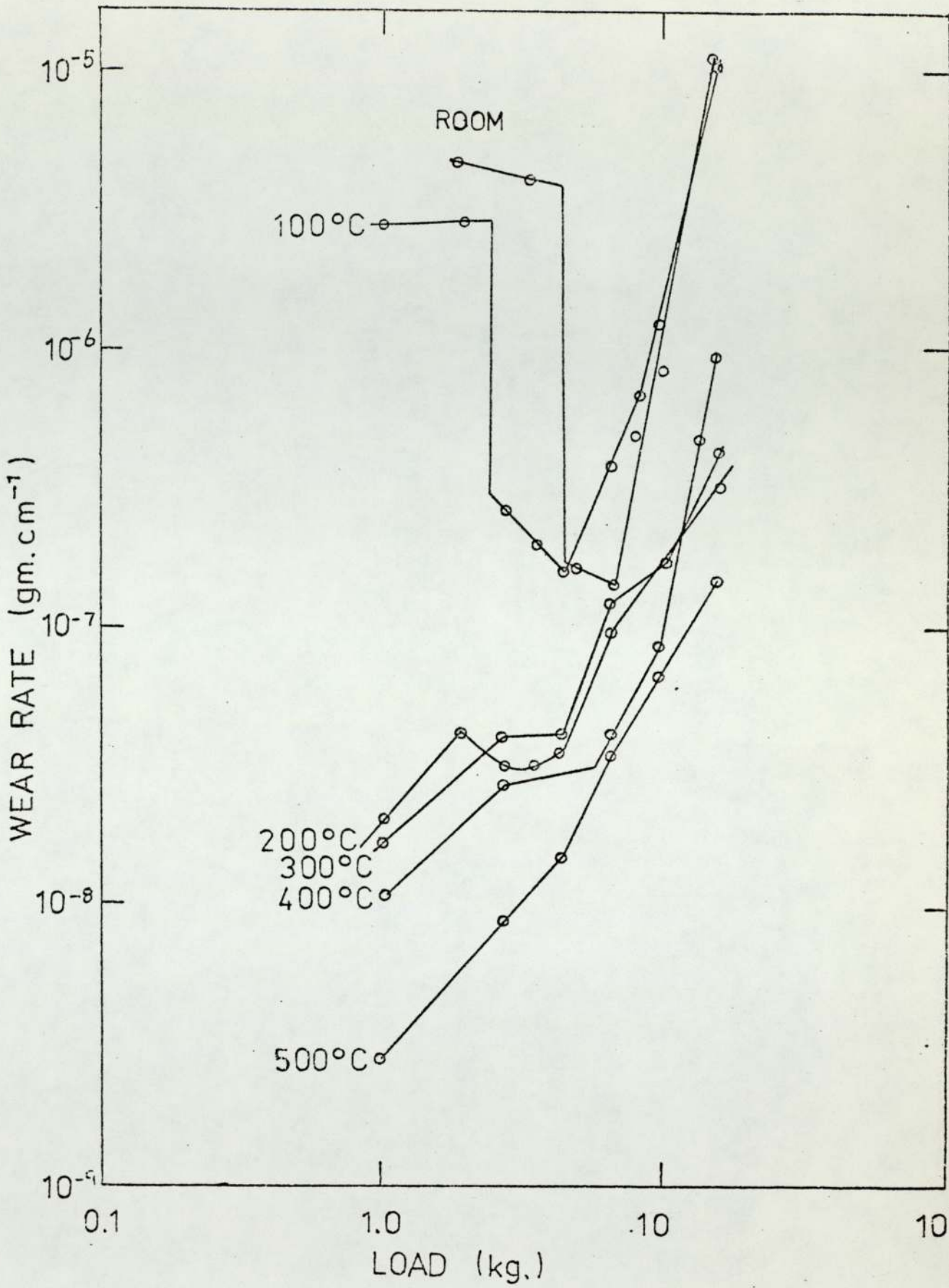


Figure 3.10. Log w (weight-loss method) plotted against log W for various externally-induced disc temperatures.

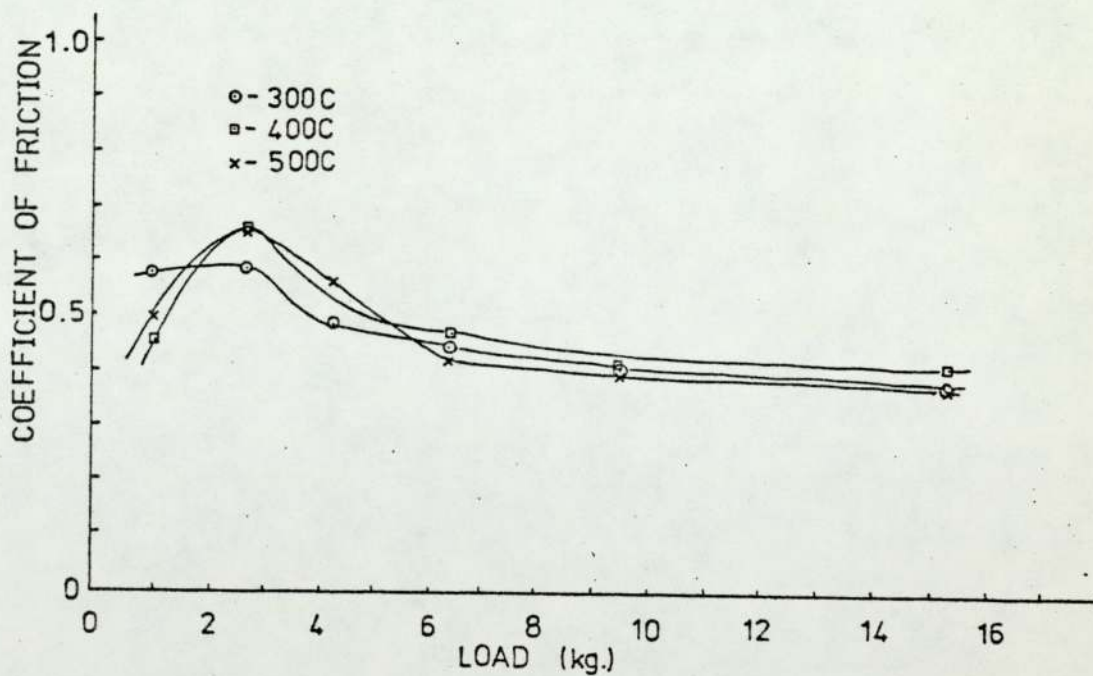
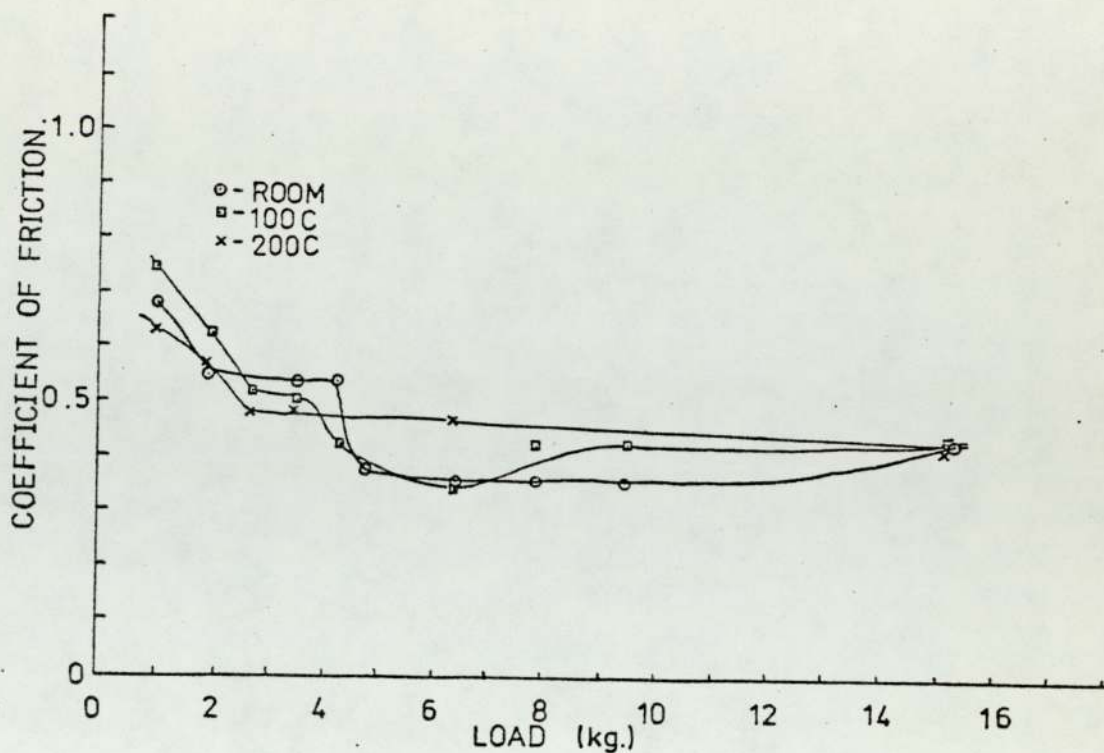


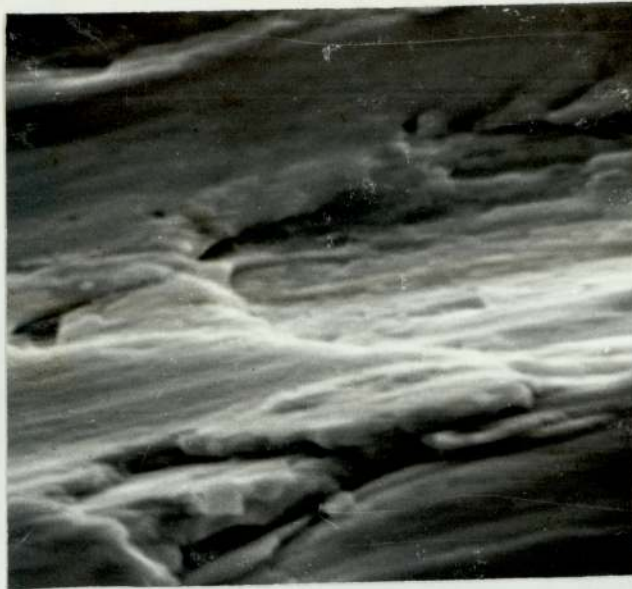
Figure 3.11. Friction coefficient versus load for various externally-induced disc temperatures.

since it may be the edge of one of the overlapping particles shown in (e).

Figure 3.13 (a) and (b) shows severe wear disc surfaces ($W = 3.25 \text{ kg}$; $V = 0.75 \text{ m.s}^{-1}$). In many respects these surfaces are not dissimilar to those of the previous mild wear surfaces; see Figure 3.13. (c) which was taken from the mild wear region shown in Figure 3.12. The major difference is in the scale of damage. It is possible that the mild wear of the pre- T_1 transition occurs at the highest regions of a rough surface produced by the long periods of run-in which occurred for these experiments. The gouges which can be seen on both areas are similar in size and it appears that the areas which would be likely to be detached as wear particles are much longer for the severe wear surfaces than the mild wear surfaces. The rough area shown in Figure 3.13(a) appears to show where a particle has been removed and its size corresponds to that of the wear particles found in the debris.

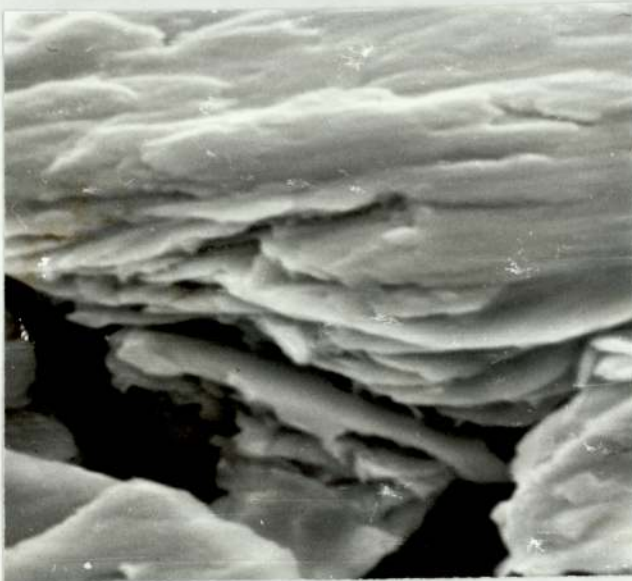
Areas from the mild wear region which occur at higher loads ($W = 1.9 \text{ kg}$; $V = 0.75 \text{ m.s}^{-1}$), in the T_2 to T_3 transition are shown in Figure 3.14. A good example of a plateau as observed by Quinn in previous mild wear studies (43) can be seen in (a). The surface of the plateau was smooth and contained cracks which ran at right angles to the direction of sliding. The height of the plateau is around $2 \mu\text{m}$. At the edges of the plateau there are small particles of oxide derived from the breakdown of larger wear particles. The oxide particles are hardened and act as abrasive particles, smoothing and polishing both wear surfaces. The proportion of the total wear which is due to this abrasive action is very difficult to estimate.

Figure 3.14(c) is very similar to that of Figure 3.12(b) showing a similar laminar nature, possibly due to oxide growth in



(a)

2 μm



(b)

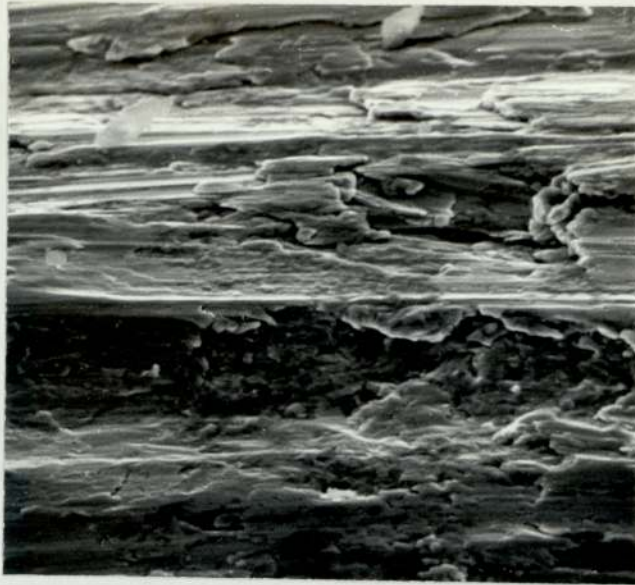
2 μm



(c)

10 μm

Figure 3.12. Scanning Electron micrographs of pre T_1 transition, mild wear disc surface. ($\bar{W} = 500 \text{ g}$; $v_1 = 0.75 \text{ m.s}^{-1}$).



(a)

10 μm



(b)

50 μm



(c)

50 μm

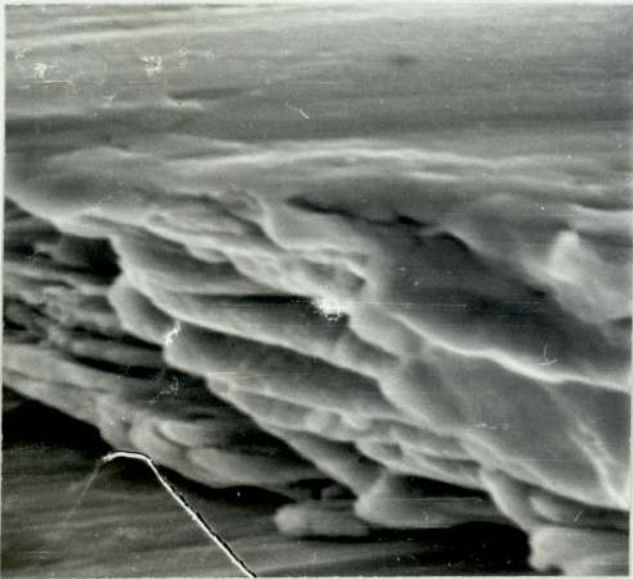
Figure 3.13. Scanning Electron micrographs of disc surfaces.
a) & b) Severe wear. ($W_1 = 3.25 \text{ kg}$; $V = 0.75 \text{ m.s}^{-1}$)
c) pre T_1 transition mild wear ($W = 500 \text{ g}$; $V = 0.75 \text{ m.s}^{-1}$)



(a)
10 μm



(b)
2 μm



(c)
2 μm



(d)
20 μm

Figure 3.14. Scanning Electron micrographs of disc surface undergoing $T_2 - T_3$ transition wear ($w = 7.9 \text{ kg}$; $v = 0.75 \text{ m.s}^{-1}$).

successive passes. Figure 3.14(d) shows a difference in general surface nature to that shown in (a) in that the surface is mainly smooth with damage occurring by removal of flakes from a sheet of oxide and not by removal of plateaux once a critical height has been reached.

Contrasting areas are also present in the T_3 region micrographs, Figure 3.15. (a) shows an area similar to Figure 3.13(b), the particle in both cases could be either near to detachment from the disc surface or could possibly be transferred material. Figure 3.15(b) shows a relatively smooth region which has been deeply gouged.

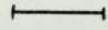
Specimens from the elevated temperature experiments which a bulk disc temperature of 500°C are shown in Figure 3.16. This temperature was selected because of its purely oxidative character. (a) shows a ridged sheet of oxide from which flakes of material have been removed revealing relatively rough areas, (b), (c) and (d) are progressively higher magnification of the edge of one of the rough regions. The oxide has a well defined thickness of around $2\ \mu\text{m}$ and does not show any evidence of laminar build up. There is considerable cracking of the surrounding oxide sheet due to a thermal fatigue mechanism or differential volume expansion of the oxide and metal subsurface. (c) shows how the very fine particles of oxide found in the debris are formed by crumbling of the oxide sheet.

The micrographs obtained from the pin surfaces which correspond to the disc surfaces shown previously did not provide the same variety of features, although the same surface character was displayed in each case. Figure 3.17 gives a selection of micrographs obtained from each region of the general wear pattern.



(a)

20 μm

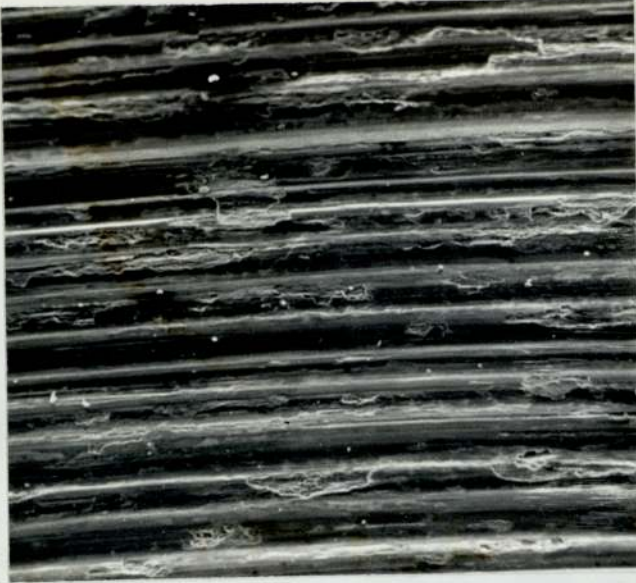


(b)

20 μm



Figure 3.15. Scanning Electron micrographs of disc surface undergoing T_3 transitional wear. ($w = 15.3 \text{ kg}$; $v = 1.0 \text{ m}\cdot\text{s}^{-1}$)



(a)
100 μm



(b)
20 μm

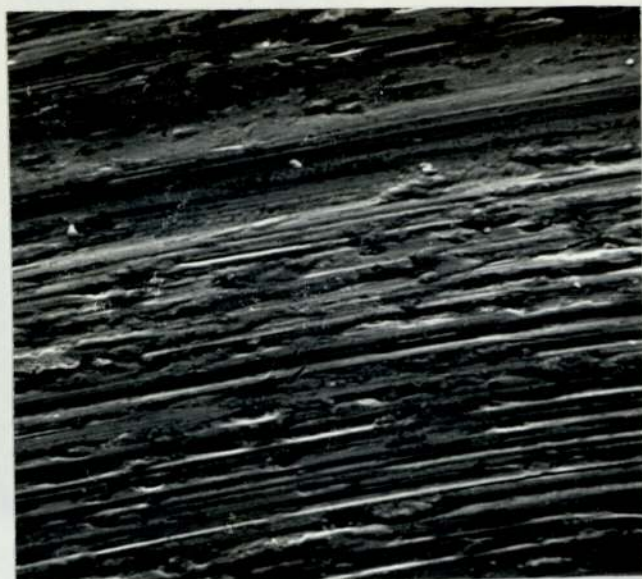


(c)
5 μm



(d)
2 μm

Figure 3.16. Scanning Electron micrographs of disc surface, from 500°C experiment. ($w = 1.0 \text{ kg}$; $v = 1.0 \text{ m.s}^{-1}$)



(a)

20 μm



(b)

20 μm



(c)

20 μm



(d)

50 μm

Figure 3.17. Scanning Electron micrographs of pin surfaces.
a) pre T_1 transition mild wear. b) severe wear.
c) T_2 - T_3 transitional wear. d) T_3 transitional wear.

3.8

Scanning Electron Micrographs of Debris

This technique was employed in order to determine both the shape and size of the debris from each type of wear. Although the sizes of the particles varied from one regime to another the same plate-like particles occurred in every sample.

The size of the particles from the T_2 - T_3 mild wear region (Figure 3.18 (a) and (b)) fall within a narrow range (50 to 30 μm) compared to that found for both the severe and post- T_3 wear. The bright metallic severe wear particles were mostly greater than 20 μm in length and gave the appearance of being covered with very much smaller particles of debris (see Figure 3.18 (c) and 3.19(a)), with diameters of a few micrometers or the thickness of the plates which make up the bulk of the debris, the larger particles were up to approximately 1mm. A similar variation in size was found for the particles from the post- T_3 region the largest particles found were smaller than those from the severe wear experiments at around 0.1mm, the smaller particles did not show the apparent adherence to the large particles as found previously. Figure 3.19 (c) shows a large particle from the post- T_3 region which exhibits a large amount of cracking along the apparent direction of sliding and perpendicular to it, which appears to generate the small particles.

3.9

Optical micrographs of sections of debris

A few samples of debris were selected and sectioned and then examined using an optical microscope, some examples of which are shown in the following section. This technique was used in order to determine the nature of the oxidation which took place in the wear above the T_3 transition. In this region it was thought that oxidation may have taken place at the surface of the large wear particles at the point of removal from the wearing surfaces. Some evidence of this can be seen in Figures 3.20(a) and (b) which show

large particles of metal with some indication that a thin oxide layer is present at the edges of the particle section. The particle in Figure 3.20(a) shows sign of deformation and oxidation apparently within the particle. Severe wear particles in section are shown in Figures 3.21(a) and (b) again show the wide range in particle sizes. Figure 3.21(a), light etching of the section showed the large degree of deformation occurring during severe wear.

Figure 3.21(c) shows typical debris from the experiments in which the heat flow technique was applied. It can be seen that a large proportion of the debris consists of unoxidised metal particles.

3.10

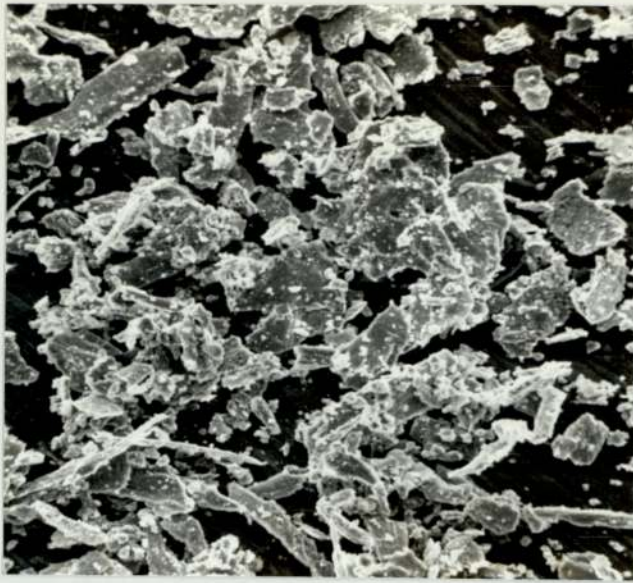
X-Ray Results

3.10.1.
Heat flow experiments ($V = 2 \text{ m.s}^{-1}$)

3.23 → Debris was examined from two experiments at 2 m.s^{-1} at different loads, 4.3 and 1.0 kg. The debris from the 4.3 kg experiment was also sectioned see Figure 3.21(c). It can be seen from the wear rate versus load graph for these experiments Figure 3.24 that two slopes can be drawn, - one through experiments 1,2 and possibly 3 and another through 3, 4, 5, 6 and 7 - the experiments which lie on the steeper slope were used in the heat flow considerations. The debris from the 1.0 kg experiment, which lies on the lower slope, was selected for comparison.

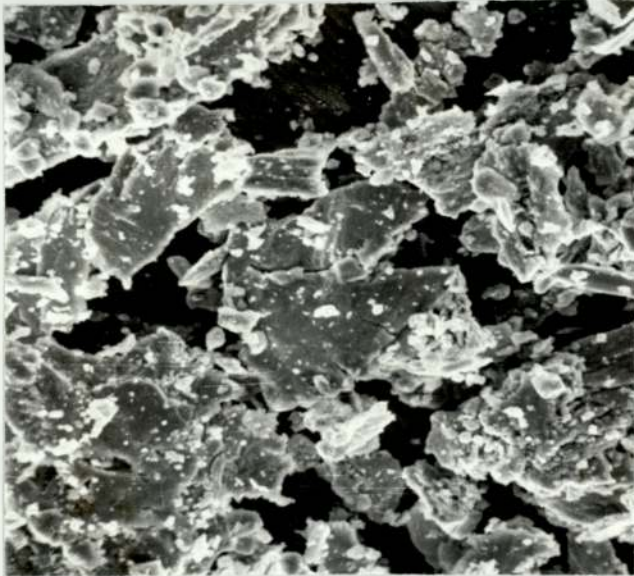
In each case the debris consisted of mainly black particles which were metallic in appearance together with a much finer powder. 4.3 kg - the film indicated that the black oxide was in fact FeO, there was no indication that there was any other oxide present. The major Fe lines were also visible.

1.0 kg - FeO lines were also present on this film but were very much weaker, the Fe lines were about the same intensity and again no other oxide lines were present.



(a)

20 μm



(b)

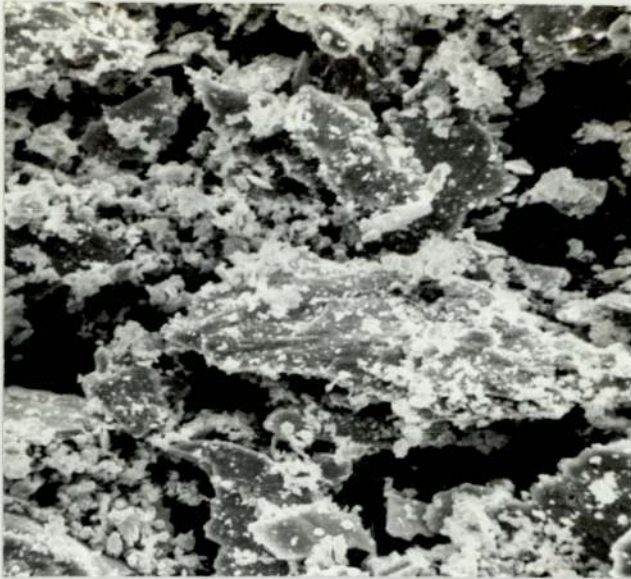
10 μm



(c)

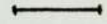
20 μm

Figure 3.18. Scanning Electron micrographs of Debris.



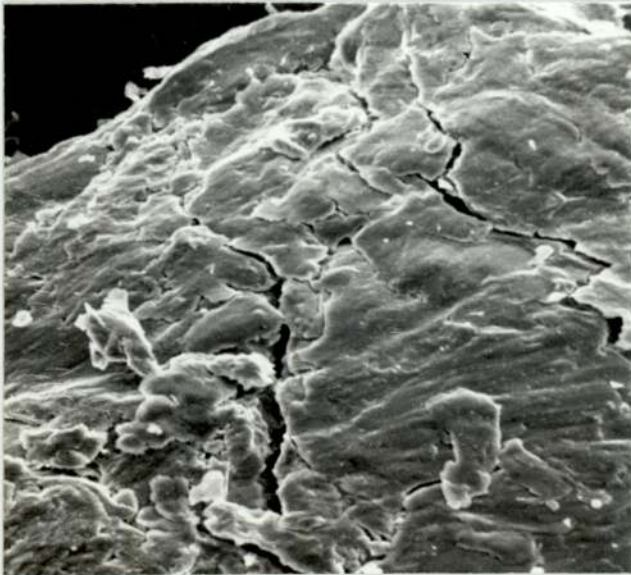
(a)

10 μm



(b)

100 μm



(c)

10 μm

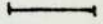
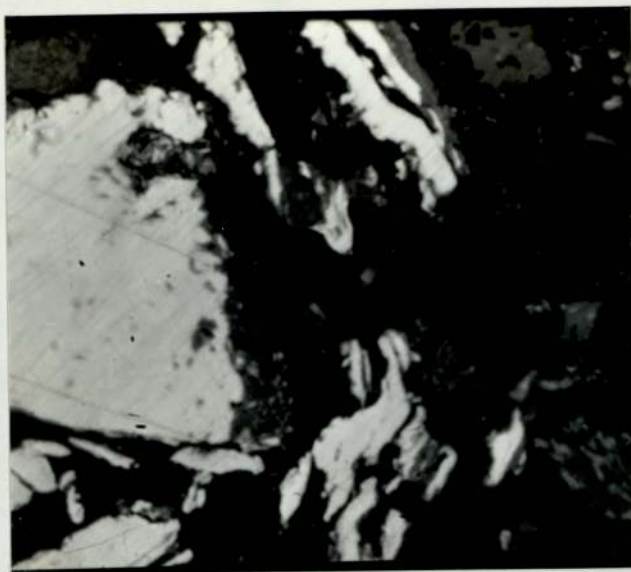
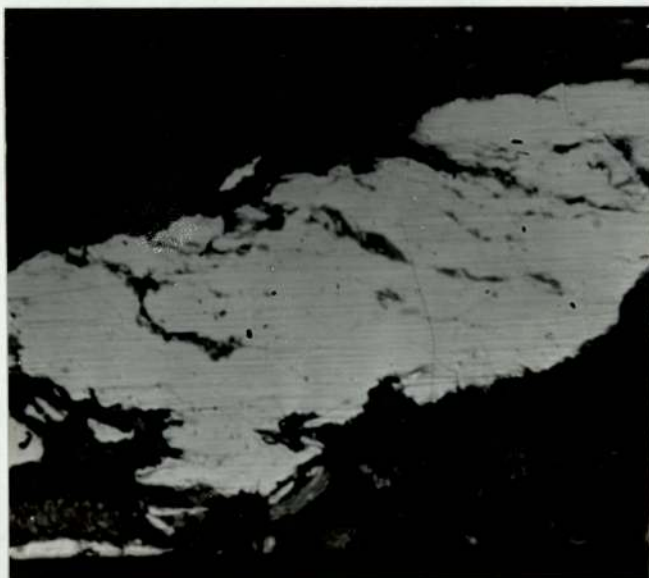


Figure 3.19 Scanning Electron micrographs of Debris.



(a)

5 μm

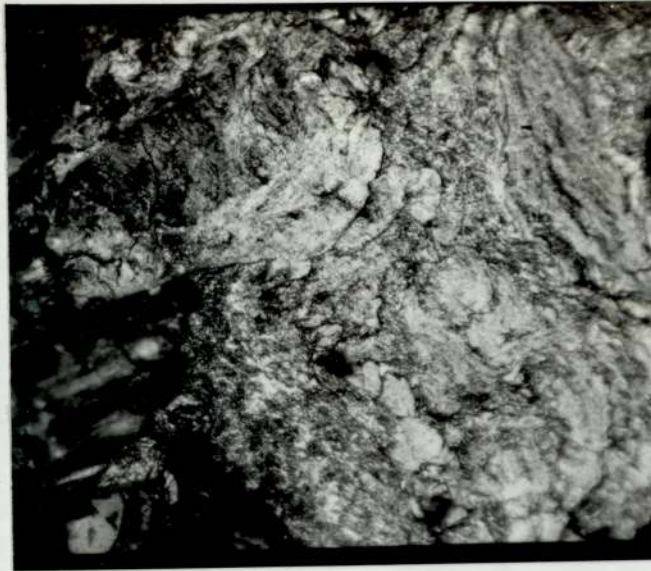


(b)

10 μm



Figure 3.20. Optical micrographs of sections of debris.



(a)

50 μm



(b)

0.5 mm



(c)

10 μm

Figure 3.21. Optical micrographs of sections of debris.

X-Ray Results

3.10.2, General Wear Pattern

Mild wear below T_1

The debris from this region was very fine light brown powder of Fe_2O_3 oxide.

Severe wear, T_1-T_2

As expected the bright metallic particles did not contain any detectable oxide and only the Fe lines were present.

Mild wear, T_2-T_3

Two specimens from this range were selected from the experiments with a sliding speed of 1 m.s^{-1} , and with no external heating.

6.4 kg - this experiment gave a wear rate in the middle of this region and instead of the expected lines corresponding to Fe_3O_4 or a mixture of Fe_3O_4 and Fe_2O_3 oxides, the debris which consisted of black particles and powder produced Fe and faint lines of FeO.

4.37 kg - this load was near the T_2 transition and the debris appeared to be the same as that from the 6.4 kg experiment.

Wear above T_3

The debris from this region was similar to that collected from the T_2-T_3 region but appeared to be more metallic especially at the higher loads. For the experiments with sliding speed of 1 m.s^{-1} the debris gave Fe lines with faint lines of FeO; at the highest load employed (15.3 kg) the FeO lines were barely visible.

X-Ray Results

Elevated Temperature experiments

100C -- Debris from all the experiments at this disc temperature which exhibited some form of mild wear were analysed. The oxide

produced from the experiments at loads immediately above the T_2 transition load was a mixture of Fe_3O_4 and Fe_2O_3 . As the loads increased to the T_3 transition load the oxide gradually changed into predominately FeO . At the highest load used (15.3kg) where the wear rate was higher than the severe wear at lower loads the debris consisted of large metallic particles with some very fine black oxide powder. Only Fe lines were detectable.

200, 300 and 400C -- Samples of debris from the 1 kg experiments were analysed to examine the oxide from the very low wear rates which were found when the severe region was suppressed by the increase in disc bulk temperature. The oxide produced at all disc temperatures was very similar to that found in the T_2 - T_3 transition region for the 100C experiments with possibly a larger proportion of Fe_2O_3 .

500 and 600C -- As the bulk disc temperature was increased the intensity of the Fe lines decreased and at these temperatures were not detectable. The oxide produced at 500C was mostly Fe_2O_3 with some Fe_3O_4 . The experiments at 600C where the disc wear was very much greater than the pin wear produced large amounts of a dark red powder of Fe_2O_3 .

3.11

Heat Flow experiment results

The results of the Heat Flow analysis performed on the pin for the experiments at a track speed of 2.0 m.s^{-1} are given in Table 1. Details of the theory are given in Quinn (40) and in the appendix (3). Using this method two parameters are calculated (a) T_s , the temperature of the surface of the pin outside of the real area of contact. It is the temperature resulting from the instantaneous flashes of energy conversion at the real areas of contact (due to plastic flow or some microscopic process) averaged over the whole surface and remains constant for an equilibrium process.

(b) δ_{expt} is the proportion of heat generated at the real areas of contact, where

$$\delta_{\text{expt}} = \frac{H_1}{H_{\text{total}}}$$

and H_1 is the heat flow per second at the interface between the pin and disc, H_{total} is the product of the frictional force at the pin (F), and the linear speed of the pin (U).

TABLE 1 - HEAT FLOW PARAMETERS

EXPT. NO.	LOAD (W) (N)	FRICTION FORCE (F) (N)	THERMOCOUPLES			HEAT FLOW			H_{total}	δ_{expt} %	T_s 'C
			T_a	T_b	T_c	H_1	H_2	H_3			
1	4.90	2.48	42	37	31	0.47	0.37	0.35	4.96	9.65	45
2	18.93	9.41	91	62	52	2.34	2.01	1.93	18.82	12.47	106
3	26.48	10.33	105	81	63	2.12	1.78	1.69	20.66	10.26	118
4	34.33	13.05	134	80	59	4.97	3.79	2.63	26.10	19.06	186
5	42.18	16.45	192	102	71	6.99	6.37	6.11	32.90	21.26	223
6	49.05	19.62	144	95	71	4.02	3.34	3.19	39.24	10.25	173
7	62.78	25.74	194	120	83	5.23	5.11	4.87	51.48	10.16	199

Figure 3.22(a) is a graph of the derived value of T_s versus the applied load (W), it shows a gradual increase in temperature at the surface with load, which is interrupted by a possible transition at around 40N. Figure 3.22 (b), also shows a similar transition in the plot of the measured value T_a at the same load. The form of these curves and the significance of the transition will be discussed at a later stage.

The transition shown in the graphs of T_a and T_s is also present in the plot of the equilibrium mild wear rate (w_{expt}) against load

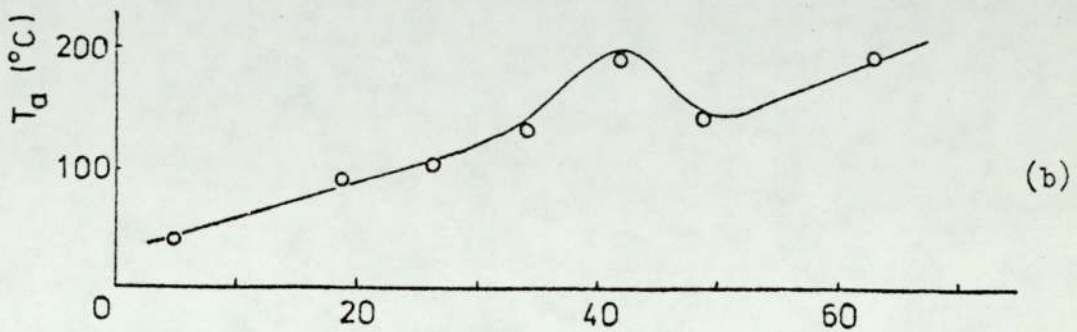
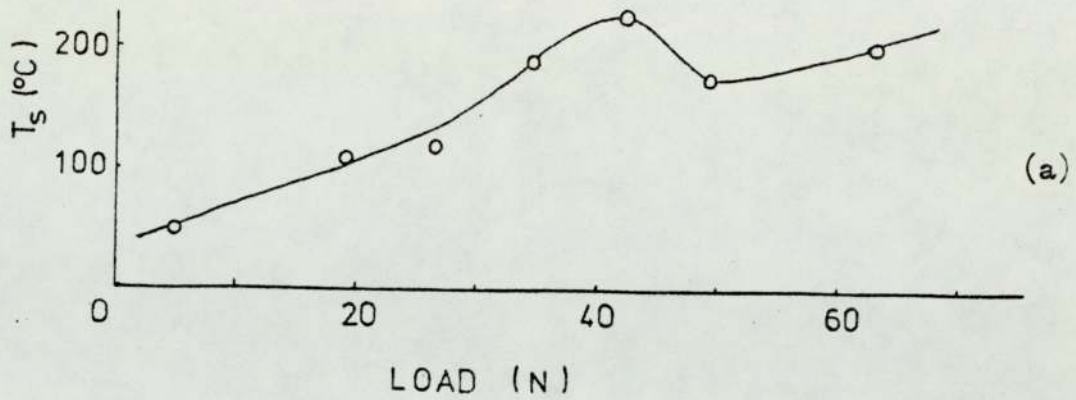


Figure 3.22(a) Graph of thermocouple reading (T_a) versus applied load
(b) Graph of surface temperature (T_s) versus applied load

Figure 3.23. The reproducibility of these wear rates was very good, experiments 3, 6 and 7 had previously been run without the heat flow measurements and the wear rates obtained were identical. These wear rates were also plotted on Figure 3(2); the transition was not as noticeable on the log-log plot.

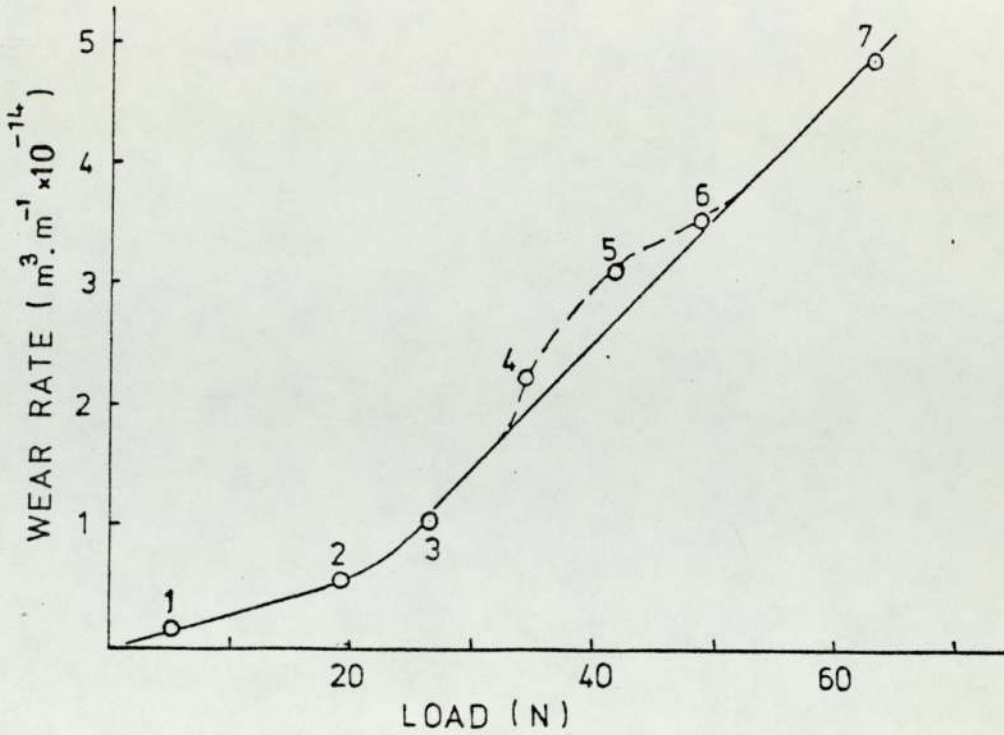


Figure 3.23. Graph of pin wear rate (w_{expt}) versus applied load

The wear rates for experiments 1 and 2 appear to lie on a different slope to the other experiments; this minor transition is also evident on the previous graphs of wear rate for both 2.0 and 4.0 m.s⁻¹ shown in Figure 3(2).

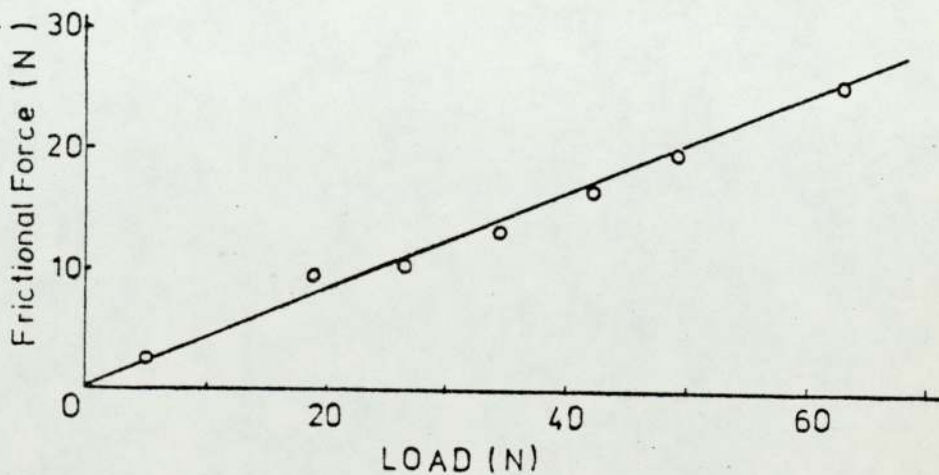


Figure 3.24. Graph of frictional force(F) at the pin versus applied load

Figure 3.24 shows that the frictional force at the pin (F) increases with applied load and does not show any transitions.

CHAPTER 4

DISCUSSION OF GENERAL WEAR PATTERN RESULTS

4.1. Introduction

To investigate the effect of elevated temperatures, i.e. externally induced ambient disc temperatures, on the general wear pattern of EN8 steel, it was necessary in the first case to establish the values of load and speed which would produce all or part of the pattern, within the loads available.

A linear track speed of 1.0 m.sec.^{-1} was selected with the aid of the results of Welsh (12) for various plain steels with approximately the same hardness. It was not possible to compare the results directly due to the difference between the machines and their specimen geometry. There is, however, some agreement in the shape and positions of the patterns for the present experiments.

Each transition is discussed in the first place with respect to the 'room' temperature experiments in which the sliding speed was varied.

The 'elevated temperature' wear experiments are discussed in terms of the effect of externally induced ambient specimen temperatures upon the "wear rate versus load" graphs produced from the 'room' temperature experiments at 1.0 m.s^{-1} . The results of physical analysis of sliding specimens and debris and friction measurements are used to support the discussions.

4.2.

The T_1 Transition

The present work only includes the observation of this transition at one speed (0.75 m.s^{-1}). The original intention was to chart the movement of all the transitions with speed and with temperature. The T_1 transition lies outside the range of conditions for these

experiments. A decrease in track speed would have increased the T_1 and T_2 transition loads, but T_1 is known to change less rapidly with speed than T_2 so further decrease of track speed may have displaced T_2 to much greater loads. The T_1 transition could have best been brought to higher loads, without losing T_2 by increasing the initial bulk hardness.

Welsh found that the behaviour at the light loads at which the transition occurred was not always reproducible, this was also found in the present work. Some experimental difficulties were experienced at the lowest loads, as mentioned previously and for similar conditions of load and speed the wear regime encountered could be mild or severe. When mild wear occurred the wear rates were very low (around $10^{-9} \text{ mm}^3 \text{ mm}^{-1}$) with low friction and the production of light brown Fe_2O_3 . The microhardness of the worn surfaces reached hardnesses corresponding to the first critical hardness found by Welsh. In the author's view oxidation is only possible at the areas of contact immediately following asperity separation. The total heat generated at the interface was very small and could not develop a measurable thermal gradient along the specimen pin length.

4.3.

The T_2 Transition

This was the most readily observed transition, occurring at fairly well defined loads. The effect of sliding speed on the transition load was found to be as expected by inspection of the curves obtained by Welsh. The transition load decreased with increasing sliding speed until at around 2.0 m.s^{-1} it was not observed. The similarity between the curves obtained by Welsh, at the same speeds and carbon content, and the present work was good and several features were reproduced. The slope of the logarithmic plot of the wear rates in the mild wear region preceding the T_1 transition and

the severe wear before the T_2 transition is normally close to unity (i.e. the wear rate is proportional to load). Welsh found that for high carbon steels the slope of the wear immediately following the T_2 transition is also near unity, the T_3 transition occurs at a higher load and the overall slope of the ensuing wear is much greater than unity. For low carbon steels the T_2 and T_3 transitions merge together and the result is a region immediately following the T_2 transition with a slope greater than unity. The latter was found to be true for the EN8 steel used in the present investigation; this point is very relevant to the discussion of the application of heat flow methods to the division of heat at sliding interface undergoing mild wear.

The seemingly odd behaviour of the wear curve at around 7 Kg for the experiments at 1.25 m.s^{-1} (Figure 3.1) was probably the same as that shown by Welsh for a similar steel and conditions of load and speed (Page 37, Figure (5(a), ref. 12). Although an explanation is not forwarded for this minor event it serves to show that very similar conditions were used in both sets of experiments and that some comparisons can safely be drawn for other effects.

Welsh found that the T_2 transitions coincided with a critical hardness being reached at the surface. The actual value for his experiments was found by etching and tempering experiments, and not from direct measurement of the microhardness of worn surfaces. The hardness curves drawn from the microhardness results gave conflicting behaviour at the T_2 transition, to provide a consistent explanation of the transition he used a different approach, investigating the surface hardness as a function of sliding distance. Phase hardening to high values does occur in the early stages of rubbing where the change from severe to mild wear takes place. Once the transition has taken place, the hardness does not necessarily continue at a

high level and will only do so if the T_3 load is exceeded. The results of the microhardness tests on the worn surfaces of the pin and discs in the present work only serve to show that that hardening has in fact taken place during rubbing. The graphs show that the hardness of the pin surface increased dramatically with load for the low speed experiments, compared with the more gradual increase of the surface hardness with increasing load for the 2.0 m.s^{-1} experiments. Similar hardness levels, to those found by Welsh, were reached for the T_1 and T_2 transitions which are associated with the 1st and 2nd critical hardnesses.

4.4.

The T_3 Transition

This transition is usually taken to occur approximately at the minimum load required to cause permanent surface hardening. In the present work a pin on disc configuration was used and Welsh (12) a pin on ring; in each case there is thermal asymmetry and it is thought that features of this transition are associated with this asymmetry. Similar divergencies between the wear rate of the pin and disc were observed in the region following the T_2 transition but were not as apparent as those found by Welsh. It would seem from the absence of a significant mild wear region, with a slope of near unity, between the T_2 and the T_3 transition, that, in the present work the carbon content of the steel is such that the T_3 transition has merged with the T_2 transition to some extent.

The divergence of the wear rates of the rubbing members could be due to a number of factors such as an increase in the scale of transfer of material from the now much softer pin, or, to impregnated particles of oxide acting in an abrasive fashion. Of more interest, perhaps, is the question of how the surfaces wear in the region immediately following the T_3 transition. Although the wear appears

at first to be purely oxidative, the magnitude of the wear rates and the rate at which they increase with load would seem to indicate that the wearing mechanism involves more than just the production and removal of oxide. The analysis of debris samples from this region have confirmed that the wear mechanism involves severe wear with the production of metal particles which have been oxidised to some extent after removal. It is possible that the oxidation which occurs at the surfaces reduces friction levels which results in smaller damage to the surfaces but still larger than the more oxidative wear mechanism which occurs between the T_2 and T_3 transitions.

4.5.

Surface Temperatures and the General Wear Pattern

The present work has not attempted to measure surface temperatures throughout the wear pattern since the method of estimating such temperatures, favoured and used in the detailed examination of mild wear which follows, is not suitable for severe wear rates. Previous examinations by Lancaster (11) and Welsh (12) do not provide any real explanation of transitional behaviour in terms of surface temperature estimates and indeed do not agree upon whether the influential temperature is the mean surface temperature of the flash temperature.

Indications of surface temperatures have been taken from observations of physical changes in the wearing surfaces and from the type of oxide present in the wear debris. Most recently Molgaard (64) has taken the first detection of the presence of FeO oxide to indicate that a surface temperature of 570°C exists. This method is complicated by the question of which temperature this actually represents and also by the possible difference between oxidation taking place under rubbing and static conditions. An indication of the ambient temperatures can possibly be drawn from the elevated

temperature wear experiments which are discussed later.

4.6.

Friction measurements

Friction measurements were made for all experiments and reveal changes in friction levels throughout the wear pattern which correspond to changes in wear character. This aspect of wear has not been given any importance in previous discussions of the general wear pattern. In the present work the measurement of friction has been used to confirm changes in wear character which had already been indicated by other measurements.

4.7.

The elevated ambient temperature wear experiments

The aim of this section of research has only been partially fulfilled, since only one speed was used for the elevated temperature. Nevertheless, the trends in the wear behaviour of mild steel can be seen. It is probable that trends are all that one can hope to perceive from such research, due to the prohibitive length of time required for a graph such as Figure 3.9, where every point represents the slope of a "wear volume versus distance slid" graph carried out over 3 or 4 hours running.

The first point emerging from this research is the apparent "disappearance" of the T_2 transition with increasing temperature of the disc above $T_E = 100^\circ\text{C}$. It is interesting to compare this result with the speed varying experiments where a similar "disappearance" of the T_2 transition occurred at the relatively low sliding speeds above 1.25 m.s^{-1} . It is tempting to suggest that similar thermal conditions exist in both sets of experiments and that more concentrated research in this particular topic would produce estimates of the surface temperatures responsible for the T_2 transition and the ensuing mild wear. The exact thermal conditions existing in the elevated ambient temperature experiments must be considered carefully,

however. The method of producing elevated ambient temperatures used in this research (external heating of the disc alone) enhances the thermal asymmetry of the already geometrical asymmetrical test piece configuration. It has already been noted from the behaviour of the $T_E = 100^\circ\text{C}$ curve at high loads that the combination of induced and frictional heating complicates the interpretation of the wear curves obtained. It would perhaps be worthwhile to consider the use of more symmetrical physical and thermal configuration for experiments intended for a basic study of wear processes.

The "wear rate versus load" curves for $T_E = 200, 300$ and 400°C exhibit a well defined kink in the otherwise steady increase in wear rate with increasing load. It is possible that at loads of around 1 kg the induced temperature was sufficient to tip the delicate balance between severe and mild wear in favour of mild wear. At higher loads the induced temperature is not adequate to completely overcome the frictional and physical factors such as surface hardening responsible for the T_2 and T_3 transitional wear character. The ambient disc temperature required to overcome these factors appears to be around 500°C .

The 500°C curve lies significantly below the 200, 300 and 400°C curves particularly at the low loads and from X ray diffraction it was found that the debris at 500°C contained a much higher proportion of Fe_2O_3 oxide. The scanning electron micrographs also show the highly oxidative character of the worn surfaces.

CHAPTER 5

DISCUSSION OF THE HEAT FLOW EXPERIMENTS AND OXIDATIONAL WEAR THEORIES

5.1. Welsh (12) and Lancaster (24, 11) have provided an understanding of the general wear pattern in terms of surface hardening and simple wear mechanisms. It is generally accepted that it is difficult to cover the entire range of wear in as much detail as one would like

in one report or series of experiments. The number and complexity of the parameters involved normally limit the researcher to a particular section of the pattern. An attempt must then be made to fit the conclusions into the general wear behaviour. In this way the present work attempts to develop existing theories of wear relevant to the mild wear regime. The most developed ideas on oxidative wear are described in a recent paper by Quinn (40), in which he has expanded his ideas on the role of surface temperatures, the division of heat and their relation to a simple surface model. The results obtained indicated interesting trends in the values of the number of contacting asperities, N , the critical oxide film thickness, ξ , flash and skin temperatures. Using similar experimental techniques and treatment of the results, one can investigate the "post- T_2 " transition region in the light of the general wear pattern and also provide further data for Quinn's approach to this difficult area. The analysis of the results obtained in the present work did not provide such a good correlation between experiment and theory and it was not possible to compare the behaviour of the various parameters over a similar wear pattern. A number of modifications were made to the parameters used, and to the surface model in an attempt to find a pattern to the results. At this stage it would be suitable to give a brief description of Quinn's method.

5.2.

A brief description of Quinn's method

An analytical expression was deduced for the division of heat (δ theory) at the pin-disc interface, in terms of a surface model consisting of N asperities of approximately the same area of contact upon which an oxide film thickness is situated.

Following Archards approach to the estimation of flash temperatures and using the simple surface model an expression for

δ_{theory} can be found:-

$$\delta_{\text{theory}} = \frac{T_d}{(T_d + T_p)}$$

The proportion of heat generated at the real areas of contact (δ_{expt}) is given by:-

$$\delta_{\text{expt}} = \frac{H_1}{H_{\text{total}}}$$

where H_1 is the heat flow down the pin at the Tip as shown in Figure 2.3 and is determined from the heat flow calculations described earlier.

The first stage of a computer program produced values of N and ξ which provide good correlation between δ_{theory} and δ_{expt} . The second stage was based on the assumption that $w_{\text{theory}} = w_{\text{expt}}$ the expression used for the theoretical wear rate was taken from Quinn's Oxidational Wear Theory:-

$$w_{\text{theory}} = \frac{W d A_p \exp(-Q/R T_0)}{U P_m f^2 P_o^2 \xi^2}$$

where T_0 (in deg K) is the temperature at which oxidation occurs during wear and is assumed to be equal to T_c , the contact temperature, and $d = 2(W / .N.P_m)^{1/2}$.

Using this assumption and the values of T_0 associated with each N and stepping through a range of values for ξ , various values of Q were found. Only those combinations of N, ξ , and T_0 which gave $Q = 96 \text{ kJ.mole}^{-1}$ were selected. A summary of the resulting trends produced from such combinations are given in the following section.

5.3. Quinn's Results

Load 5.9 -29.4 N : Speed 5.11 m.s⁻¹

Quinn found that at the speed and loads used, the values of ξ ($= 2.3 \pm 1.3$) and T_0 ($= 239 \pm 33$) were consistent with previous work. N , however had a higher range of values than expected (400-2000) but were consistent if it was assumed that, at any instant, all the N asperities were making contact on only 1 or so plateaus of contact.

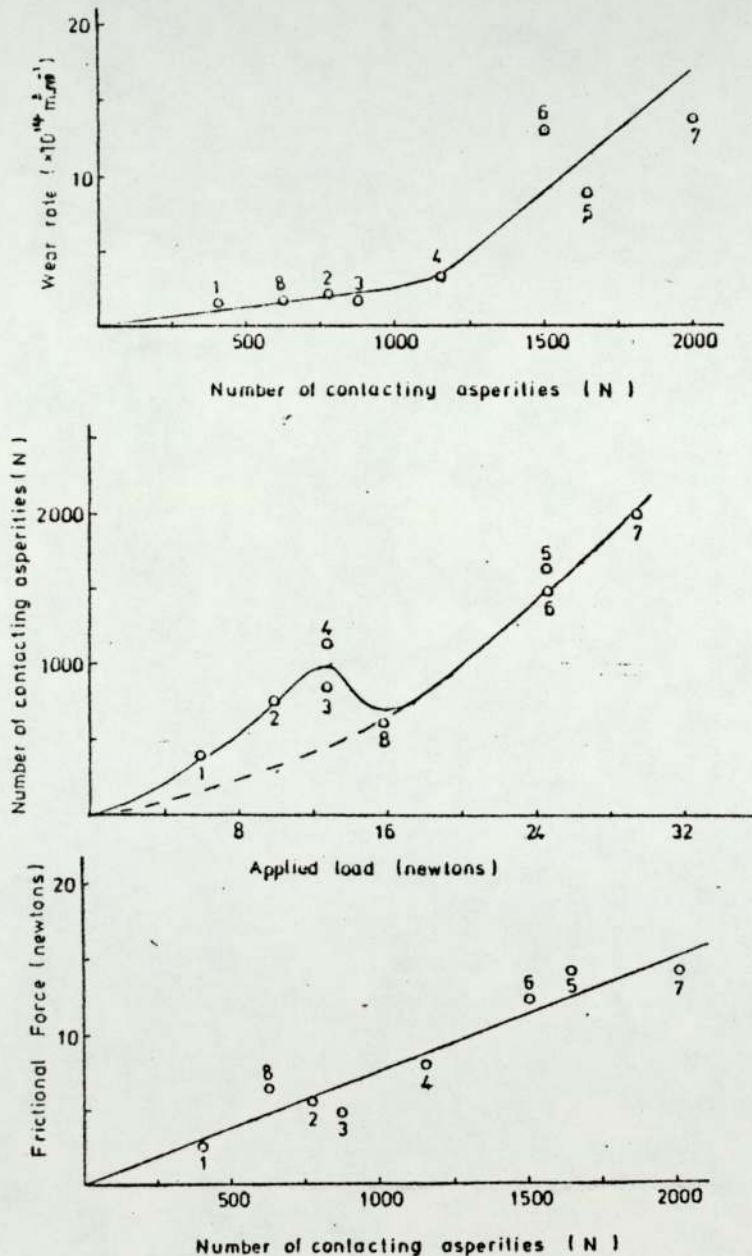


Figure 4.1 Graphical results from Quinn(40)

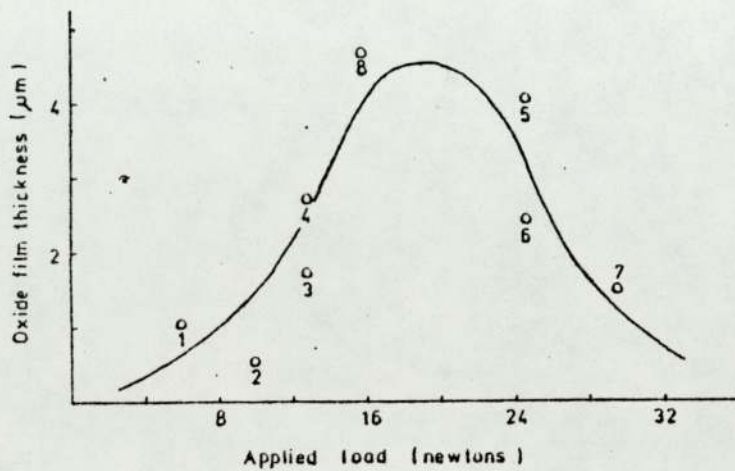
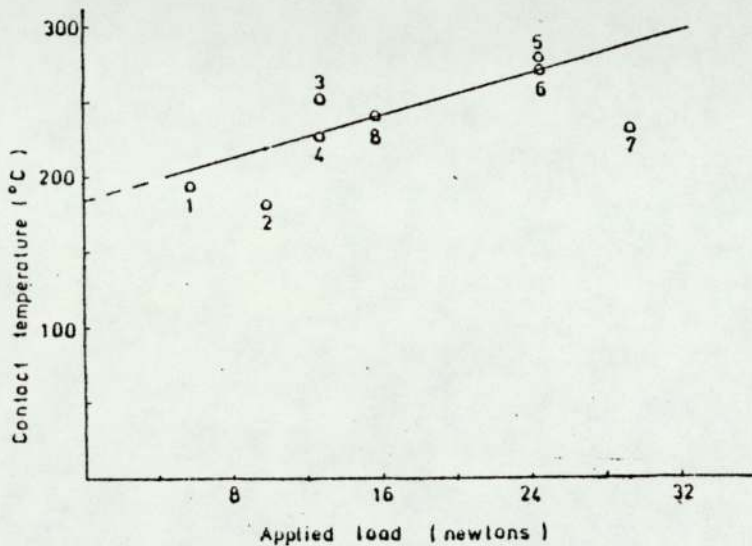
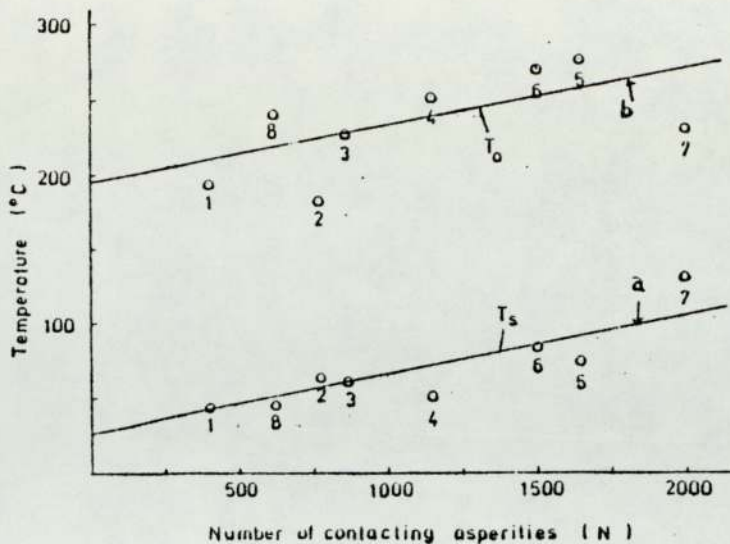


Figure 4.2 Graphical results from Quinn(40)

5.4.

The application of Quinn's method to the present work

A computer program was written to perform the same operations as that used by Quinn. Although the actual programs were in some respects different, Quinn's results could be reproduced accurately. An interactive-type computer was used to make the search process more flexible and efficient. A flow diagram is given in appendix 1.

No recognisable pattern could be found in the results, at least not to the same degree that had been found by Quinn. It is difficult to present the results obtained in a concise fashion, since if the value of Q was taken to be $96\text{kJ}\cdot\text{mole}^{-1}$, not all of the experiments provided corresponding values of N , T_0 and ξ . If however, the results were selected on the basis that ξ had a constant value of $1\mu\text{m}$, some form could be found and the results examined. There appeared to be two sets within the experiments, 1, 2, 3 and 4, 5, 6, 7, these sets lie on different slopes of the wear rate against load graph, Figure 3.23. When various refinements were made to the values of parameters and to expressions in the calculations, the effect on the correlations were disturbing, since small changes in somewhat arbitrary parameters resulted in large differences in the values of Q and N . Where Q had previously been the basis upon which the values of all the other parameters were selected.

It would be suitable at this stage to discuss the technique in detail and consider the relevance of the values of N , T_0 , and Q which can be obtained.

5.5.

The theoretical wear rate

Quinn uses the expression for the wear rate produced by his Oxidational Wear theory (27), the equation relates to a particular mechanism of wear involving the continuous formation and removal, by a micro-fatigue process, of an oxide film. There are a limited number

of wear theories which attempt to describe oxidative wear, Uhlig (65) Yoshimoto and Tsukizoe (54), Tenwick and Earles (29) and Tao (58). Of these only Uhlig suggests a mixed mechanism, in this case for fretting corrosion. It is convenient to assume that the wear is due to a single mechanism which is not generally the case.

In oxidative wear theories a general assumption made, is that all the material which is transformed by attrition to free debris has previously been oxidised. Once in an equilibrium wear regime and at a steady state, the rate of oxidation will equal the attrition rate. This balance is upset if a significant proportion of material does not undergo oxidation and is removed by a second mechanism. This becomes important when the theoretical and experimental wear rates are compared, as in the second stage of the computer program. From visual examination of the debris from the relevant wear experiments it was noticed that there was a large proportion of wear particles which were much larger in size, when the particles were examined using physical methods of analysis it was observed that some particles were metal which had only been oxidised superficially, if at all. In the present work, the wear taking place at loads above the T_2 transition and below the T_3 , although conforming to mild wear characteristics does not appear to be pure oxidational wear. The effect of this is to make the values of Q produced from the substitution of w_{theory} for w_{expt} incorrect.

It would appear to be necessary to estimate the ratio of 'mechanical' wear to oxidative wear in this wear regime. If the ratio is high then the controlling process in wear will not be the oxidation process. A rough estimate of the ratio might be obtained by determining the ratio of oxide to metal in the debris (by weighing and reduction).

5.6.

The effect of changing various parameters on the values of N and Q

5.6.1.

Physical properties

The values of the various physical properties used for evaluating δ_{expt} and δ_{theory} are given in Appendix 2. The values of these parameters are dependent upon the materials and temperatures which are considered suitable. That is, they are dependent upon the mechanism of wear which is envisaged. Considering the material aspect, there are two possibilities, first that the physical properties of the bulk material are applicable, second, the surface properties of the rubbing members which are known to have undergone physical changes during rubbing. Whether the relevant material is the bulk steel, worn or phase hardened steel or oxide, their physical properties will depend upon temperature. In the present work it was decided for simplicity to use the known bulk properties of the steel for the temperature range 20-100°C (from ref. 68 and Appendix 2), this view was also adopted by Quinn. No attempt has been made to determine the effect of using different physical properties with the exception of the flow pressure, P_m .

5.6.2.

The flow pressure, P_m

The flow pressure, of a bulk specimen varies with temperature, decreasing slowly with increasing temperature up to around 400°C and then falling rapidly to uncertain values above 600°C.

In the present work, the measured micro-hardness of the burnished patches on the pin and disc showed, as expected, that surface hardening had taken place during wear. The average hardness for all the experiments was within the range of the second critical hardness noted by Welsh (12), i.e. between 550-780 V.p.n. The relationship between hardness and flow pressure is not direct and is dependent on the material itself. The T_2 transition takes place

when the surface has undergone phase hardening to form a pseudo-martensitic or white etching layer. The direct effect of an unsuitable P_m will be in the size and number of the areas of contact. This was investigated by varying P_m from 1.3 to $4.3 \times 10^9 \text{ N.m}^{-2}$ which corresponds to hardnesses of 260 to 1300 V.p.n. In the middle of this range at 600 to 800 V.p.n. (3.0 to $3.3 \times 10^9 \text{ Nm}^{-2}$) the effect would appear to be small. If however the P_m value corresponding to the bulk hardness at room temperature were used a drastic change in the real area of contact ($= W/P_m$) would occur.

Table II

The effect of various values of P_m on N , T_0 and Q .

Heat flow experiment 7

For $\xi = 1 \mu\text{m}$; $W = 63\text{N}$; $V = 2.0 \text{ m.s}^{-1}$

P_m ($\times 10^9 \text{ Nm}^{-2}$)	N	Q (kJ mole^{-1})	T_0 ($^{\circ}\text{C}$)
1.3	626	107	257
2.3	349	114	303
3.3	242	121	350
4.3	185	129	396

5.7.

The division of heat

The theoretical deduction of the division of heat at the interface is based on work by Molgaard et al (38, 39) and was then applied to a specially designed pin-and-disc wear machine by Quinn.

An estimation of the contact temperature (T_0) is made from the estimate of δ theory:-

$$T_C = (\delta \text{ theory } T_p) + T_S$$

since oxidation temperature is taken to be equal to the contact temperature (or very nearly so) the value of δ_{theory} is very important. At this stage if the estimate of δ_{theory} is assumed to be reliable we can now consider its importance in the Quinn method. The first stage of the computer program involves the comparison of δ_{theory} with δ_{expt} , the question which now arises, is how reliable is the value of δ_{expt} ? Since a given δ_{expt} determines δ_{theory} and the combination of N and ξ associated with that particular δ_{theory} , it is very important that δ_{expt} is accurate. The effect of different values of δ_{expt} on the values of N, Q and T_C is shown in Table III. The experimental error in the value of δ_{expt} has not been determined. It can be seen that it is the value of N which is most affected by δ_{expt} . If we imagine that the error in δ_{expt} of ± 0.02 , this would result in a range of values of N, in the case given, of 457-153.

The effect of changes in the value of δ_{expt}

δ_{expt}	N	Q	T_C
0.05	1046	101	267
0.06	921	105	282
0.07	636	109	297
0.08	457	112	312
0.10	255	120	346
0.11	196	124	363
0.12	153	129	383
0.13	120	133	402

Table III. The effect of changes in the value of δ_{expt} on N, Q and T_C
 (Expt. no.7; original $\delta_{\text{expt}} = 0.102$; $\xi = 1.0 \mu\text{m}$)

It is interesting to note that Quinn's values of δ_{expt} range from around 1-5% whilst the present values range from 10-21%.

Since

$$\delta_{\text{expt}} = \frac{H_1}{H_{\text{total}}} \quad \text{where } H_{\text{total}} = FxU$$

The increase in δ_{expt} is mainly due to a speed effect since the sliding speed used was less than Quinn's (2.0 m.s^{-1} as opposed to 5.11 m.s^{-1}) or perhaps to better thermal contact between the pin and disc, provided by increased metal-metal contact.

5.8.

The critical oxide thickness, ξ , and the distance over which wearing contact is made, d.

Under the mechanism proposed by Quinn, the thickness ξ is built up on each asperity after $1/K$ passes and is formed whilst still in contact. In the original proposal (27) no particular reason was given for the assumption that a critical thickness of oxide was reached. In (40) the values of ξ and d obtained indicated that from geometrical considerations, the asperity will become unstable when its height is greater than its width. The values obtained for ξ ($= 2.3 \pm 1.3 \mu\text{m}$) and d ($= 2.8 \pm 0.52 \mu\text{m}$) are consistent with previous experimental observations (61). In the present work d was typically an order of magnitude greater than ξ .

A possible modification was considered bearing in mind the comments by Rowe and Fowles (66) and Berry (62) on the Oxidational Wear Theory. Both Berry and Rowe suggest that since the oxide wear particles are supposed to be removed initially as flakes, then this must be accounted for in the development of a wear equation.

Following the Archard Wear law ($w = K \cdot \frac{W}{F_m}$), Rabinowicz states that K incorporates a shape factor and that $K = \frac{K'}{3}$ for spherical particles only, this is apparently ignored by Quinn. Quinn replied to this by

restating that his particular interpretation of K allows him to neglect the shape of the particles. In any case, if the suggestion made by Rowe is considered, i.e. that K should be multiplied by a factor of $1/\xi$ and not d/ξ^2 , it can be seen that if $\xi = d$, as suggested by Quinn, then in both cases K is multiplied by effectively the same factor.

The role of oxide thickness is an important one, basically it has two main effects on the wearing system. Firstly, due to the nature of the oxidation process, the thickness determines the rate of oxidation. Secondly, once a certain thickness of oxide has built up, on any asperity either by a single encounter or by a number of passes, attrition will take place through abrasion or fatigue.

Care must be taken to ensure that the correct interpretation of \bar{m} and d are used when comparing different theories, for instance take the theory proposed by Tenwick and Earles (29) and the Oxidational Wear Theory.

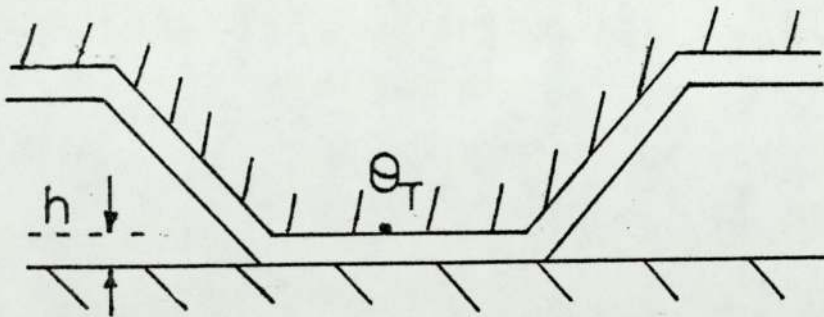


Figure 4.3. Typical Asperity Contact visualized by Tenwick and Earles.

Tenwick and Earles visualise a model in which only one asperity forms the real area of contact and that it remains continually in contact with the opposing surface until an oxide wear particle is formed. It

should be noted that the oxide layer is also present over non-contacting areas. When a critical thickness, h_c , is reached the oxide becomes detached. In Quinn's model there are a large number of asperities (200-2000) in contact at any given time, in order to make this consistent with the electron microscope evidence (61) of a small number of large plateaux, it was assumed that all of the contacts exist on one plateau and that only one plateau is in contact at any instant. The critical oxide thickness (ξ_c) was assumed to be equal to the height of the large plateau. Wear takes place by a fatigue process, the plateau surface exhibiting cracking, and breaking into flakes a few microns thick. These flakes are subsequently broken up into wear particles with comparable diameters. It is difficult to accept the assumption that ξ_c is the height of the plateaux in contact, and also visualise the role of the asperities in the wearing process, unless perhaps, each asperity becomes weak when its height approaches its diameter and contributes to the fatigue of the whole of the plateau surface. Quinn and Sullivan (63), in a review of oxidational wear, have questioned the importance of the plateau in the understanding of mild wear.

The problems which have arisen from the consideration of the critical oxide thickness are also applicable to d in some ways. If the contact is assumed to be a plateau region then d would correspond to the length of the plateau, if this plateau forms the real area of contact ($N=1$) and $A = W/P_m$ then d is simply established, if only asperities are visualised, then d is presumably N times smaller. Only if asperities exist on plateaux does d become confused.

5.9.

The Activation Energy of Oxidation in Wear, Q

It is usual to assume that the oxidation which takes place at the surfaces obeys a parabolic rate law in the temperature range

300-800C and is expressed in the following form:-

$$\Delta m^2 = k_p \cdot t$$

where $k_p = A_p \exp(-Q/RT_0)$

Q and A_p are temperature dependent; in most cases it is only the value of Q which is emphasised but the value of A_p can vary by two orders of magnitude depending upon the source of data. The effect of different values of the Arrhenius Frequency factor can be shown by simple calculations of the rate constant:-

(1) If $A_p = 3.2 \times 10^6 \text{ kg}^2 \text{ m}^{-4} \text{ s}^{-1}$ (ref. 52)
Q = 96 kJ mole⁻¹
and $T_0 = 473^\circ\text{K}$
then $k_p = 3.1 \times 10^6 \text{ kg}^2 \text{ m}^{-4} \text{ s}^{-1}$

(2) If $A_p = 1.2 \times 10^4 \text{ kg}^2 \text{ m}^{-4} \text{ s}^{-1}$ (ref. 51)
Q = 193 kJ mole⁻¹
and $T_0 = 473^\circ\text{K}$
then $k_p = 1.1 \times 10^4 \text{ kg}^2 \text{ m}^{-4} \text{ s}^{-1}$

The rate constants differ by two orders of magnitude and is produced by the change in A since the change in Q has negligible effect upon the exponential term. When values of Q_p which are not derived from known oxidation data are incorporated into wear rate calculations it is necessary to consider a corresponding value for A_p .

One of the most important problems in oxidative wear studies is the matching of the activation energies predicted from wear studies to known values of the activation energy of oxidation. First of all the question must be asked, how representative are the values of oxidation data derived from static bulk experiments to the oxidation which takes place at rubbing interfaces? Derived values of

Q cover a wide range and are generally much lower than the static values normally used. This is normally explained by the fact that it is reasonable to assume that the surfaces are highly energised and that oxidation takes place much more readily. It has been known for some time that plastic deformation will increase the oxidation rates for iron and steel in the temperature range 200-600C and the detection of exo-electron emission from rubbing surfaces show that the surfaces can become activated. Whether some of the lower values are justifiable for these reasons is open to question, indeed some authors do not think that it is necessary to accept that the value of Q in wear will be very different to the known static values.

There are two most commonly used sources of values of both Q and A_p , Caplan and Cohen (52) with abraded specimens and Kubaschewski and Hopkins (51) with hydrogen-annealed specimens. Quinn (40) has recently found that the value of Q which provides the most consistent fit between theory and experiment, was Caplan and Cohens value of 96 kJ/mole, for the temperature range 450-580C. Molgaard (64) has also suggested that the value of Q for oxidation in wear is the same as for standard oxidation studies. It will be seen in the present investigation that Q is an extremely sensitive parameter, mainly due to nature of the exponential expression for the oxidation rate. In comments by Berry (62) on Quinn's original hypothesis, he points out this sensitivity and Molgaard (64), in spite of recommending that Q can be fixed at the standard static value, illustrates the sensitivity of Q to small changes in other wear parameters (a 30 per cent change in Q for a 10°C change in the mean rubbing temperature). In fact he gives a number of values of Q for a set of assumed values of the temperature of oxidation, for the range 550-600C the range of Q (96-251 kJ/mole) was nearly the same as that quoted by Caplan and

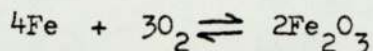
Cohen for the temperature range 400-700C. Molgaard (30), however, in an earlier paper, suggested that, in any event, he thought that it was unlikely that the oxidation process is a controlling process in wear, and that the basic factors are the mechanical properties of the oxide formed in wear.

It has already been stated that the most important factor in the oxidation process is the temperature of oxidation, T_0 , this factor will be discussed in detail at a later stage. There are a number of other factors which are important to the understanding of the oxidation process but are not normally considered in the formulation of a wear equation. Factors such as the partial pressure of the oxygen in the rubbing vicinity, the type of oxide, the mode of formation, the diffusivity of the oxide and the deformation of the oxide.

If a steady state situation is considered such as may occur during the equilibrium mild wear of two interacting oxidised surfaces it is possible that if the existing oxide contains a high density of disconformities it would provide a greater area of reaction.

The relative diffusion rates of the metal and oxygen ions through the existing oxide would appear to affect both the rate of oxidation and also the site of oxidation, since if the metal ions diffuse at a much greater rate towards the hot interface than the oxygen ions diffuse into the cooler subsurface, then oxidation would tend to take place near to the interface, and perhaps at a higher temperature than occurring nearer to the metal-oxide interface.

The conditions at the interface favour oxidation because a concentration of oxygen in the irregularities of the surface by the high local pressures set up when two bodies are brought into contact under load.



The equilibrium is driven to the right in accordance with Le Chateliers law because a drop in pressure results.

The factors briefly mentioned above have been researched in some detail in static oxidation studies but not in rubbing situations. It is accepted that the study of the oxidation process in wear is a very difficult proposition but it is felt that more consideration of such factors should be taken in future mean studies.

5.10.

The influential temperature, T_C , T_O or T_S ?

The question of which temperature is the most influential in the wear process is a controversial one. The value of T_O is of particular interest since it is the temperature used to calculate probable values of Q upon which the values of N and ξ are selected.

Primarily one needs to decide whether oxidation takes place in the contacting or non-contacting periods. Quinn assumes that $T_O = T_C$ or very nearly so, which infers that oxidation takes place during contact or perhaps that it occurs immediately after separation of the asperities before the temperature has fallen appreciably. On the other hand it is also suggested that T_S is the controlling temperature since any given point on the surface will spend more time out of contact. A simple order of magnitude calculation by Archard (28) appears to justify the assumption that T_C is the most influential by showing that, the amount of oxide grown at the mean surface temperature will be negligible compared to that grown at the higher contact temperature.

Instinctively it would appear that oxidation during contact would be limited by restricting the availability of oxygen to the reaction sites. A more reasonable assumption is that oxidation

takes place very quickly after contact when the surface is still activated. Whether the surface revealed after contact is of bare metal or of oxide, depends on the assumed mode of wear. The contact temperature, T_C , was determined from the theoretical division of heat and is the value found when $\omega_{theory} = \omega_{expt}$. Quinn found that T_O (using $T_O = T_C$) showed a linear relationship with W and with N , and that $T_O - T_S$ was constant at around 1700C which agreed with his previous work.

In the present work T_O was taken to be equal to T_C and no pattern could be found in the results, as mentioned previously. Unfortunately an error in the value of T_O leads to some misleading, but on retrospect, interesting results. Instead of using the value of T_O in degrees Kelvin for the rate equation, degrees Celsius was used. At this stage it was noticed that the original program used by Quinn also contained the same mistake. The recalculated values consequently found by Quinn were different but the same trends or patterns were observed. In the present work a recognisable pattern was found only when the erroneous calculations were made. Briefly, these results indicated that T_O remained constant at around 500C, N increased linearly with W , and $T_O - T_S$ was not constant but decreased with W . Since no pattern could be found in the correct analysis it is perhaps worthwhile to consider the incorrect analysis further.

It was possible to find some correlation in the results when T_O was 273C lower than T_C . Since it is reasonable to assume that T_O lies somewhere between T_C and T_S , a corresponding value of T_O was selected and used in the analysis. Quinn (37) using a different wear theory to that used in the present work (Quinn (27)) suggested that T_C estimated from X-ray analysis of wear debris, which corresponded to the oxidation temperature, was around 200C greater

than T_S . Tenwick and Earles (29) have also suggested a similar relationship between T_O and T_S .

The results of using $T_O = T_S + 170$ are given in Table IV

Expt. No.	Q_p (kJ mole)	N	T_C (°C)
1	104	223	207
2	112	44	328
3	113	107	252
4	129	17	490
5	137	12	605
6	120	198	310
7	125	261	339

Table (IV) Values of N, T_C and Q_p assuming $T_O = T_S + 170$ and $\bar{v} = 1 \mu\text{m}$.

Experiments 4 and 5 stand out and seem to interrupt any pattern or trend in the results. This has been noticed in previous print-outs and has been taken to indicate a possible transition in the wearing process since the wear rates and surface temperatures change character at these loads.

It has also been proposed that T_S is representative of the oxidation temperature, this possibility cannot be easily incorporated into Quinn's method since oxidation would take place during non-contact periods and over the whole of the apparent area of contact. This is contrary to the assumptions of the Oxidational Wear theory. Yoshimoto and Tzukizoe (54) based a wear theory on oxidation occurring during non-contact periods, the mechanism proposed was such that oxide is removed at every pass and grows to a constant thickness before the next pass. The resulting expression for w_{theory} contains constants for logarithmic oxidation which are

as subject to uncertainty as those for parabolic oxidation.

5.11.

The contact temperature, T_C

The Archard approach to the estimation of contact and flash temperatures has been used in the present work. This theory was developed by Jaeger originally and simplified by Archard. Temperatures are calculated using a moving heat source analysis where the energy input is modelled as a plane heat source moving along the surface. It is often found that the predictions made using either analysis are higher than expected. A recent paper by Malkin and Marmur (67) suggest that the energy may be distributed within a thin layer rather than concentrated within a plane. Subsequent comparisons showed that their predictions were lower and could be up to half of that obtained using the moving plane source solution. The ideas put forward are too recent to attempt to incorporate into the present examination, but could be considered in future research. Since the predictions of contact and flash temperatures are lower than those normally obtained using the Archard Theory, they may be used to bring together theoretical and experimental estimates.

5.12

The number of asperities in contact beneath the pin, N.

There is no real factual evidence for values of N, Quinn extrapolated the results of experimental work on carbon brushes by Bickerstaff (69) to provide some comparison in order to explain the unexpected high values of N which he obtained. Using the same extrapolation at 60N load N would be around 5000. The result of allowing for higher values of N to be reached in the computer (originally the ~~maximum~~ value was 2000) was that extremely small values of a and ξ were given and the difference between T_C and T_S was reduced. An increase in the real area of contact at higher loads could possibly explain the effect on the surface temperatures but it is difficult to reconcile the unacceptable reduction of both a and ξ . Quinn found that N was proportional to W and that when they were plotted against wear rate the graphs exhibited the same form which included a change in wear rate slope. This change in slope is normally attributed to a change in the wear mechanism and in the value of K. Further work on this particular effect would give some insight of the possible interdependence of these parameters which is not possible at the present.

CHAPTER 6

CONCLUSIONS

A wear testing machine was constructed which was capable of measuring continuously the friction, wear and heat flow between specimens for a wide range of loads, speed and externally-induced ambient temperatures. The machine was designed such that it could be readily modified to suit a variety of tribological experiments for example, the construction of a controlled atmosphere environment which could be used to investigate wear in hostile conditions. One recommendation which could be made is that for future work on basic wear mechanisms of elevated temperatures it would be better if facilities were incorporated to enable the ambient temperature of the specimen pin to be raised in order to eliminate the effects of thermal asymmetry.

The effect of externally induced elevated temperature upon the "wear rate versus load graphs" has been examined for the first time. Although the aim of this work has only been partially fulfilled, that is, only one sliding speed was used, the trends in the wear behaviour of mild steel can be seen from the amount of work carried out. This type of research involves a large number of experiments which take a long time to arrange and carry out which makes more detailed examinations prohibitive. The observation of trends of behaviour for other speeds and material combinations would, however, be very useful to the development of guides to the use of engineering metals and the widely increasing variety of surface treatments now used to improve tribological characteristics.

The first point emerging from this research is the relative ease in which both temperature and speed can overcome the tendency

of low carbon steel to wear in the severe mode. Mild wear was nearly always obtained at higher load, speeds and temperature. Since mild wear can be acceptable for some unlubricated situations, especially where high temperatures are involved then this research indicates that mild steel may be a useful material in these situations. It may also be argued that the wear behaviour pattern found by Welsh may not be very representative in engineering conditions.

The variation of wear rate with load revealed wear rate transitions similar to those reported by Welsh. The shape of the "wear rate versus load" graphs were strongly dependent upon the externally-induced ambient specimen temperatures. Similar transitions and shapes were also obtained by increasing the sliding speeds.

The effect of increasing the specimen disc bulk temperature was very similar to that observed, when the sliding speed was increased. That is, all wear rate transitions are displaced to lower loads resulting, in the disappearance of the T_1 and T_2 transitions leaving a wide range of loads over which mild wear persists. Severe wear only occurring during the early stages of a wear test when the surfaces are running-in.

Insufficient data prevents the author from suggesting any firm explanation of the possible interrelation between the speed and ambient temperature effects in terms of surface temperature estimates for instance. It is felt that with certain modifications to the wear test method such as heating the pin as well as the disc and the measurement or estimation of rubbing temperatures for all of the numerous tests which would be necessary, the combination of speed and specimen temperature variation would produce valuable information.

The second part of the research was concentrated upon mild wear and in particular to the measurement of the dimension of heat at the sliding interface and to the estimation of surface temperatures in such a way that existing oxidational wear theories could be examined. An existing method, proposed by Quinn, was used in the present work.

A critical analysis of the method with particular attention to the proposed oxidation wear theory was carried out, in conjunction with a more detailed physical examination of the wear taking place for the experiments in which the heat flow was measured.

The following conclusions were reached. Firstly, that the wear mechanism for the heat flow experiments did not conform to the type of wear upon which the original work by Quinn was based, although there were a number of similarities in the variation of wear rate and surface temperature (T_s and T_a) with load. The importance of physical analysis of wear surfaces and debris in determining the character of wear in any wear investigation is shown in this particular circumstance.

In attempting to overcome the failure to fit the results of the heat flow analysis within Quinn's oxidational wear theory, and subsequent efforts to modify certain aspects, a critical examination of existing wear theories was made. An accepted disadvantage of present wear theories and predictive expressions for wear rates is the large variety and number of variables which can be incorporated. The introduction of computer methods to this problem has proved to be very useful in that a large number of combinations of the various variables can be analysed which might otherwise have proved to be a daunting task.

The speed and specimen temperature varying experiments have indicated that the most commonly encountered region of the general wear pattern is the mild wear region above the T_2 transition and includes the T_3 transition. It was found that the wear in this region was not purely oxidative and that the wear also included the removal of unoxidised material. This was not limited to the region of the wear pattern which appeared to be above the T_3 transition. For the particular conditions of material, hardness, load and speed used it is suspected that the T_2 and T_3 transitions are not as distinct as might possibly be encountered. Before attempting to correlate experimental data with theoretical considerations it is necessary to firmly establish the character of the wear taking place.

It is the author's view that although the method proposed by Quinn to relate the division of heat at sliding interfaces to a surface model is not fully developed it provides a new basis for further work concerning mild wear. If a method for providing realistic estimates of the surface temperatures generated during severe wear could be found, a better understanding of the general wear pattern would be possible.

REFERENCES

1. FINK, M., Wear Oxidation, A New Component of Wear, Trans.Am. Soc.Steel Treating, Vol.18, 1930, p.204
2. MAILANDER, R. and DIES, Contributions to the Investigations of the Processes taking place during wear, Arch.Eisenhutt, Wes., Vol. 16, 1943, pp.385
3. SIEBEL, E. and KOBITZSCH, R., Verschleisserscheinungen bei gleitender trockner Reibung, VKI Verlag, (Berlin), 1941
4. HOLM, R. Electric Contacts Handbook, Springer-Verlag (Berlin), 1958, p.199
5. BURWELL, J.T. and STRANG, C.D., 'On the Empirical Law of Adhesive Wear', J.Appl.Phys., Vol.23, 1952, p.18
6. ARCHARD, J.F. and HIRST, W., The Wear of Metals under Unlubricated Conditions, Proc.Roy.Soc. (London), Vol.A236, 1956, p397
7. BOWDEN, F.P. and TABOR, D., The Friction and Lubrication of Solids, Oxford University Press, 1950
8. DYSON, J. and HIRST, W., The True Area of Contact Between Solids, Proc.Phys.Soc. (London), Vol.B67, 1954, p.309
9. COCKS, M., "The Effect of Compressive and Shearing Forces on the Surface Films present in Metallic Contacts", *ibid.*, Vol.B67, 1954, p.238
10. KERRIDGE, M. and LANCASTER, J.K., The Stages in a Process of Severe Metallic Wear, Proc.Roy.Soc.(London), Vol.A236, 1956, p.250

11. LANCASTER, J.K., The Formation of Surface Films and the Transition between Mild and Severe Wear, *ibid.*, Vol.A273, 1953, p.466
12. WELSH, N.C., The Dry Wear of Steels, *Phil.Trans.Sec.(London)*, Vol. A257, 1965, pp.31-70
13. BURWELL, J.T., Survey of possible Wear Mechanisms, *Wear*, Vol.1, 1957-58, p.119
14. ARCHARD, J.F., Contact and Rubbing of Flat Surfaces, *J.Appl.Phys.*, Vol.24, 1953, p.24
15. ARCHARD, J.F., Single Contacts and Multiple Encounters, *ibid.*, Vol.32, 1961, p.1420
16. EYRE, T.S. and MAYNARD, D., Surface aspects of Unlubricated Metal-to-Metal Wear, *Wear*, 18 (1971), 301-310
17. BLOK, H., Determinations of Surface Temperatures under Extreme Pressure Lubricating Conditions, *Proc.World Congr.Petrol.*, 2nd Paris, 1937, 471-486
18. BLOK, H., Theoretical Study of Temperature Rise at Surfaces of Actual Contact under Oiliness Lubricating Conditions, *Inst. Mech.Eng.*, *Proc.General Discussion Lubrication and Lubricants*, 2, 222-235 (1937)
19. JAEGER, J.C., Moving Sources of Heat and the Temperature at Sliding Contacts, *Proc.Roy.Soc.New South Wales*, 56, 203-224 (1942)
20. HOLM, R., Calculation of the temperature developments in a contact heated in the contact surface, and the application to the problem of the temperature rise in a sliding contact, *J.Appl.Phys.*, 19, 361-366 (1948)

21. ARCHARD, J.F., The Temperature of Rubbing Surfaces, *Wear*, 2, (1959), 438-455
22. BARBER, J.R., Distribution of Heat between Sliding Surfaces, *J.I.Mech.Engrg.Sci.*, 9, No.5, (1967)
23. EARLES, S.W.E. and POWELL, D.G., Surface temperature and the periodic breakdown between unlubricated steel surfaces, *Asle.Trans.*, 11, 109-120, (1968)
24. LANCASTER, J.K., The Influence of Temperature on Metallic Wear, *Proc.Roy.Soc. (london)*, A273, 1963, 466
25. HIRST, W. and LANCASTER, J.K., The Influence of Speed on Metallic Wear, *ibid*, A259, 1960, 288
26. QUINN, T.F.J., The Effect of "Hot-Spot" Temperatures on the Unlubricated Wear of Steel", *Asle,Trans.* 10, (1967) 158
27. QUINN, T.F.J., "Oxidational Wear", *Wear*, 18, (1971), 418
28. ARCHARD, J.F., A Review of Wear Studies, N.A.S.A. Symposium on Interdisciplinary Approach to Friction and Wear, Paper 5
29. TENWICK, N. and EARLES, S.W.E., A Simplified Theory for the Oxidative Wear of Steels, *Wear*, 18, (1971), 381-391
30. MOLGAARD, J., A Discussion of Oxidation, Oxide Thickness and Oxide Transfer in Wear, *Wear*, Vol.40, (1976), 277-291
31. SHORE, H., "Thermoelectric Measurement of Cutting Tool Temperature", *J.Wash.Acad.Sci.*, 15, 85, (1925)
32. HERBERT, E.G., "The Measurement of Cutting Temperatures", *Proc.Inst.Mech.Engrs.*, 1, 289, (1926)
33. FUREY, M.J., "Surface Temperatures in Sliding Contact," *Asle.Trans.*, 1, 133, (1964)

34. LING, F.F., "Juncture Conditional Moving Interfaces", Surface Mechanics, Wiley-Interscience, 65, (1973)
35. LING, F.F. and SIMBINS, T.E., "Measurement of Pointwise Juncture Condition of Temperature at the Interface of Two Bodies in Sliding Contact", Jolt, Trans.ASME, 85, 481, (1963)
36. VASILAKIS, J.D. and LING, F.F., "A Novel Method of Measuring Temperature due to Sliding in Ultra-high Vacuum", Space Tribology, European Space Agency, Neully, France, 87 (1975)
37. QUINN, T.F.J., "An experimental study of the thermal aspects of sliding contacts and their relation to the unlubricated wear of steels", Proc.Inst.Mech.Engrs., 183, Pt.3P, 129, (1968-69)
38. GROSBERG, P, McNAMARA, A.B. and MOLGAARD, J., "The Performance of Ring Travellers", J.Text.Inst., 56, T24, (1965)
39. GROSBERG, P. and MOLGAARD, J., "Aspects of the Wear of Spinning Travellers: The Division of Heat at Rubbing Surfaces", Proc.Instn.Mech.Engrs., 181, Pt.3L, 16, (1966-67)
40. QUINN, T.F.J., The Division of Heat and Surface Temperature at Sliding Steel Interfaces and their Relation to Oxidational Wear, Asle Preprint No.76-IC-2B-I (paper to be published in ASLE. Trans. in 1977)
41. RABINOWICZ, E., Friction and Wear of Materials, John Wiley & Sons, 1965, Chapter 6.
42. KERRIDGE, M. and LANCASTER, J.K., The Stages in a Process of Severe Metallic Wear, Proc.Roy.Soc. (London), A236, (1956) 250
43. QUINN, T.F.J., "The dry wear of steel as revealed by Electron Microscopy and X-Ray Diffraction", Proc.Inst.Mech.Engrs., 182, Pt.3N, 1967-68

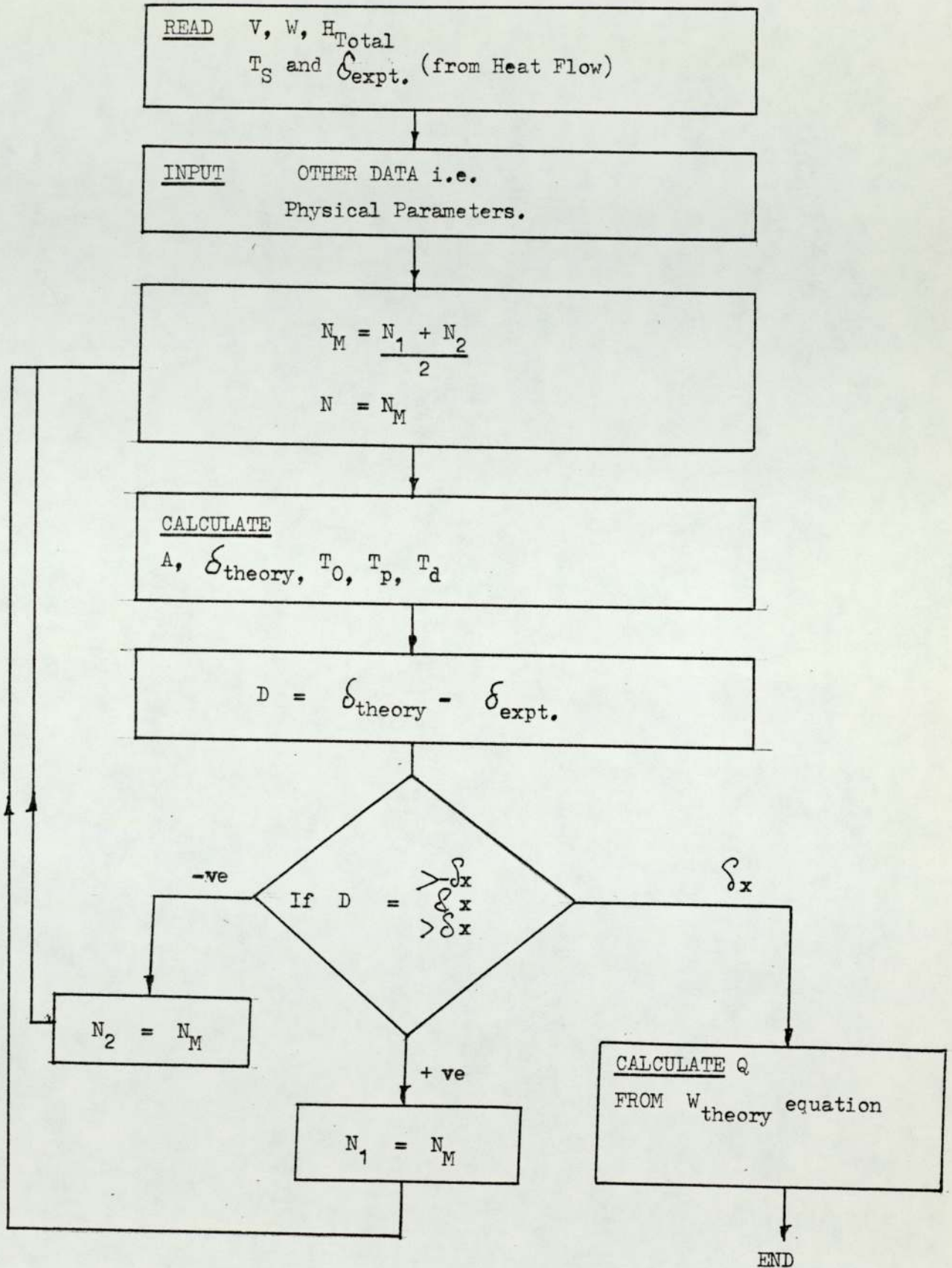
44. FINKIN, E.F., Speculations on the Theory of Adhesive Wear, *Wear*, 18, (1971), 381-391
45. SUH, N.P. The Delamination Theory of Wear, *Wear*, 25, (1973) 111-124
46. KRAGELSKII, I.V., (L.Ronson & J.K.Lancaster, trans.): Friction and Wear, Butterworths Scientific Publ. (Wash.D.C.) p.98
47. KRUSCHOV, M.M. and BABICHEV, M.A., Research on the Wear of Metals, Ch.7, NEL Translation No. 892
48. SEDRICKS, A.J. and MULHEARN, T.O., Mechanics of Cutting and Rubbing in Simulated Abrasive Processes, *Wear*, 6, (1963), 457
49. SEDRICKS, A.J. and MULHEARN, T.O., The Effect of Work-Hardening on the Mechanics of Cutting in Simulated Abrasive Processes, *ibid*, 7, (1964), 451
50. MULHEARN, T.O. and SAMMUELS, L.E., The Abrasion of Metals; A Model of the Process, *ibid*, 8, (1962), 478
51. KUBASCHEWSKI, O. and HOPKINS, B.E., "Oxidation of Metals and Alloys", Butterworths, London, 1962
52. CAPLAN, D. and COHEN, M. "The Effect of Cold Work on the Oxidation of Iron from 400 to 650C", *Corrosion Science*, 6, (1966), 321
53. CLARK, W.T., PRITCHARD, C. and MIDGLEY, J.W., Mild Wear of Unlubricated Hard Steels in Air and Carbon Dioxide, *Proc.Inst. Mech.Engrs.*, 182, Pt3N, (1967-68), 97-106
54. YOSHIMOTO, G. and TSUKIZOE., On the Mechanisms of Wear between Metal Surfaces, *Wear*, 1, (1957-58), 472
55. QUINN, T.F.J., "An Experimental Study of the Thermal Aspects of Sliding Contacts and their Relation to the Unlubricated Wear of Steel", *Proc.Inst.Mech.Engrs.*, 183,Pt 3P, 1968-69, 129

56. GOOD, J.N. and GODFREY, E., Changes found on Run-in and Scuffed Surfaces of Steel, Chrome Plate and Cast Iron, N.A.C.A. Tech. Note 1432 (1947)
57. JOHNSON, R.L., GODFREY, D. and BISSON, E., Friction of Solid Films on Steel at High Sliding Velocities, N.A.C.A. Tech.Note 1578 (1948)
58. TAO, F.F., A Study of Oxidation Phenomena in Corrosive Wear, ASLE.Trans., 12, (1969), 97-105
59. ARCHARD, J.F. and HIRST, W. An Examination of a Mild Wear Process, Proc.Roy.Soc.(london), A238, 1957, 315
60. DUNCKLEY, P.M., QUINN, T.F.J. and SALTER, J., Studies of the Unlubricated Wear of a Commercial Cobalt-base Alloy at temperatures up to about 400C, ASLE Trans. Vol.19, 3, 221-223 (1976)
61. QUINN, T.F.J., "The Dry Wear of Steels as revealed by Electron Microscopy and X-ray Diffraction", Proc.Inst.Mech.Engrs., 182, Pt.3M, 201 (1968)
62. BERRY, G.A., Comments on "Oxidational Wear", Wear, 18, (1971) 499
63. QUINN, T.F.J. and SULLIVAN, J.L., "A Review of Oxidational Wear", Proc. of the International Conf. on Wear Materials, April 1977, St.Louis, to be published in J.of Lub.Tech.Trans. ASME 1978
64. MOLGAARD, J. and SRIVASTAVA, V.K., The Activation Energy of Oxidation in Wear, Wear, 41 (1977), 263-270
65. UHLIG, H.H., Mechanism of Fretting Corrosion, J.Appl.Mech., Vol.21, 1954, p.401

66. ROWE, C.N. and FOWLES, P.E., Discussion of ref. 26.
67. MALKIN, S. and MARMUR, A., Temperatures in Sliding and Machining Processes with Distributed Heat Sources in the Subsurface, Wear, 42 (1977) 333-340
68. SMITHELLS, C.J., Metals Reference Book, Vol.3, 4th Edition 1967, Butterworths
69. BICKERSTAFFE, A.E., "The Real Area of Contact between a Carbon Brush and a Copper Collector", Proc. 15th Holm Seminar on Electric Phenomena, Illinois Institute of Technology, Chicago, 1969, p. 41.

APPENDIX 1

Flow Diagram



For a given Q values of N, T₀, T_S, T_C and S are obtained.

APPENDIX 2

Values of the experimental parameters used for evaluating δ_{expt} and T_s :

- K_i = conductivity of insulating medium
= $1.045 * 10^{-1} \text{ J.m}^{-1} . \text{C}^{-1}$
- K_s = conductivity of EN8 steel
= $51.83 \text{ J.m}^{-1} . \text{s}^{-1} . \text{C}^{-1}$
- K_o = thermal conductivity of mixed oxide
= $2.1 \text{ J.m}^{-1} . \text{s}^{-1} . \text{C}^{-1}$
- R_a = inner radius of copper heat sink
= $(7.95 \pm 0.03) * 10^{-3} \text{ m}$
- R_t = radius of pin
= $(3.175 \pm 0.001) * 10^{-3} \text{ m}$
- C = Conductance of thermocouple wire
= $1.174 * 10^{-5} \text{ J.m.s}^{-1} . \text{C}^{-1}$
- U_r = rate of rotation = $382 \pm 5 \text{ rpm}$
- U = speed of disc at the pin
= $2.0 \text{ m.s}^{-1} \pm 1.3 \text{ percent}$
- K_x = kinematic viscosity of air = $\frac{u}{\rho_a} = 13.98 * 10^{-6} \text{ m}^2 . \text{s}^{-1}$
- N_{Re} = $9.08 * 10^2$
- N_{Nu} = 16
- K_{air} = $2.711 * 10^{-2} \text{ J.m}^{-1} . \text{s}^{-1} . \text{C}^{-1}$
- h = $68.30 \text{ J.m}^{-2} . \text{s}^{-1} . \text{C}^{-1} \pm \text{percent}$

$$\rho_s = \text{density of EN8 steel} = 7.84 * 10^3 \text{Kg.m}^{-3}$$

$$c = \text{specific heat of EN8 steel} = 4.81 * 10^2 \text{J.Kg}^{-1}.\text{C}^{-1}$$

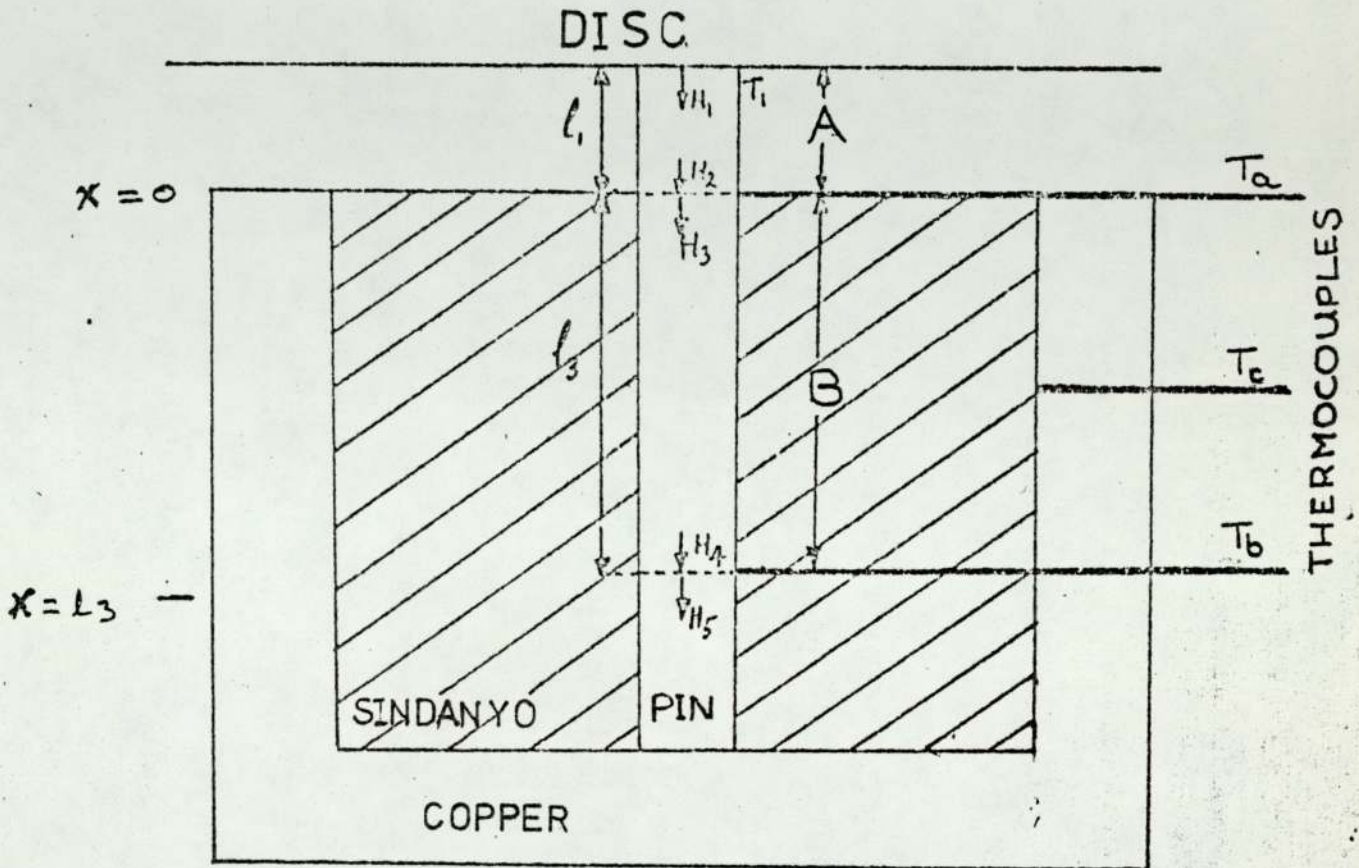
$$P_m = 3.26 * 10^9 \text{N.m}^{-2}$$

$$\text{Diameter of wear track} = 1 * 10^{-1} \text{m}$$

APPENDIX 3

Heat Flow Theory

The following theory was used by Quinn (40) and also in some unpublished work and was originally developed by Dr. R. Coy. (A.1)



Section 'B' of the pin.

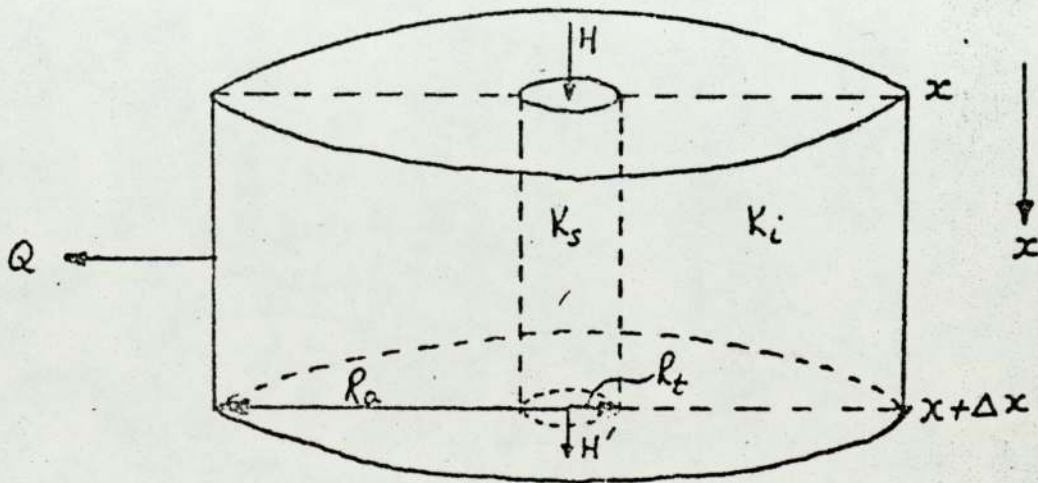


FIGURE 3.2

We consider a cylinder between the limits $x = 0$ and $x = 1$,
 and the cylindrical outer surface at $r = R_a$ is the outer
 radius of the Sindanyo. The radius of the pin is R_t .

Consider the steady state equilibrium of a thin slice through
 the insulator and the pin (FIG 3.2). The distance between
 the planes is Δx , x being in the direction of the pin axis.

T_x is the temperature of the pin at x . The axial heat flow
 through the pin at x is

$$H = -K_s \pi R_t^2 \frac{dT_x}{dx} \quad (3.1)$$

and at $x = \Delta x$ the heat flow is

$$H' = -K_s \pi R_t^2 \left(\frac{dT_x}{dx} + \frac{d^2T_x}{dx^2} \Delta x \right) \quad (3.2)$$

K_s = Thermal conductivity of steel.

Ignoring the change in temperature from $x + \Delta x$, the radial
 heat flow through the Sindanyo per unit length of pin is

$$Q = \frac{2 K_i \pi (T_x - T_c)}{\log_e (R_a / R_t)} \quad (3.3)$$

K_i = Thermal conductivity of Sindanyo.

For equilibrium equation (3.1) must equal the sum of (3.2)

and (3.3). Therefore

$$K_s \pi R_t^2 \frac{d^2T_x}{dx^2} = \frac{2 K_i \pi (T_x - T_c)}{\log (R_a / R_t)} \quad (3.4)$$

Putting

$$M_I^2 = \frac{2 K_i \pi \cdot (T_x - T_c)}{K_s \pi \cdot R_t^2 \log (R_a / R_t)} = \frac{d^2T_x}{dx^2} \quad (3.5)$$

$$\text{and } T = T_x - T_c \quad (3.6)$$

$$\text{we have } \frac{d^2 T}{dx^2} = M_1^2 \cdot T \quad (3.7)$$

The solution to (3.7) is

$$T = B_1 e^{M_1 x} + B_2 e^{-M_1 x} \quad (3.8)$$

$$\text{or } T_x = B_1 e^{M_1 x} + B_2 e^{-M_1 x} + T_c \quad (3.9)$$

B_1 and B_2 are constants depending on the boundary conditions.

For this section the boundary conditions are

$$\text{at } x = 0, T_x = T_a \quad \text{and } H = H_3$$

$$\text{at } x = l_3, T_x = T_b \quad \text{and } H = H_4$$

T_a and T_b are the temperatures at the upper and lower ends of the section of the pin and are known from the thermocouple readings.

From equations (3.1) and (3.9)

$$H = -K_s \sqrt{R_t^2 M_1} (B_1 e^{M_1 x} - B_2 e^{-M_1 x}) \quad (3.10)$$

Hence from the boundary conditions

$$T_a = B_1 + B_2 + T_c \quad (3.11)$$

$$H_3 = -K_s \sqrt{R_t^2 M_1} (B_1 - B_2) \quad (3.12)$$

$$T_b = B_1 e^{M_1 l_3} + B_2 e^{-M_1 l_3} + T_c \quad (3.13)$$

$$\text{Define } \bar{H}_3 = \frac{H_3}{K_s \sqrt{R_t^2 M_1}} \quad (3.14)$$

Then from (3.12)

$$\bar{H}_3 = B_2 - B_1 \quad (3.15)$$

Multiplying (3.11) by $e^{M_1 l_3}$ gives

$$(T_a - T_c) e^{M_I l_3} = B_1 e^{M_I l_3} + B_2 e^{-M_I l_3} \quad (3.16)$$

Subtract (3.13) from (3.16) gives

$$(T_a - T_c) e^{M_I l_3} - (T_b - T_c) = B_2 (e^{M_I l_3} - e^{-M_I l_3})$$

$$\text{or } B_2 = \frac{(T_a - T_c) e^{M_I l_3} - (T_b - T_c)}{2 \sinh M_I l_3} \quad (3.17)$$

substituting for B_2 in (3.11) gives

$$B_1 = (T_a - T_c) - \left(\frac{(T_a - T_c) e^{M_I l_3} - (T_b - T_c)}{2 \sinh M_I l_3} \right)$$

$$\text{or } B_1 = \frac{-(T_a - T_c) e^{-M_I l_3} + (T_b - T_c)}{2 \sinh M_I l_3} \quad (3.18)$$

and substituting for B_1 and B_2 in (3.15) gives

$$\bar{H}_3 = \frac{(T_a - T_c) e^{M_I l_3} - (T_b - T_c) + (T_a - T_c) e^{M_I l_3} - (T_b - T_c)}{2 \sinh M_I l_3}$$

$$\bar{H}_3 = \frac{(T_a - T_c) \cosh M_I l_3 - (T_b - T_c)}{\sinh M_I l_3} \quad (3.19)$$

or

$$H_3 = K_s R_t M_I^2 \left(\frac{(T_a - T_c) \cosh M_I l_3 - (T_b - T_c)}{\sinh M_I l_3} \right)$$

Heat flow through the thermocouple.

Let C = conductance of the thermocouple wire, i.e. C = heat flow per second per unit temperature gradient in degrees centigrade per cm along the length of the thermocouple wire, then the heat flow along the thermocouple is equal to

$$H_2 - H_3 = \frac{C (T_a - T_c)}{R_a - R_t} \quad (3.20)$$

We are here dealing with the thermocouple, which measures T_a and we assume that the temperature of the thermocouple wire at the outer cylindrical surface of the Sindanyo is equal to T_c . The length of the thermocouple in the Sindanyo is $R_a - R_t$.

We now use a function E given by

$$E = \frac{(T_a - T_c) C}{K_s R_t^2 M_I (R_a - R_t)} \quad (3.21)$$

and with this from equation (3.20) we obtain

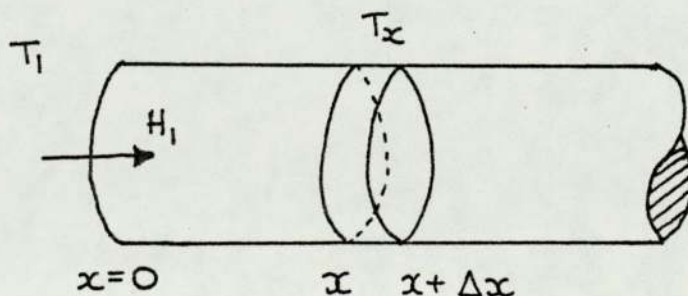
$$\bar{H}_2 = \bar{H}_3 + E \quad (3.22)$$

where $\bar{H}_2 = \frac{H_2}{K_s \lambda R_t^2 M_I}$

Section 'A' of the pin.

Consider a cylindrical rod, frictional heating being produced at $x = 0$, it is assumed that there is no temperature gradient along the radii of the rod, but that nevertheless heat is transferred from the rod surface to the air.

The temperature of the rod at $x = 0$ is taken to be the body temperature T_I .



Consider an element of length Δx at x .

The heat conducted across a plane at x is

$$-K_s \pi R_t^2 \frac{dT_x}{dx} \quad \text{and} \quad -K_s \pi R_t^2 \left(\frac{dT_x}{dx} + \frac{d^2T \Delta x}{dx^2} \right)$$

$$\text{The heat transferred to the air is } 2\pi R_t^2 h (T_x - T_c) \Delta x \quad (3.23)$$

h = heat transfer coefficient from the pin surface to its environment, where the ambient temperature of the air flowing past the pin is assumed to be equal to T_c .

Hence the thermal equilibrium of the element is

$$-K_s \pi R_t^2 \left(\frac{dT_x}{dx} + \frac{d^2T \Delta x}{dx^2} \right) + 2\pi R_t^2 h (T_x - T_c) \Delta x = -K_s \pi R_t^2 \frac{dT_x}{dx} \quad (3.24)$$

$$\text{From this } \frac{d^2T_x}{dx^2} = \frac{2h}{K_s R_t} (T_x - T_c) \quad (3.25)$$

$$\text{Putting } T = T_x - T_c \text{ and } z = \left(\frac{K_s}{2hR_t} \right)^{\frac{1}{2}} \quad (3.26)$$

$$\text{we get } \frac{d^2T_x}{dx^2} = \frac{T}{z^2 R_t^2} \quad (3.27)$$

The general solution is

$$T = B_1 e^{x/zR_t} + B_2 e^{-x/zR_t} \quad (3.28)$$

$$\text{or } T_x = B_1 e^{x/zR_t} + B_2 e^{-x/zR_t} + T_c \quad (3.29)$$

The boundary conditions are

at $x = 0$ $T_x = T_I$ and $H = H_I$

at $x = l_I$ $T_x = T_a$ and $H = H_2$

$$\text{Thus } T_I = B_I + B_2 + T_c \quad (3.29a)$$

$$H_I = \frac{K \pi R_t}{z} (B_2 - B_I) \quad (3.30)$$

Using equation (3.1) and differentiating equation (3.29)

$$T_a = B_I e^{1_I/zR_t} + B_2 e^{-1_I/zR_t} + T_c \quad (3.31)$$

$$H_2 = \frac{-K \pi R_t}{z} (B_I e^{1_I/zR_t} - B_2 e^{-1_I/zR_t}) \quad (3.32)$$

subtracting (3.32) from (3.31) gives

$$B_I = \frac{1}{2} \left((T_a - T_c) - \frac{zH_2}{K \pi R_t} \right) e^{-1_I/zR_t} \quad (3.33)$$

similarly

$$B_2 = \frac{1}{2} \left((T_a - T_c) + \frac{zH_2}{K \pi R_t} \right) e^{1_I/zR_t} \quad (3.34)$$

substituting (3.33) and (3.34) into (3.29a) and (3.32)

$$\begin{aligned} T_I &= \frac{1}{2} (T_a - T_c) (e^{-1_I/zR_t} + e^{1_I/zR_t}) \\ &\quad + \frac{1}{2} \cdot \frac{zH_2}{K \pi R_t} (e^{1_I/zR_t} - e^{-1_I/zR_t}) + T_c \end{aligned} \quad (3.35)$$

$$\text{or } T_I = (T_a - T_c) \cosh(1_I/zR_t) + \frac{zH_2}{K \pi R_t} \sinh 1_I/zR_t + T_c$$

$$(3.36)$$

similarly

$$H_I = \frac{K_s R_t}{z} \pi \left[\frac{1}{2} \left((T_a - T_c) (e^{1_I/zR_t} - e^{-1_I/zR_t}) \right) + \frac{zH_2}{K_s \pi R_t} (e^{1_I/zR_t} + e^{-1_I/zR_t}) \right]$$

$$\text{or } H_I = \frac{K_s \pi R_t}{z} (T_a - T_c) \sinh 1_I/zR_t + H_2 \cosh 1_I/zR_t \quad (3.37)$$

Equations (3.36) and (3.37) give the body temperature and the heat flow through the rubbing surface respectively, assuming that $T_a - T_c$ and H_2 are known from the previous section.

Before the temperature of the tip of the pin can be calculated values for the heat transfer coefficient to the air must be obtained. M^CAdams (Ref. A.1) has plotted a universal curve for air flowing normally to single cylinders, corrected for radiation to the surroundings. He plots Nusselt Number N_{mi} against Reynolds Number N_{re} where $N_{mi} = \frac{hD}{K_{air}}$ and $N_{re} = \frac{DU\rho}{\mu} = \frac{DU}{\nu}$

$$(3.38)$$

D = Diameter of the pin.

K_{air} = Thermal conductivity of air

U = Air Speed

ρ_a = Density of air

μ = Viscosity of air.

ν = Kinematic Viscosity of air.

N_{re} can be calculated and a value for N_{mi} obtained from the graph, hence a value for 'h' can be obtained.

- Ref. A.1. R.COY. "An investigation of the mechanism of the unlubricated wear of EN26 steel using several physical techniques" M.Sc. thesis. Aston University Sept. 1971.
 A.2. McAdams, W.H. Heat Transmission. New York, McGraw-Hill 3rd edition(1954)

The effect of elevated temperatures and speed upon the wear of mild steel

SYNOPSIS Experiments are described in which mild steel (EN8) pins are slid against mild steel disks at various loads, speeds and externally-induced disk temperatures. At low speeds, and at disk temperatures less than about 150C, the "wear rate versus load" graphs revealed transitions similar to those reported by Welsh in 1964. For a wide range of higher speeds and higher disk temperatures, however, it is shown that this transitional behaviour does not occur, i.e. mild wear persists at all loads. The importance of this result in so far as the wear behaviour expected of mild steel is discussed. Suggestions for further work involving the analysis of these results in terms of a modified oxidational wear theory are also discussed.

INTRODUCTION

1. There has been a marked increase in the amount of research in Tribology devoted to investigating the wear of materials, in particular of steels, under unlubricated conditions of continuous sliding. This research has arisen in response to the needs of the aerospace and nuclear power industries, where systems are expected to function reliably without conventional lubrication. A further complication occurs with most of these systems in that they are often required to function at elevated temperatures. Other industries, notably the steel manufacturing and forming industry, also have problems involving the wear of materials at elevated temperatures, where no conventional lubrication is possible. The present research, in fact, is related to the wear of guides used in hot rolling strip mills.

PREVIOUS WORK

2. The definitive paper on the unlubricated wear of metals must be that written by Archard and Hirst in 1956 (ref. 1). In this paper, they define wear as being either "mild" or "severe", in terms of (i) final surface roughness (ii) whether or not the contact between the surfaces is metallic (severe) or non-metallic (mild), and (iii) whether or not the wear debris is metallic (severe) or oxidized (mild). Although other classifications have been proposed for wear, this particular one has stood the test of time, due mainly to its dependence upon observable characteristics.

3. Using the Archard and Hirst classification, Welsh (ref.2) showed that most of the previously inexplicable wear behaviour of steels could be understood in terms of transitions from mild to severe wear (T_1) and from severe to mild (T_2) in the "wear rate versus load" graphs. Welsh pointed out that it was necessary to cover the

whole range of loads and speeds in order to get the characteristic wear pattern. He varied the carbon and chromium content of his steels and found that these characteristic patterns (and in particular the transitions) were strongly influenced by these alloying constituents, mainly through hardness changes but also through the influence of these constituents on the oxidation-behaviour. Welsh indicates that load and speed are mainly important because of their influence upon the temperatures at the real areas of contact, but he does not attempt to determine these temperatures.

4. Welsh did not use elevated temperatures for any of his experiments. Various researchers have carried out elevated temperature wear experiments, notably Lancaster (ref.3 and 4), but none has obtained the characteristic pattern of the type recommended by Welsh (ref.2), namely the variation of wear rate with load for changes in the other parameters, such as speed, metallurgical composition and ambient temperature. Lancaster's experiments were concerned with the wear of 60/40 leaded brass on tool steel, a combination which is well-known for its reproducible severe wear under most typical sliding conditions.

5. The aim of the present research was to obtain the characteristic wear patterns (i.e. wear rate versus load) for a common steel (EN8) (often used as replaceable pads in the guides in hot rolling steel strip mills) with sliding speed and ambient (surface) temperatures as the independent variables.

THE EXPERIMENTAL APPARATUS

6. The test machine built and used for the continuous sliding experiments described herein was the pin and disk machine shown in Fig. 1. It was designed to fulfil a wide range of applications in wear testing. It is capable of a range of loads from 1 to 500N, a range of

speeds from 0.3 to 7.5 m.s⁻¹ and a range of disk temperatures up to 700C. Ancillary equipment consists of devices to measure and continuously record the various desired temperatures, wear rates, friction and the speed.

7. The machine has one or two unusual features worth mentioning here. Firstly, the pin is loaded against the back of the disk, as shown in Figure 2. This allowed for easy mounting of the disk on the main shaft and easy heating of the disk without the risk of distortion. The main shaft was designed to withstand this unusual configuration. Facilities were provided for cooling the needle roller bearing at the front and the angular contact bearing at the back of the bearing assembly. At no time were these bearings at temperatures greater than 60C, even when the disk was running at 720C. Secondly, the pin was held in a heat flow calorimeter fixed to the loading arm in a similar fashion to that described by Grosberg and Molgaard (ref.5). The division of heat at the pin surface can be deduced from calculations involving the 3 thermocouple measurements taken at 2 points along the (insulated) length of the pin and at the inside surface of the copper calorimeter.

8. The drive system and friction measurement were fairly standard. The wear rate, i.e. the volume of pin material per unit sliding distance at the pin, was calculated from the decrease in pin height, monitored by a Linear Voltage Differential Transformer (LVDT), which sensed the forward movement of a plate fixed to the load shaft, the latter being loaded pneumatically for loads from 10N to 500N and by a dead-weight method for loads below 10N. To keep the friction between the load shaft and its bearings down to an insignificant amount, it was found to be necessary to exclude contamination (especially from wear debris) by enclosing the whole of the loading arm in a metal box.

9. The heater assembly consisted of a domestic cooker ring fixed to the face of the disk opposite to that on which the pin was loaded. The heater was supplied, via carbon brushes, by a 270 volt Auto-Transformer, providing disk temperatures up to 720C, readily controlled at any temperature to within $\pm 5C$, provided settled conditions were reached in an experimental run. The bulk disk temperature was measured using a thermocouple spot-welded to the wearing face of the disk at the radius of the asbestos spacer between the disk and the main shaft. Ancillary experiments indicated that this temperature was only about 10C more than at the sliding radius for most temperature settings.

EXPERIMENTAL DETAILS

10. The mild steel used for the pins and the disks was BS970, EN8 which has the following composition:-

C	Si	Mn	S	P
0.35-0.45%	0.05-0.35%	0.60-1.00%	0.060%	0.060%

The disks were cut from black bars and randomly ground to around 0.2 μ m (0.004 μ m) Centre Line Average (CLA). The pins were taken from cold-rolled rods and turned to a smooth finish. The

bulk hardness of the pin and disk material was 210 \pm 10 VPN. The disk dimensions were 0.12 m diameter and 12.7 mm thick; the pins were 38.1 mm long and 6.35 mm diameter. The disks and pins were degreased by washing in acetone and petroleum ether prior to each experiment.

11. Before the start of each elevated temperature run, the bulk disk temperature was raised to the desired value and maintained for about 15 min with the pin loaded against the disk, but with no sliding. The run was then started and adjustments made to the temperature until a steady wear rate was obtained at the desired temperature. There was very little further adjustment necessary once these steady state conditions were achieved, except when transitions (T_1 or T_2) occurred, in which case adjustments were necessary to overcome the few degrees change in temperature brought about by these transitions.

12. Welsh (ref.2) maintains that the wear of both surfaces should be measured when dealing with pin and disk experiments. Although provision for measuring the wear rate of the pin has been included in the machine, the disk wear rate (averaged over the whole run) had to be found from weighing before and after on a Triple-Beam balance. This was not an accurate method, being only sensitive to changes in weight greater than 10⁻⁴ kg. For comparison, the pins were weighed before and after experiments using an electronic chemical balance.

RESULTS

The effects of changing speed (at room temperature)

13. Fig. 3 shows how the wear rate of the pin and disk varied with load for the 0.75 m.s⁻¹ experiments. These are average values obtained by weight loss measurements. Clearly, the wear pattern is similar to the "classical" picture presented by Welsh (ref.2), with a T_1 transition (from mild to severe wear) at about 3N and a T_2 transition (from severe to mild wear) at about 80N. Note that the pin and disk are wearing at approximately the same rate. The corresponding graph of pin wear rate versus load, as measured by the LVDT, is shown in Fig.4, together with the pin wear rates for 1.0 and 1.25 m.s⁻¹. The wear rates at loads below the T_1 transition have not been plotted, but they were of the same order of magnitude as that found by weighing for the 0.75 m.s⁻¹ experiments. Fig. 4 shows that the form of the graphs are similar for each speed, with the T_2 transition occurring at lower loads as the speed is increased. Thus for speeds less than, or equal to 1.25 m.s⁻¹, one obtains the classical Welsh (ref.2) behaviour for mild steel sliding against itself without any external heating supplied.

14. Figure 5, a graph of wear rate versus load for the 4.0 m.s⁻¹ experiment, is typical of those obtained at the higher speeds. It can be seen that the wear rates are low (between 10⁻⁸ and 10⁻⁶ g.cm⁻¹) and comparable with the "post- T_2 " mild wear rates for the lower speed experiments (see Fig.3). The disk exhibits a lower wear rate, at a given load, for most of the experiments, which might indicate transfer is occur-

ing from pin to disk. All the surfaces exhibited the characteristics of mild wear (i.e. shiny oxidized surfaces and oxidized wear debris). All the indications are that this graph represents "post- T_2 " behaviour. This was confirmed, to some extent, by the LVDT measurements of the wear rate, as shown in Fig. 6, for the experiments carried out at 2.0 and 4.0 $m.s^{-1}$. It is interesting to note that this form of "wear rate versus load" graph is often found in published wear data, especially with a change in slope around 10 to 30N e.g. see Fig. 4 of Quinn's (ref. 6) paper in which a low alloy, medium-carbon steel was slid at 8 $m.s^{-1}$ in a typical pin-on-disk configuration.

15. The effect of speed upon the friction is shown in Fig. 7 (for higher speeds) and Fig. 8 (for the lower speeds). These graphs can be summarized by saying that equilibrium (or characteristic) frictions (about 0.4) are obtained at much lower loads (about 40N) for the higher speeds, compared with the 80 to 100N for the lower speeds. Clearly the high friction coefficients obtained with the low speeds and low loads are to be associated with the transitions in the wear mechanisms indicated in Fig. 3 and 4. In the author's view, this is one of the main uses for friction measurement in a wear experiment, namely it confirms changes indicated by other measurements.

16. The effect of speed upon the micro-hardness of the worn pin surface is shown in Fig. 9 (for a speed of 0.75 $m.s^{-1}$) and Fig. 10 (for a speed of 2.0 $m.s^{-1}$). These graphs show that the hardness of the pin surface increased dramatically with load for the low speed experiments, compared with the more gradual increase of the surface hardness with increasing load for the 2.0 $m.s^{-1}$ experiments.

The effects of changing disk temperature

17. The experiments at various elevated disk temperatures were all carried out at a speed of 1 $m.s^{-1}$, at temperatures up to 500C. The form of the "wear rate versus load" graphs are shown in Fig. 11, where now one sees an apparent "disappearance" of the T_2 transition with increasing the temperature of the disk above 100C. This should be compared with the "disappearance" of the T_2 transition at speeds above 1.25 $m.s^{-1}$ for the speed-varying experiments. The coefficient of friction versus load graphs (not shown) all indicated an equilibrium value of about 0.4 at all temperatures for loads greater than about 60N.

DISCUSSION

18. The aim of this research has only been partially fulfilled, since only one speed was used for the elevated temperature experiments. Nevertheless, the trends in the wear behaviour of mild steel can be seen from the amount of work already carried out. It is probable that trends are all that one can hope to perceive from such research, due to the prohibitive length of time required for a graph such as Fig. 11, where every point represents the slope of a "wear volume versus distance slid" graph carried out over 3 or 4 hours running!

19. The first point emerging from this research is the relative scarcity of severe wear and the abundance of mild wear as one alters load speed and disk temperature. This is a typical steel used in many industrial applications, the selection of this material often being made on the basis of its availability and cheapness rather than on a tribological basis. Nevertheless, this work indicates that mild wear is nearly always obtained at higher load, speeds and temperatures. Since mild wear can be acceptable for some unlubricated situations, especially where high temperatures are involved, then this research indicates that the commonly-held view of mild steel as a poor material for tribological situations may be in error. This, by itself, is a worthwhile piece of knowledge.

20. The second point is also related to the scarcity of severe wear, since it leads one to enquire how representative is the Welsh (ref. 2) behaviour pattern (as typified by Fig. 3 and 4 of this paper) for steels other than mild steel? There seems to be an increasing amount of evidence building up to support the suggestion that the typical wear pattern should be more like that of Fig. 6, namely a linear increase in the logarithm of the wear rate when plotted against the logarithm of the load, with sometimes a slight "kink" in the line indicating a change in specific wear rate.

21. Having shown that the T_2 transition is not too important in the wear behaviour of mild steel one can now concentrate on the mild wear situations indicated by Fig. 11 (for disk temperatures equal to or greater than 200C) and Fig. 6 (for speeds equal to or above 2 $m.s^{-1}$). Although there is plenty of variation about the lines on Fig. 11, one can see that the lines for 200, 300 and 400C all lie significantly above the 500C line. Does this mean that a different form of metal-substrate or surface oxide is formed at the highest disk temperatures? What is the temperature at the real areas of contact between the pin and the disk. Is the increase in wear rate with load due to an increase in this temperature? These and many other questions will have to be answered by further work, probably along the lines used by Quinn (ref. 7), where he measured the division of heat and the surface temperatures at sliding steel interfaces and related these to the wear rate (assuming an oxidational wear theory). Clearly, Quinn's approach will have to be modified to take into account the effect of oxidation at the elevated temperatures used in the present experiments.

22. The effect of speed upon mild wear is not really shown by Fig. 6, although there may be a decrease in wear rate with increased speed, for a given load. This trend will have to be confirmed by further work. It is probable that this trend is also due to increased temperatures at the real areas of contact, caused by the increased speed of sliding. In this case, Quinn's (ref. 7) approach can be applied directly, since there is not the complication of externally induced surface temperatures. This will be the subject of a later publication, which will also deal with the application of physical techniques (e.g. X-Ray diffraction, electron diffraction, electron microscopy and electron probe microanalysis) to the study of the changes in composition and topography of both the wearing surfaces and the wear debris brought about by the increased temper-

atures. The metallographic changes in the sub-surface region will also be studied.

ACKNOWLEDGEMENTS

23. This research was made possible as a result of cooperation between the University of Aston in Birmingham, the Corporate Laboratories of the British Steel Corporation (BISRA) in London, and the Science Research Council under the Cooperative Awards in Science and Engineering (CASE) Scheme. The authors would like to thank Mr. C.J.S. Chapman and Mr. F. Lane, of the University of Aston in Birmingham, for their help with the design and fabrication of the elevated temperature wear test rig.

REFERENCES

1. ARCHARD J.F. and HIRST W. The Wear of metals under unlubricated conditions. Proc.Roy. Soc., A236, pp 397-410, 1956.
2. WELSH N.C. The dry wear of steels
I The General Pattern of Behaviour
II Interpretation and Special Features
Trans.Roy.Soc., Phil.Trans., A257, pp 31-79, 1965.
3. LANCASTER J.K. The influence of temperature on metallic wear. Proc. Phys.Soc. B, 70, pp 112-119, 1957.
4. LANCASTER J.K. The formation of surface films at the transition between mild and severe metallic wear. Proc.Roy.Soc. A 273, pp 466-483, 1963.
5. GROSBERG P. and MOLGAARD J. Aspects of the wear of spinning travellers. The division of heat at rubbing surfaces. Proc.Instn.Mech.Engrs. 181, Pt. 3L., 1966-67.
6. QUINN T.F.J. The effect of "hot-spot" temperatures on the unlubricated wear of steel. ASLE Transactions, 10, pp 158-168, 1967.
7. QUINN T.F.J. The division of heat and surface temperatures at sliding steel interfaces and their relation to oxidational wear. ASLE Transactions Preprint No 76-LC-2B-1. Paper presented at the ASLE/ASME Lubrication Conference in Boston, Massachusetts, October 5-7, 1976.

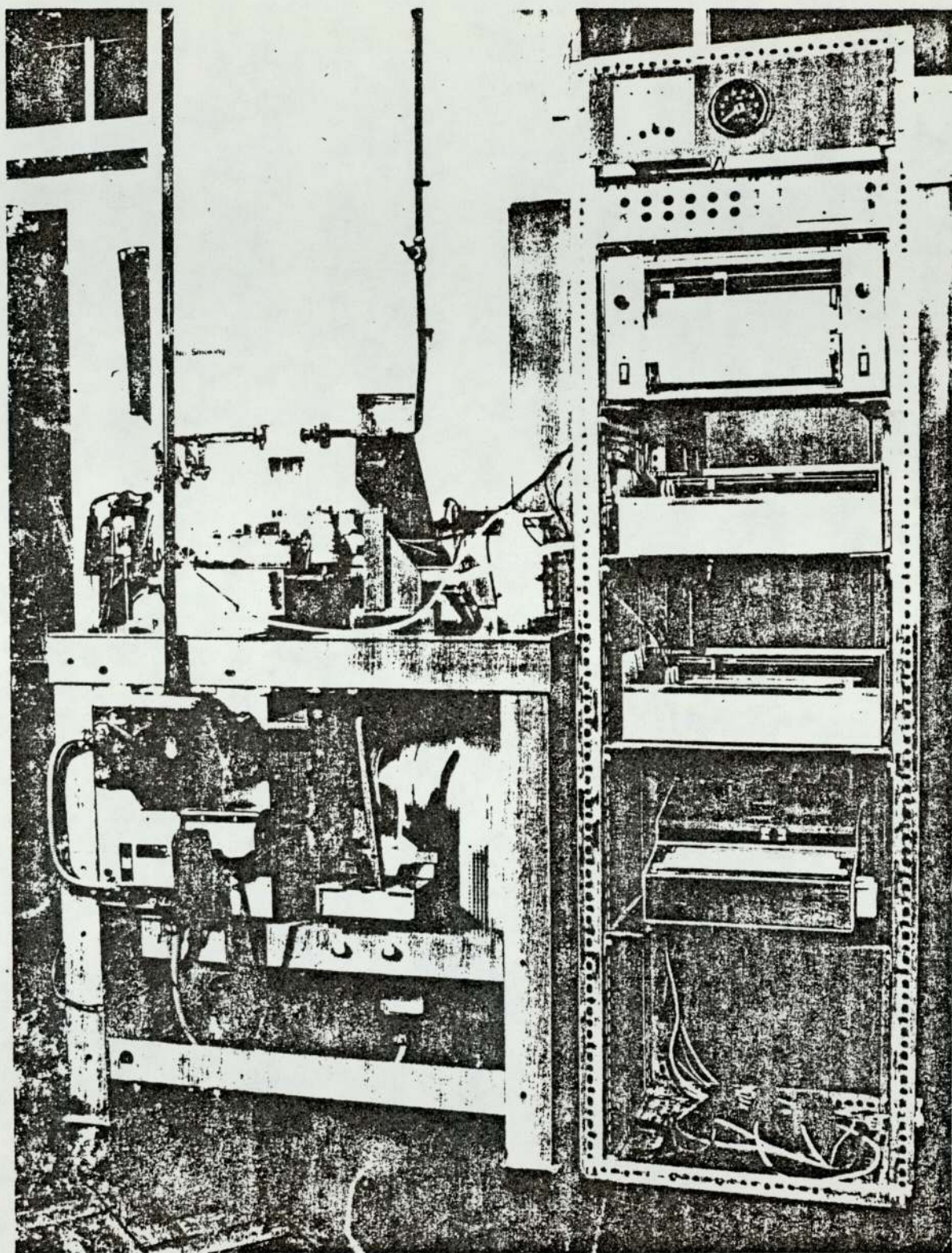


Figure 1 : General view of elevated temperature pin and disk

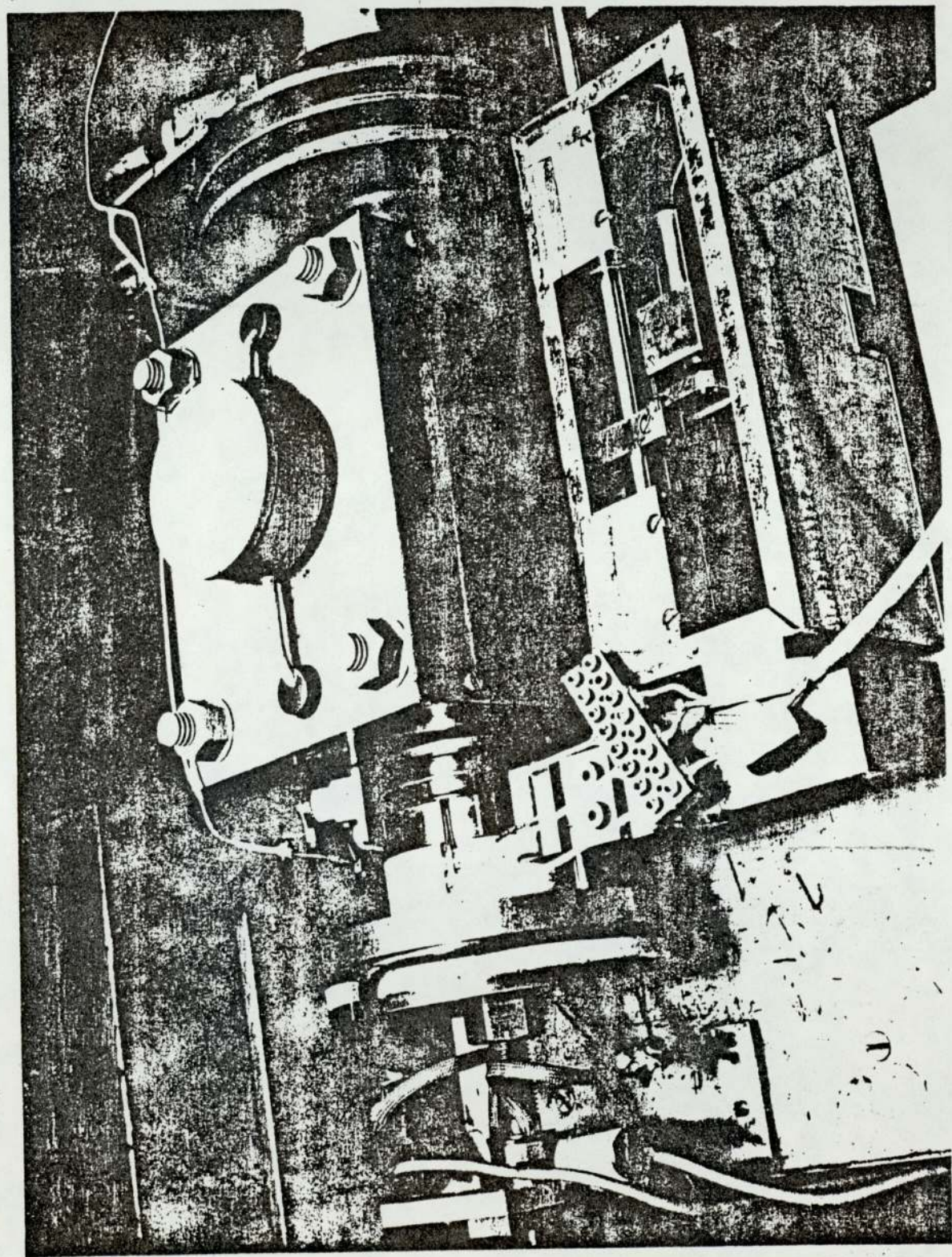


Figure 2: Close-up view of pin and disk
and microwave equipment

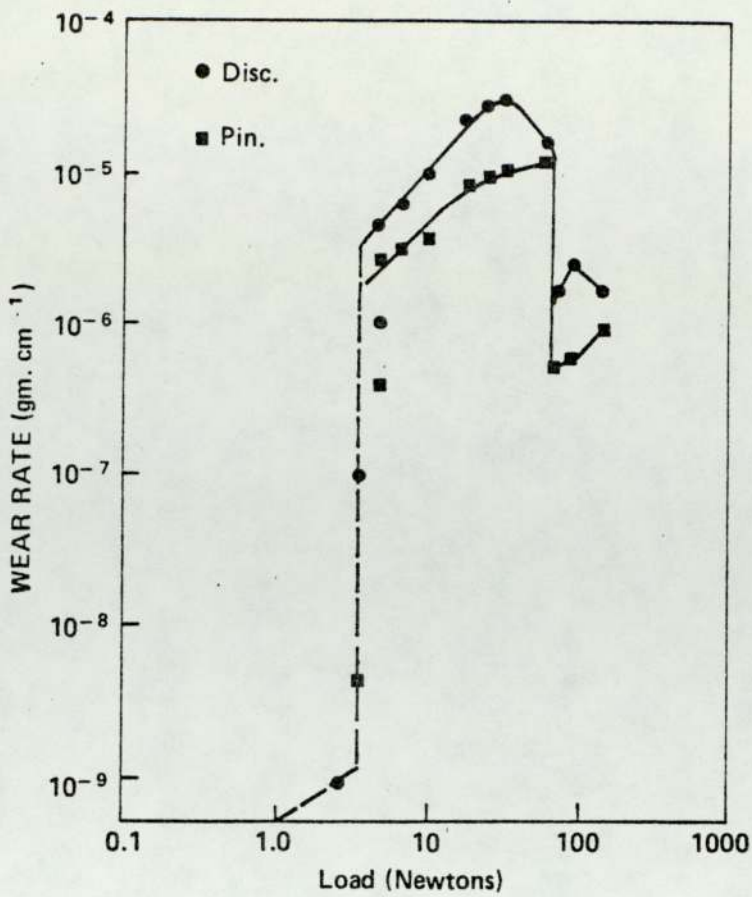


Figure 3: Wear rate (weight-loss method) versus load; sliding speed : 0.75 m.s^{-1}

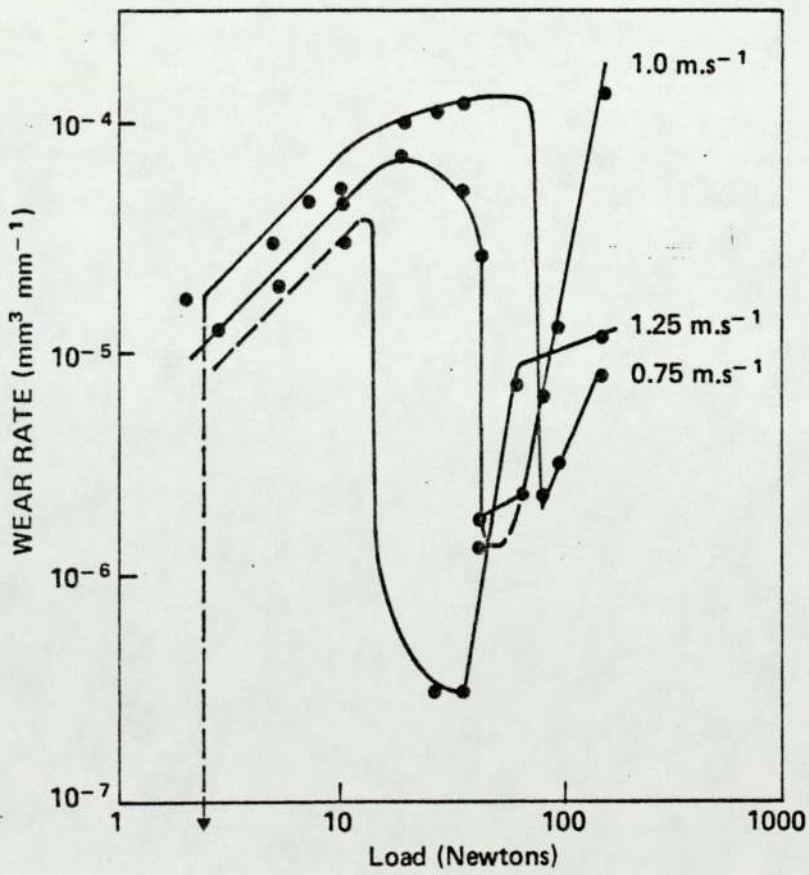


Figure 4: Wear rate of pin versus load for the lower sliding speeds

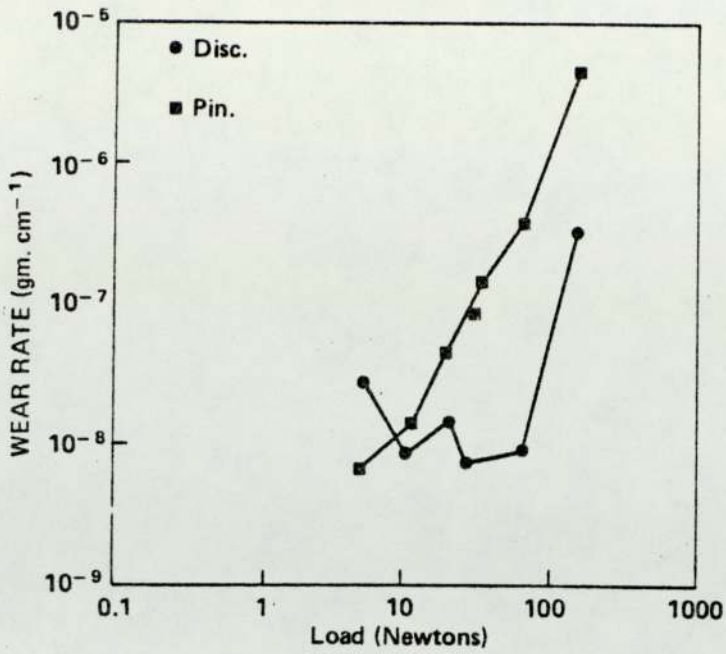


Figure 5: Wear rate (weight-loss method) versus load; sliding speed : 4.0 m.s^{-1}

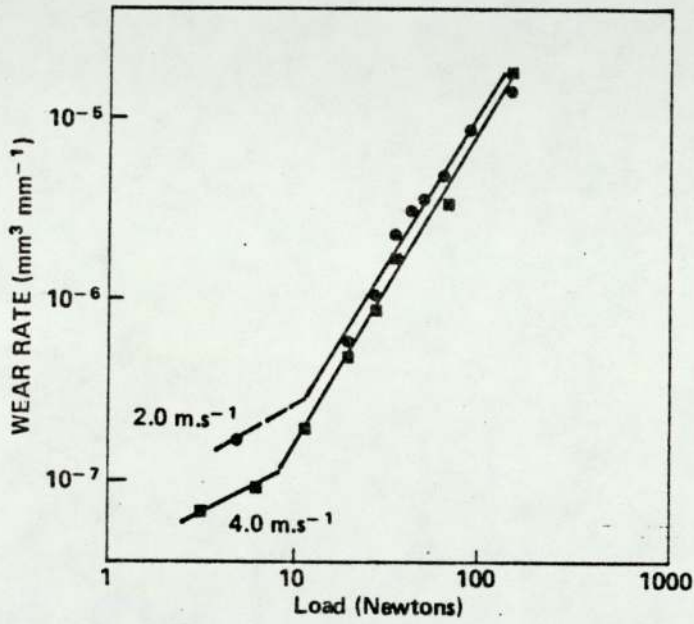


Figure 6: Wear rate of pin versus load for the higher sliding speeds

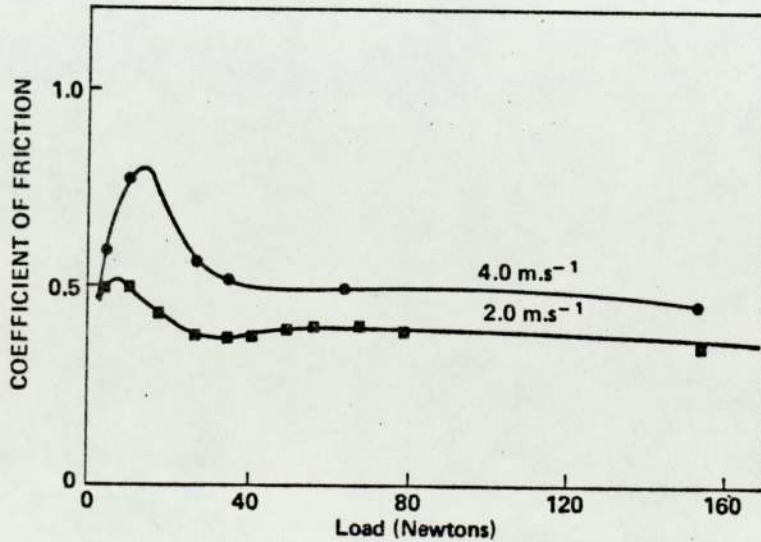


Figure 7: Friction coefficient versus load for higher speeds

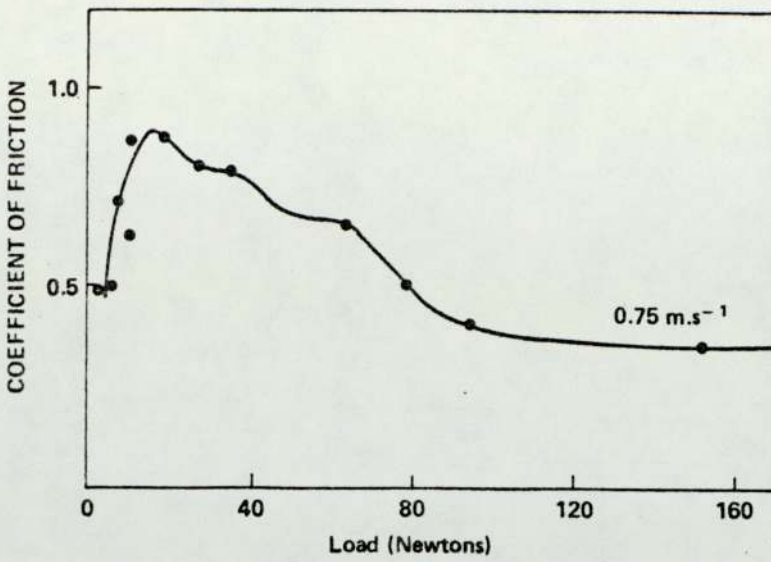


Figure 8: Typical graph of friction coefficient versus load for lower speeds

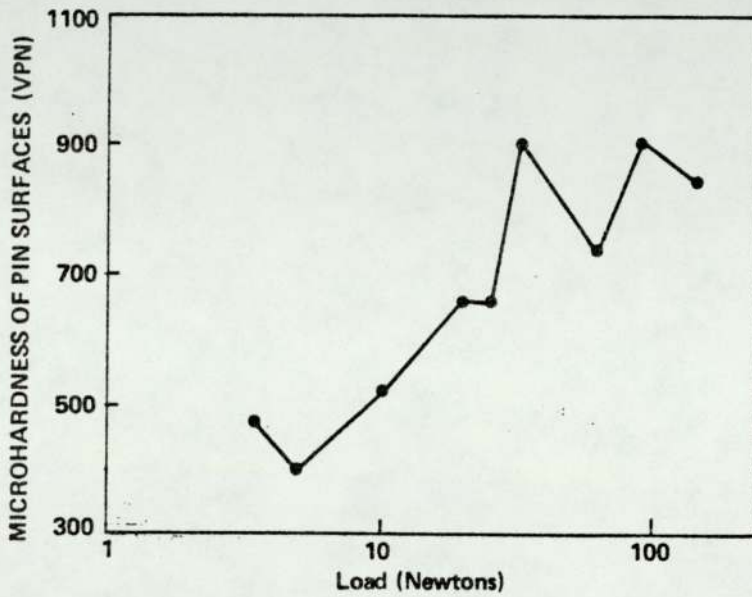


Figure 9: Microhardness of pin surfaces sliding speed : 0.25 m.s^{-1}
No externally - induced heating.

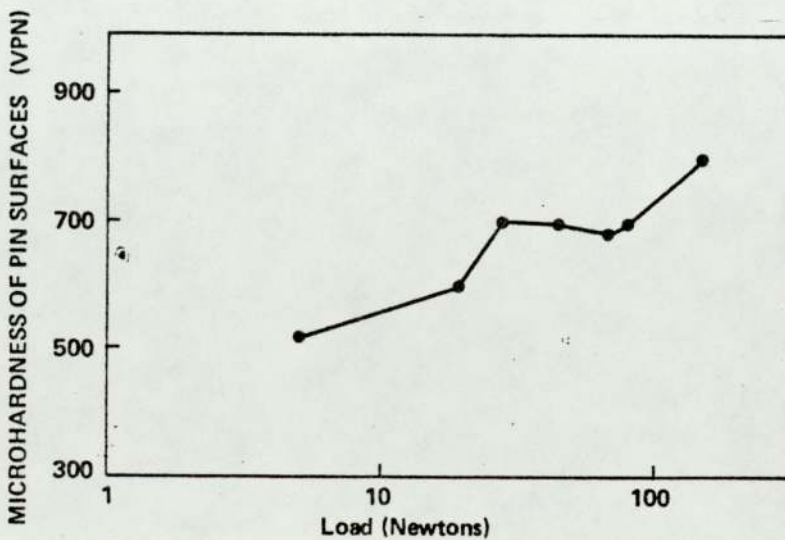


Figure 10: Microhardness of pin surfaces after wear
Sliding speed : 2.0 m.s^{-1} ; No external heating

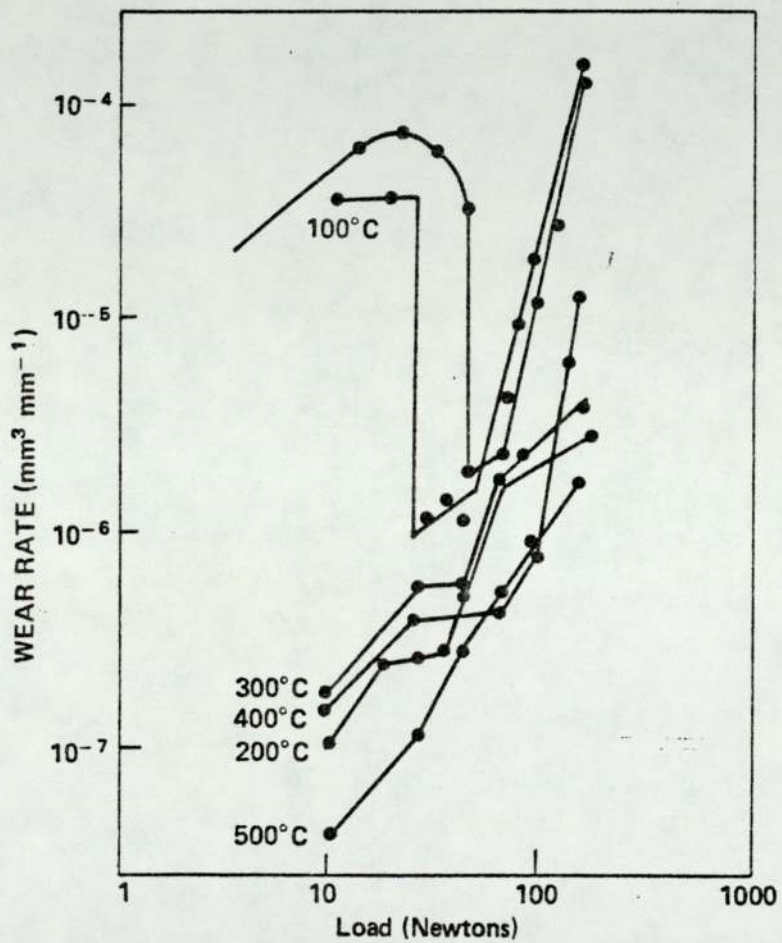


Figure 11: Wear rate of pin versus load for various externally-induced disk temperatures.



Studies of the Unlubricated Wear of a Commercial Cobalt-Base Alloy at Temperatures up to about 400 C

P. M. DUNCKLEY, T. F. J. QUINN*, and J. SALTER

The University of Aston in Birmingham
Birmingham B47ET, England

Pins of a commercial cobalt-base alloy (Stellite 31) have been worn against disks of the same material at room temperature and at various externally-induced ambient temperatures between about 100 C and 400 C, under continuous and reciprocating sliding conditions without lubrication. An unexpected maximum in the wear rate versus ambient temperature curve occurred at about 200 C for specimens which had previously been exposed to ambient temperatures less than the temperature of any given experiment. On entirely new specimens, however, this maximum could not be detected, although there was a pronounced decrease in the wear rate at around 200 C. Friction coefficients, pin temperatures, surface topographies, and the compositions of the wear debris were determined for these experiments, and significant changes were also noted to occur at disk temperatures around 200 C.

The changes in wear, friction, temperature, wear debris composition, and surface topography around 200 C are discussed in terms of the onset of a mild wear mechanism in which the spinel oxides of chromium and cobalt are assigned important roles.

INTRODUCTION

The unlubricated wear of cobalt-base alloys has received very little attention from previous investigators, which is surprising in view of the extensive use of such materials in aircraft engine manufacture. There has been some work by Peterson, Florek, and Lee (1) and Foley, Peterson, and Zapf (2) on the unlubricated sliding of pure cobalt at elevated temperatures and low speeds. Dunckley and Johnson (3) have also carried out some elevated temperature experiments with cobalt. Huppman and Clegg (4) have carried out experiments, without any form of external heating, on the friction and wear of an 8 percent Fe-Co alloy. The main conclusion

Visiting Professor of Mechanical Engineering at Virginia Polytechnic Institute and State University, Blacksburg, Virginia 24061 (1974-75)

to be drawn from previous work on the wear of cobalt is that there may be an effect of a crystallographic change of the room-temperature hexagonal structure to the high-temperature face-centered cubic structure, upon the friction coefficients and wear rates at surface temperatures around 450 C.

Jesper (5) has carried out the most definitive work on the wear of cobalt-base alloys of the type often used in high-temperature applications. All his work, however, dealt with reciprocating sliding, as compared with the continuous sliding work mentioned above. The average speed of sliding during the oscillations was very small and the load was also insufficient to cause much frictional heating. He showed (5) that the reciprocating sliding of Haynes Stellite 25 against itself exhibited a low wear rate at temperatures greater than about 400 C. However, at temperatures around 300 C, the wear rate was about two orders of magnitude greater than at 400 C and about one order of magnitude greater than at room temperature. Jesper (5) also reported a similar minimum in the "wear-resistance versus ambient temperature" curve for Nimonic 80 wearing against Haynes Stellite 25. The comparatively high wear of cobalt and cobalt-base alloys at the lower ambient temperatures could have important practical implications, since this type of alloy is often used in gas turbine engines.

The significance of the ambient temperature is somewhat blurred by the fact that, undoubtedly, the wearing surfaces were at some temperature in excess of ambient, according to the speed of sliding and the applied load. Only for slow sliding speeds and low loads, can one neglect the effects of frictional heating upon the temperature of the sliding contacts. It is difficult to assess this actual temperature of contact, although Archard (6) has shown how to get approximate values for the excess temperature over ambient for steels. In this paper, an attempt will be made to deduce the most probable temperature of the contact areas, since this is clearly more relevant than the ambient temperature.

This paper describes some pin and disk experiments

carried out with the cobalt-base alloy commercially known as Stellite 31. A first set of continuous sliding experiments was carried out with a fresh pin and disk surface for each of the externally-induced temperatures of the disk. A second set of experiments was carried out at increasing disk temperatures from about 30 C to 400 C, with the same disk and the same pin. Although the surfaces were polished and cleaned prior to each run, the metallurgical properties of the bulk of the material of the disk and the pin must have been affected by the prolonged heating of the previous experiment. This second set of experiments was carried out with much more elaborate measuring instruments; namely, friction and pin temperatures were determined, as well as the wear rate and the disk temperatures. By way of comparison, some results obtained on a reciprocating sliding test rig, consisting of a spherical button rubbing against a flat plate, are also described.

X-ray diffraction analysis of the wear debris from these experiments was also carried out wherever there was enough debris to be used in the X-ray powder cameras. The topographies of selected surfaces were also examined using transmission electron microscopy of replicas of the worn surfaces.

EXPERIMENTAL DETAILS

The Pin and Disk Wear Machine

The machine used for the continuous sliding experiments was a modification of a machine described elsewhere (7). Essentially, the machine consisted of a horizontal pin holder which enabled the pin to be loaded pneumatically against the flat face of a disk which was held in a chuck attached to a variable speed drive, the axis of which was horizontal. The modifications enabled the disk to be externally heated to about 400 C. The disk temperature was measured with a thermocouple placed in the surface of the disk near to the wear track.

For the first set of experiments, the pins were wedge-shaped, about 0.6 mm thick, and were held in a chuck which was allowed to pivot about an axis which was coincident with the axis of the disk. The frictional drag of the rotating disk on the pin caused the chuck system to rotate against a restraining force provided by a spring (for the first set of experiments) or a distance transducer (for the second set of experiments). The amount of rotation, or the force causing the transducer to change its output, was measured respectively by a sensitive dial gauge or a pen recording instrument. Both methods of measuring the frictional drag were calibrated as a function of the moment required to cause the rotation.

For the second set of experiments, the pins were cylindrical and the temperatures at three places A, B, and C (as shown in Fig. 1) were continuously measured. These temperatures can be used for calculations of heat flow along the pin, but in these experiments they were used to give only rough estimates of the actual temperature of the pin surface.

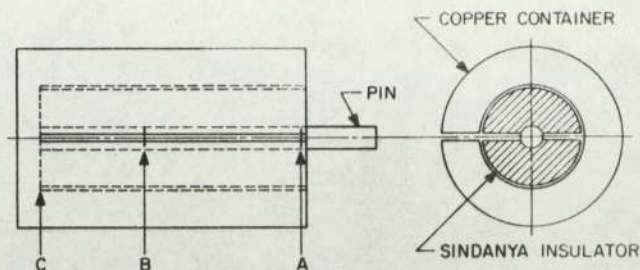


Fig. 1—Pin holder used for measuring temperatures of pin

The Specimens

The disks were circumferentially ground from a cast ingot of Stellite 31. The composition of the ingot was 50 percent cobalt, 20 percent chromium, 15 percent tungsten, 10 percent nickel, together with small amounts of iron, manganese, and silicon. When cast, the hardness of the ingot was about 325 Brinell maximum. The pins for these experiments were fabricated from a slice of the same ingot used for the disks.

Method of Measuring Wear

In the first set of experiments, the wedge shape of the pins readily allowed a measure of the volume of material removed from the pins during sliding by pressing the pin against a piece of aluminum foil, backed by tissue paper and thin metal sheet, to give an impression of the scar width. The width of the impression was measured with a travelling microscope. Thus, the measurement of scar width could be carried out in the shortest possible time with the minimum possible disturbance to the system, especially to the specimen alignment. Comparison of the final scar widths measured directly from the pins and from the impressions confirmed that this technique was sufficiently accurate for the purposes of the experiments.

In the second set of experiments, the decrease in height of the cylindrical pin was measured directly with a travelling microscope.

Electron Microscopy and X-Ray Diffraction

Electron microscopy was used for examining surface topographies. The disks were examined using a replicating technique involving two-stage, plastic and carbon, shadowed replicas. This technique is fairly conventional and needs no elaboration here.

X-ray diffraction of the wear debris was also very conventional. The debris was placed in a fine capillary tube of noncrystalline glass, and irradiated in an X-ray powder camera using molybdenum X-rays. The exposure times were about twelve hours. Such long times were necessary in order to detect the minor constituents present in the wear debris.

The Button-on-Plate Experiments

The button-on-plate experiments consisted of a spherical button loaded against a flat plate. This plate was reciprocated at 1,500 cycles/min with a peak-to-peak

plitude of 2.5 mm. The normal load between the plate and button was 5.7N. The wear was obtained by measuring the widths of the scar formed after a fixed number of cycles and calculating the volume of material removed from the button. This method can only give an average wear rate (where wear rate is measured in units of volume removed per unit sliding distance). If there is a change from severe to mild wear [see Ref. (8) regarding these classifications of unlubricated wear] during the course of 10^5 cycles, the average wear rate will be very different from the equilibrium mild wear rate, especially if mild wear is only just beginning to set in. Various ambient temperatures, from room temperature up to 400 C or more, were obtained by enclosing the button, the button loading arm and the plate in a thermostatically-controlled furnace.

Two-stage carbon, shadowed replicas were obtained from worn parts of the plate, and transmission electron micrographs obtained from these replicas. The plate of this reciprocating sliding apparatus corresponds to the disk of the continuous sliding rig, since a particular location was not in contact with the button over the whole length of the stroke.

EXPERIMENTAL RESULTS

Wear Experiments

The load used for both sets of experiments with the pin and disk machine was 9.8N. The disk temperature for the room temperature experiments was about 35 C. The room temperature was about 20 C, so that it would mean that frictional heating contributed about 15 C to the temperature of the disk surface.

The externally-heated experiments were carried out at 100 C, 200 C, and 270 C in the first set of experiments, and 130 C, 200 C, 350 C, 400 C and 410 C in the second set of experiments. The linear speeds were all 1.00 ± 0.10 m/s. Each experiment took about five or six hours, with the wear scar width or pin height being measured every half-hour. The slope of the graph of volume of pin material removed versus distance of sliding is conventionally taken to be the equilibrium wear rate.

The line is straight for the whole of the experiment and also passes through zero, as shown in Fig. 2 for the room temperature experiments, it can be assumed that severe wear (β) has been occurring. It will be shown that the other characteristics of severe wear were also present in the room temperature experiments, namely, comparatively rough surfaces and mainly metallic wear debris (see later sections).

In this description of the results of these experiments, the capital letters A, B, C, D are assigned respectively to the room temperature, 100 C, 200 C and 270 C experiments of the first set; the numbers 1, 2, 3 + 4, 5, 6 and 7 are assigned respectively to the room temperature, 130 C, 200 C, 350 C, 400 C and 410 C experiments of the second set. Experiments A and 1, which were both carried out without any external heating, gave results which lie approximately on the same straight line passing

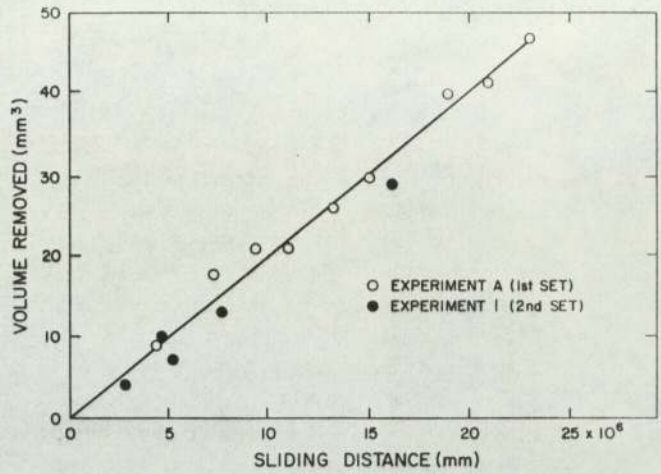


Fig. 2—Volume of pin material removed versus distance of sliding: Disk temperature about 30 C (no external heating).

through zero when the volume removed is plotted against the sliding distance (Fig. 2). This is important; since, for both Experiment A and Experiment 1, the pin and disk were new and had not been exposed to any previous heating since being fabricated.

On the other hand, there is a marked difference between the two sets of experiments for externally-induced disk temperatures, as shown in Fig. 3. Experiments 3 and 4 (carried out at 200 C after the pin and disk had already been exposed to previous heating cycles) gave a straight line (of slope 3.45×10^{-6} mm³/mm) which passes near to zero, for the wear volumes plotted against distance slid. This is markedly different from the slope of the line representing the results of Experiments B and C (carried out at 100 C and 200 C).

It is unfortunate that the machine was modified after Experiment D (at 270 C), since only one point had been obtained for that experiment. Clearly, however, the average wear rate was about 0.35×10^{-6} mm³/mm, almost an order of magnitude less than the room temperature

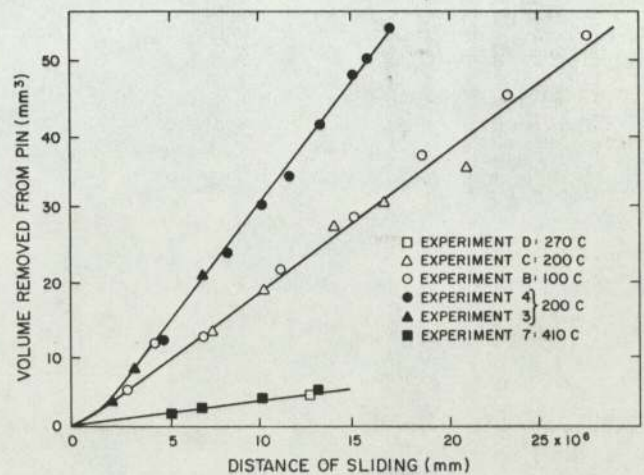


Fig. 3—Volume of pin material removed versus distance of sliding for various disk temperatures.

ar rate of 2×10^{-6} mm³/mm. Furthermore, it will be shown (in later sections) that the wear debris contained fines and the surfaces were comparatively smooth, which are two of the characteristics of mild wear (8). It is interesting to note that the one point for Experiment 7 (the pre-heated pin and disk specimens worn at 200 C). This straight line also seems to go through zero, which is not characteristic of mild wear behavior. It will be shown, however, that the other characteristics of mild wear were observed in Experiment 7.

For the purposes of comparison, it is relevant, at this stage, to give a brief summary of some of the experimental results obtained in the button-on-plate reciprocating sliding experiments. Using Stellite 31 material for the button and plate, it was found that the volume of material removed from the button passed through a maximum value around an ambient temperature of 200 C. It will be recalled that the whole of the wearing system was placed in an atmosphere at a given temperature, so this ambient temperature measurement probably entails a slightly higher pin and disk temperature than that recorded by the disk thermocouples in the continuous sliding experiments. The results are shown in Fig. 4. The letters V, W, X, Y, and Z have been used to designate the unheated, 100 C, 200 C, 300 C, and 400 C experiments respectively. Several experiments were carried out at each given temperature, and the error bars indicate the range of values obtained. Note the wide range of values occurring at 200 C, namely, 0.75 ± 0.20 mm³ (i.e., a 30 percent variation) compared with

0.16 ± 0.02 mm³ (i.e., a 6 percent variation) at about 300 C.

In order to compare the reciprocating and continuous sliding experiments, it is assumed that the wear volume will be proportional to the total distance of sliding and the real area of contact for the reciprocating sliding experiments, as well as for the continuous sliding experiments. These assumptions are in accord with the Archard wear law (9). As a first approximation, one can assume that the real area of contact is proportional to the load for a given hardness (10). Hence, in Fig. 5, the wear rate per unit load (i.e., the specific wear rate) is plotted against disk temperature (for the continuous sliding experiments) or the ambient temperature (for the reciprocating sliding experiments).

From this figure, one can see that there is a more pronounced effect due to previous heating cycles than any effect of whether or not the sliding is continuous or reciprocating. There are definite maxima at about 200 C in both the reciprocating and the continuous sliding experiments (in which previous exposure to heating cycles had occurred), whereas the completely new pins and disks exhibited a gradual decrease in wear rate. If one compares the pin and disk experiments, one can see that severe wear behavior is replaced by mild wear at a much lower temperature for the fresh specimens than for the preheated specimens, about 120 C lower. Although one cannot be definite about the type of behavior exhibited by the button on plate experiments, the electron microscopy indicates that the worn surfaces were roughest at about 200 C, (see later section), so that severe wear was probably occurring at this temperature. It is gratifying to find that the specific wear rates at 200 C and 400 C were very close to each other for both sets of experiments

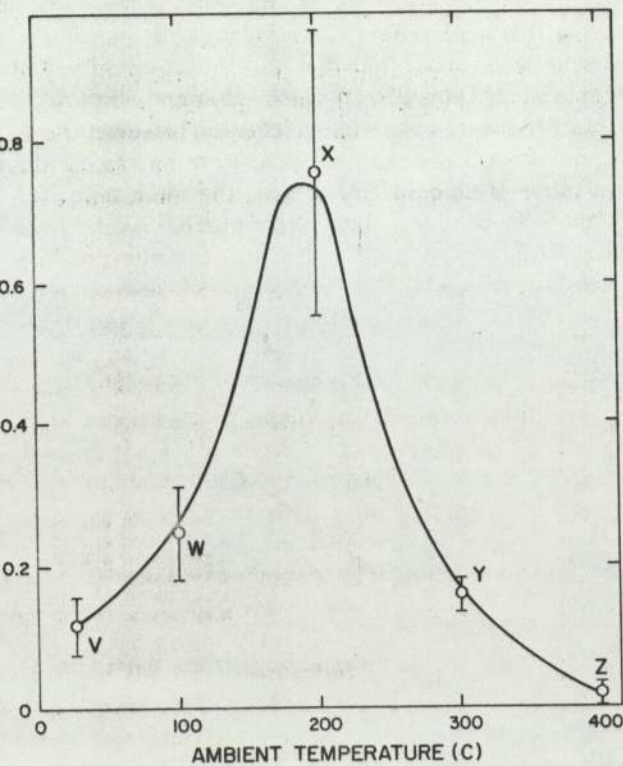


Fig. 4—Volume of button material removed during 10^5 cycles at 157 cps and a load of 5.6N, plotted against ambient temperature.

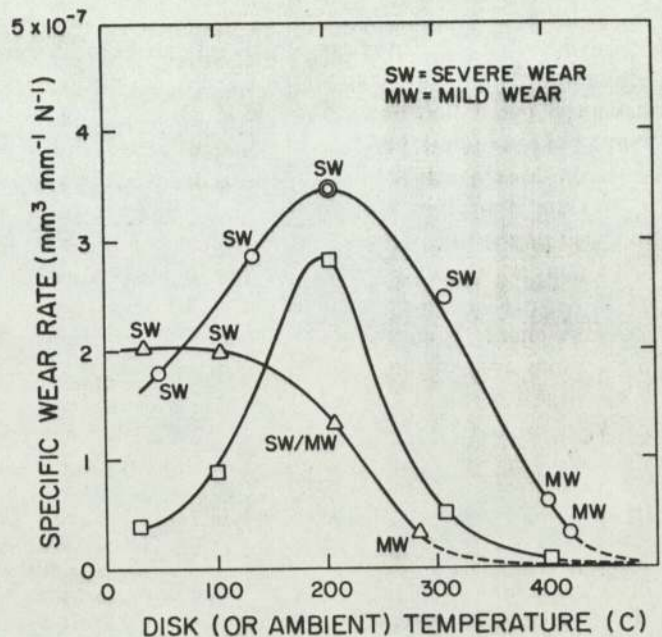


Fig. 5—Specific wear rates for unidirectional tests with fresh (Δ) and preheated (\circ) specimens and reciprocating tests with preheated specimens (\square).

which the specimens were subjected to preheating cycles.

Graphs of friction coefficients versus disk temperatures are only available for the second set of continuous sliding experiments. This was due to the inherent instability of the method used for measuring friction in the first set of experiments, especially when the wear was severe. The pin holder was not allowed to rotate in the second set of experiments, thereby ensuring a much more stable friction-measuring system. Figure 6 shows the initial and final equilibrium values of the coefficient of friction for

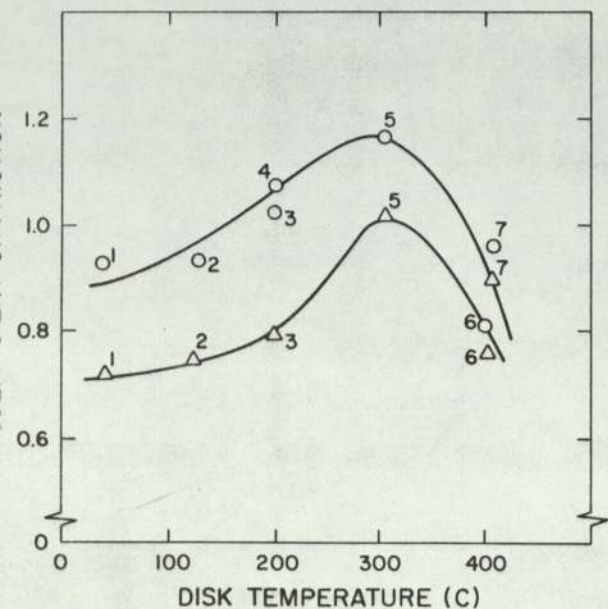


Fig. 6—Initial (O) and Final (Δ) friction coefficients for Stellite 31 pins sliding on Stellite 31 disks at various disk temperatures.

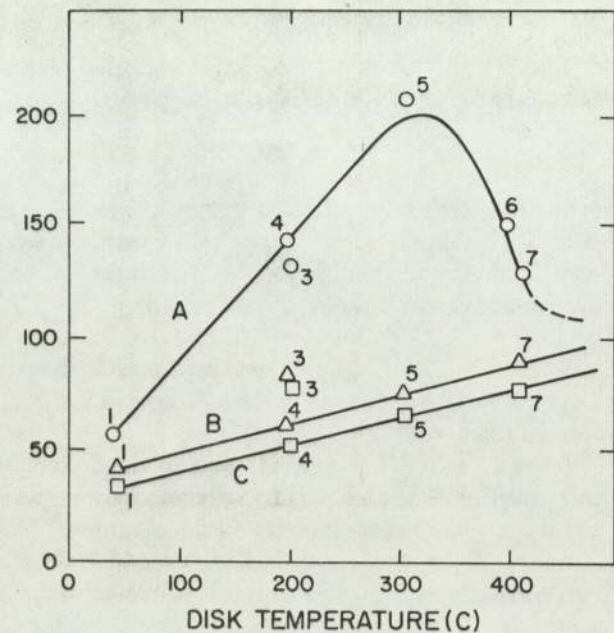


Fig. 7—Thermocouple readings at positions A, B & C of Stellite 31 pins sliding against Stellite 31 disks at various disk temperatures.

Experiments 1, 2, 3, 4, 5, 6, and 7. Clearly, the friction began to rise at about 200 C and reached a maximum at disk temperatures of about 300 C. A similar behavior occurred in the readings of the thermocouple nearest to the pin surface (i.e., thermocouple A), as shown by Fig. 7. The thermocouple readings for Experiment 2 were invalidated by failure of the recording devices, as also were the thermocouple readings for portions B and C for Experiment 6. There is enough evidence, however, to indicate a sudden increase in the temperature gradient at a disk temperature of 400 C. This, combined with the fact that the bulk temperatures of the pin and the copper block (B and C, respectively) show merely a gradual increase in temperature with increasing disk temperature, leads one to the assumption that, above 300 C, there is either (i) a sudden loss of heat to the air through some radiative process, or (ii) that a badly-conducting film is suddenly formed at the real areas of contact when the disk has a temperature of about 350 C. An oxide film would cause this phenomenon, and it will be shown in the next section that there is indeed a sudden appearance of oxide lines in the X-ray diffraction patterns from the wear debris for temperatures above 300 C.

X-Ray Diffraction Analyses of the Wear Debris

The wear debris from both sets of continuous sliding experiments was analyzed by the X-ray powder technique (see Table 1). From the X-ray diffraction evidence, it can be seen that this cobalt-base alloy has the face-centered cubic lattice of cobalt at the lower temperatures, despite the fact that, for pure cobalt, the low temperature phase has a hexagonal structure. Evidently, the alloying of the cobalt with chromium, tungsten, and nickel has caused this phase to be retained at the lower temperatures.

There is an obvious effect of previous heat cycles on the temperature at which the oxide lines become visible in the X-ray diffraction patterns, namely, this temperature is about 200 C for the fresh specimens and about 400 C for the previously-heated specimens. The decrease in friction at 400 C (Fig. 6) and the increase in temperature gradient at 400 C (Fig. 7) for the previously-heated specimens is consistent with the assumption that the spinel cobalt oxide (Co_3O_4) is formed in sufficient quantities to affect these parameters at some temperature between 350 C and 410 C. Most oxides are poor conductors of heat and the spinel oxide of other similar metals (e.g. iron) are known to be conducive to low friction (11). It has also been shown (12) that the wear of steels is associated with a predominance of the spinel iron oxide in the wear debris, and this would clearly account for the low wear at 400 C (see Fig. 5) if a similar effect occurs with the Stellite 31 specimens.

It will be recalled that the wear rate of the fresh pin and disk specimens showed a definite decrease (from the room temperature value) when the disk temperature was 200 C (see Fig. 5). This is probably due to the formation of the spinel chromium oxide. This substance was also detected at 270 C, where the wear rate was much less

TABLE 1—IDENTIFICATION OF WEAR DEBRIS FROM THE CONTINUOUS SLIDING EXPERIMENTS

TEMP. (°C)	IDENTIFICATION			
	EXPT. NO.	1ST SERIES	EXPT. NO.	2ND SERIES
35	A	fcc cobalt	—	—
100	B	fcc cobalt	—	—
200	C	fcc cobalt + trace of unknown substance with large crystallites	3	fcc cobalt only
270	D	fcc cobalt + large crystallites of spinel chromium oxide	—	—
305	—	—	5	fcc cobalt only
400	—	—	6	fcc cobalt + crystallites (of same size as the cobalt) of spinel cobalt oxide
410	—	—	7	

200 C, thereby indicating the low wearing properties of such oxides.

At temperatures at which these transitions take place, the actual real areas of contact must be more than the recorded disk temperatures for the continuous sliding experiments. This effect will be dealt with more fully in the discussion.

Electron Microscopy of Selected Specimens

Transmission electron microscopy of replicas was used to examine the final topographies of the wear tracks on the worn plate of the button-on-plate experiments and the wear tracks on the disks of the pin-and-disk experiments. Fresh specimens were used at each temperature. Unfortunately, the experimental procedure did not allow micrographs to be taken of the tracks on the disk in the second set of pin-and-disk experiments. Figure 9 contains four electron micrographs of replicas from various areas on the worn plate used in the reciprocated button-on-plate experiments. Figure 8(a) shows the typical worn surface obtained without external heating. It is fairly rough, being covered with lumps which may be transferred material, but which could be actually coming from the surface as incipient blisters. At 100 C, the worn surface (see Fig. 8[b]), the worn surface shows these blisters to be much more pronounced. At 200 C, (not shown here) the surface was at its maximum roughness. At 300 and 400 C, however, the surface had completely changed to a topography in which large flat island plateaux had formed above the rough lumps (see Figures 8 [c] and [d]). Figure 9 shows electron micrographs of the wear tracks on the disks of the first set of pin and disk experiments.

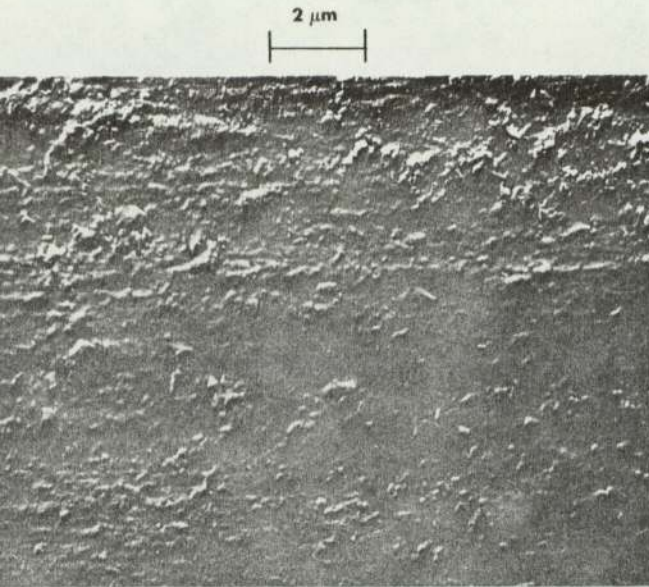
The wear track on the unheated disk (Fig. 9[a]) shows many rounded protrusions, many more than in the micrograph of the unheated plate wear track (Fig. 8[a]). For a disk temperature of only 100 C, however, the protrusions were beginning to disappear (Fig. 8[b]) and by the time 200 C was reached, they had completely disappeared leaving a very smooth topography (see Figs. 9[c] and [d]).

From the above described electron microscopy evidence, it would seem that mild wear (i.e., a smooth topography) was attained at a lower temperature for the fresh specimens than for the specimens which had been exposed to previous heating cycles.

DISCUSSION

This research has shown that the sliding wear of this particular cobalt-base alloy (Stellite 31) is strongly dependent on the previous heating cycles through which the material has been subjected. It suggests that the type of motion; i.e., continuous or reciprocating sliding, has very little effect on the wear rate. It has shown that Stellite 31 has mild wear characteristics at disk temperatures greater than 400 C regardless of type of motion or previous heat treatment.

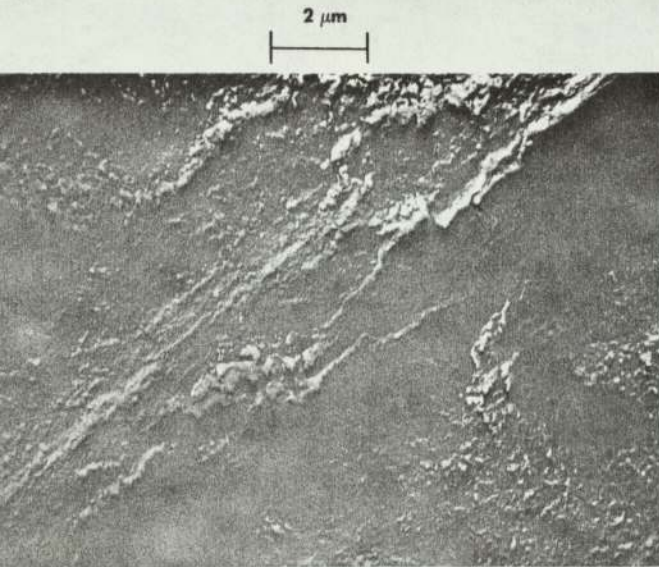
The mild wear is shown to be associated with the production of the spinel oxides of either chromium or cobalt. It would seem that the spinel chromium oxide is mainly responsible for the early onset of mild wear for the set of experiments with fresh specimens, whereas the cobalt spinel oxide is mainly responsible for the late onset of mild wear for the set of experiments with previously-heated specimens.



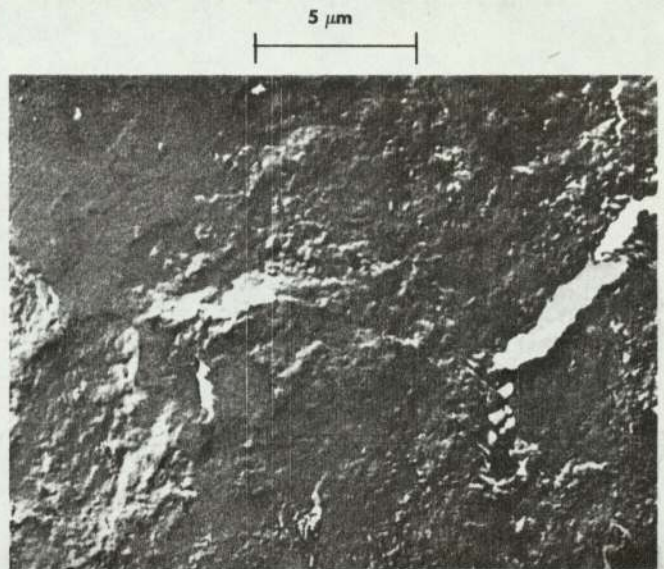
(a) The wear track on the unheated plate



(b) Wear track on the plate at 100 C



(c) Wear track on plate at 300 C



(d) Wear track on plate at 400 C

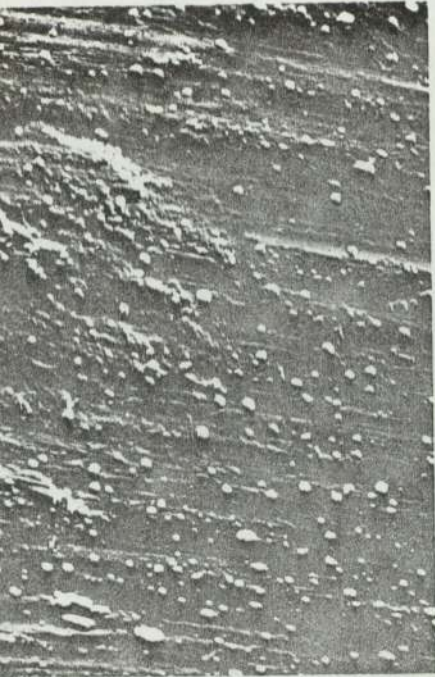
Fig. 8—Transmission electron micrographs of replicas from typical areas of the worn plate of Stellite 31 (button-on-plate reciprocating sliding experiments).

The wear-rate maximum at disk temperatures of about 100 C (for the experiments with previously-heated specimens) coincides with maximum roughness (on a microscopic scale) of the surface. However, the friction and wear maxima in temperatures show maxima at disk temperatures of about 300 C. This is not unexpected, if one assumes that the production of the spinel oxides of cobalt or chro-

mium are as beneficial (as regards friction and wear) as the spinel iron oxides are for steels (11). The debris was shown to be almost entirely fcc cobalt at the points just before mild wear set in. The beneficial effects of the oxide on the friction are not manifested until the interface is one of oxide sliding on oxide.

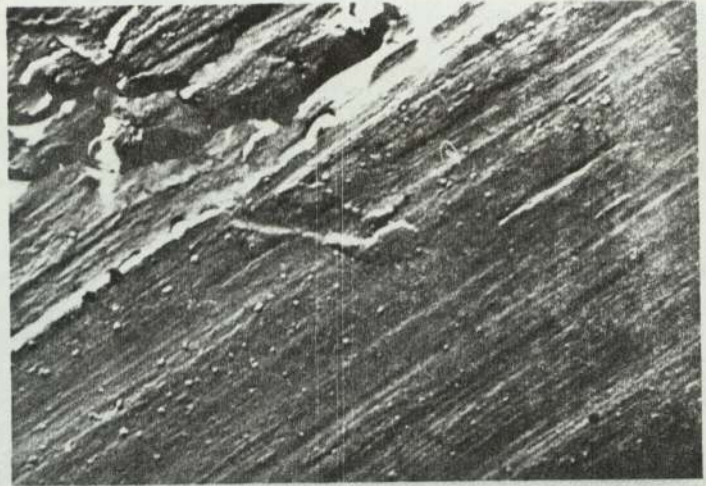
The temperatures of the real areas of contact will be

2 μm



(a) The wear track on unheated disk

2 μm



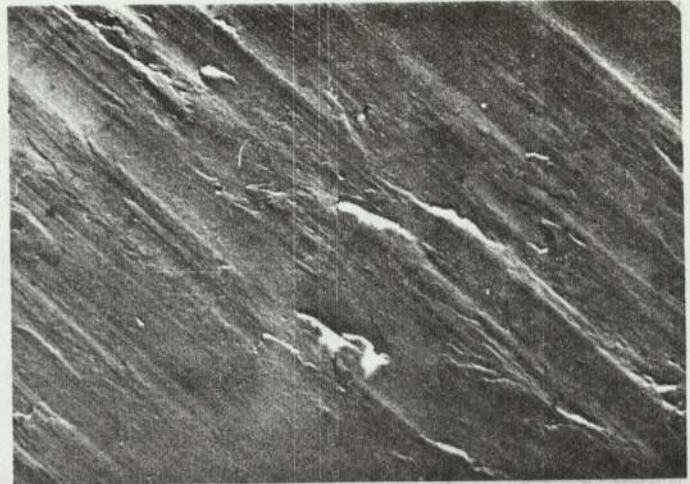
(b) The wear track on the disk at 100 C

2 μm



(c) The wear track at 200 C

5 μm



(d) The wear track at 270 C

the measured ambient or disk temperatures. Since average speed of sliding was the same for all the experiments, it is valid to compare the wear rate, friction pin temperatures as functions of the ambient or disk temperature. Any transition in these parameters at a particular externally-induced temperature will be occur at approximately the same contact temperature; i.e., real areas of contact will be at the same temperature. Consider first the effect of frictional heating on the ambient temperature of the pin. It has been shown that contribution to the ambient disk temperature from frictional heating is about 15 C for these experiments, and that this is included in the disk thermocouple measurements. The pin, however, will have an ambient temperature which depends upon the ease with which the frictional heat and the externally-induced heat can be conducted or radiated away from the interface between the pin and the disk. By extrapolating from the thermocouple measurements at positions A and B of the pin, it can be shown that the ambient temperature of the pin surface was always about 50 C more than the temperature of the disk for the severe wear experiments. In the mild wear experiments, the intervention of an oxide film between the contact of the pin and the disk probably means that a linear extrapolation cannot be made. Hence, it is not possible to estimate the ambient temperature of the pin surface for the high temperature experiments, although there is no reason to assume that the temperature will be very much different from the ambient disk temperature (400 C) and the temperature due to frictional heating (50 C). The friction coefficient is probably little different whether the wear is mild or severe, although there are second order differences (as shown by the maximum in Fig. 6).

Having shown that the bulk pin temperature was about 450 C for the mild wear experiments, it can be estimated that the contact temperature must have been about 200 C more than this, following the estimate used in some similar pin-and-disk experiments carried out with a low-alloy, medium carbon steel (13). This value of 200 C must only be regarded as an order of magnitude estimation. One can now make an estimate back to the ambient temperature of the pin surface for the mild wear experiments, namely, that 250 C should be added to the disk temperature in order to obtain the ambient temperature at the real areas of contact between the pin and the disk. Thus, the maximum in the wear rate curve can be regarded as occurring at a contact temperature of about 650 C. One must also assume that mild wear must occur at some contact temperature between 550 C and 650 C for the experiments with specimens which had previously been heated, and somewhere between 350 and 450 C for the fresh specimens.

It is not possible to deduce the significance of these temperatures by comparing with oxidation data for this cobalt-base alloy, since none exists at the present time. One needs to know why the presumably annealed specimens do not exhibit mild wear and produce the spinel chromium oxide until the temperature of the areas of contact reaches about 650 C, whereas a fresh specimen exhibits

mild wear and produces spinel chromium oxide at about 500 C. Clearly the effect of including chromium in the alloy has considerably changed its properties from those exhibited by pure cobalt. For instance, the alloy can exist in the face-centered cubic form at all temperatures, whereas pure cobalt changes from hexagonal to the face-centered cubic phase at about 450 C. Also the effect of chromium seems much more pronounced for the fresh specimens.

It is possible to conclude that this research has shown that the wear of Stellite 31 conforms very much to the mild and severe wear classifications shown to obtain in the wear of most metals and alloys, and that the formation of the spinel cobalt (or chromium) oxide is a prerequisite for obtaining mild wear. It is somewhat disquieting to note that the annealed specimens do not exhibit mild wear until a contact temperature of about 650 C is obtained, since many of the machine parts in which this alloy is used are called upon to resist wear in this temperature range. These parts will also be subject to annealing through previous heat cycles.

ACKNOWLEDGMENTS

The authors wish to acknowledge the help provided by the Mechanical Behavior Department of Rolls-Royce Aero-Engine Division, for permission to use previously unpublished data about the wear behavior of this cobalt-base alloy when used in the button-on-plate specimen geometry. They also would like to acknowledge the advice and help of M. Howse, also formerly of the Mechanical Behavior Department at Rolls-Royce.

The authors wish to acknowledge the help provided by the BISRA Corporate Laboratories of British Steel, the Science Research Council, and the University of Aston in Birmingham in providing funds and facilities to enable this research to be carried out.

REFERENCES

- (1) Peterson, M., Florek, J., and Lee, R., "Sliding Characteristics of Metals at High Temperatures," *ASLE Transactions*, 3, 101-109, (1960).
- (2) Foley, R. T., Peterson, M., and Zapf, C., "Frictional Characteristics of Cobalt, Nickel, and Iron as Influenced by their Surface Oxide Films," *ASLE Transactions*, 6, 29-38, (1963).
- (3) Buckley, D. H. and Johnson, R. L., "Marked Influence of Crystal Structure on the Friction and Wear Characteristics of Cobalt and Cobalt-base Alloys in Vacuum to 10^{-9} mm of Mercury I—Polycrystalline and Single Crystal Cobalt," NASA Technical Note D-2523 (1964).
- (4) Huppman, W. J. and Clegg, M. A., "The Tribological Behavior of Polycrystalline Cobalt as Related to Crystallographic Texture and Structure," *ASLE Transactions*, 16, 107-114, (1973).
- (5) Jesper, A. C., "Consideration of Factors Affecting the Wear Resistance of Materials Used in Gas Turbine Engines," *Proc. Inst. Mech. Engrs.*, 180, Part 3K, (1965-66).
- (6) Archard, J. F., "The Temperature of Rubbing Surfaces," *Wear*, 2, 438 (1959).
- (7) Quinn, T. F. J., "The Effect of 'Hot-Spot' Temperatures on the Unlubricated Wear of Steel," *ASLE Transactions*, 10, 158 (1967).
- (8) Archard, J. F. and Hirst, W., "The Wear of Metals under Unlubricated Conditions," *Proc. Roy. Soc.*, (London) A236, 397 (1956).

- Richard, J. F., "Single Contacts and Multiple Encounters," *J. Appl. Phys.*, **32**, 1120 (1961).
- Bowden, F. P., and Tabor, D., "The Friction and Lubrication of Solids," Oxford University Press, (1950).
- Johnson, R. L., Godfrey, D., and Bisson, E. E., N.A.C.A. Tech Note 1578 (1948).

- (12) Quinn, T. F. J., "The Application of X-Ray Diffraction Techniques to the Study of Wear," *Advances in X-Ray Analysis*, **10**, 311, Plenum Press, New York (1967).
- (13) Quinn, T. F. J., "An Experimental Study of the Thermal Aspects of Sliding Contacts and Their Relation to the Unlubricated Wear of Steel," *Proc. Inst. Mech. Engrs.*, **183**, PE 3P, 129 (1969).

DISCUSSION

DONALD H. BUCKLEY, ASLE
ASA-Lewis Research Center
Cleveland, Ohio 44135

The name spinel is given to a class of mixed oxides of the formula $R^1O \cdot R_2O_3$. Examples are $MgO \cdot Al_2O_3$ and $MgO \cdot Cr_2O_3$ (Al). Spinel generally crystallize in the cubic system with sharp edges. From the authors' paper, it is difficult to identify the spinels to which they are referring. They are simply called spinel chromium oxide and spinel cobalt oxide in the paper. Yet, there are no less than seven chrome oxides (CrO , CrO_2 , CrO_3 , Cr_2O_3 , Cr_2O_5 , Cr_3O_4 and Cr_3O_8). In addition, there are three oxides of cobalt (CoO , Co_2O_3 , and Co_3O_4). Further, there are cobalt chromate ($CoCrO_4$) and cobalt chromite ($CoCr_2O_4$). Which of these oxides and mixtures thereof are the authors calling spinel chromium oxide and spinel cobalt oxide?

The authors conclude from their experiments that mild wear is associated with the formation of the spinel cobalt (or chromium) oxide. X-ray diffraction is not sensitive to oxides normally present on cobalt alloy surfaces at room and slightly higher temperature exposures. The oxide film is just too thin for detection by X-ray diffraction. This is borne out by the authors' data in Table 1 for temperatures of 35 and 100 C. The authors do not detect oxides but only face centered cubic cobalt. This does not mean, however, that oxides are not present. They are present and could conceivably be of the spinel type to which the authors refer. The critical factor then is not the presence or the absence of oxide but rather the quantity and composition of the oxide in the contact zone.

The authors feel that because an iron oxide spinel helped to contribute to mild wear that cobalt and chrome oxide spinels would do likewise. Marked differences exist even among the simple oxides of iron (FeO , Fe_3O_4 , and Fe_2O_3) relative to wear. A similar behavior might be exhibited by the oxides of cobalt and chromium. It would certainly have been interesting had the authors conducted such a preliminary study. Metal oxide and spinel powder studies could have been conducted. The authors, however, could only assume that the spinels were beneficial.

Do the authors have an explanation for the unexpected behavior of fresh versus the previously heated specimens? One might anticipate that the thickness of the oxide would be greater for the previously heated

specimens and, therefore, mild wear would occur more readily than for the fresh specimen where the oxide layer would presumably be thinner. The authors, however, observe mild wear at a lower temperature with the fresh specimens.

Lastly, this discussant has difficulty with the terms mild and severe wear. What is severe wear to the designer of aerospace gyro-bearings is not the same as that to the steel mill lubrication engineer. To the former, one ten thousand of an inch is critical while to the latter, tenths of inches may not be. In a close tolerance ball bearing, one wear particle may be critical, while with railroad rails thousands of such particles may make little difference.

REFERENCE

- (A1) "High Temperature Technology," Edited by I. E., Campbell, John Wiley and Sons, Inc. (1956).

AUTHOR'S CLOSURE

The authors were pleased to receive Mr. Buckley's comments on their work and the following is an attempt to answer each point in turn:

- (1) Which of the oxides (mentioned in Mr. Buckley's discussion) are the authors calling "spinel chromium oxide" and "spinel cobalt oxide"?

Spinel chromium oxide: Cr_3O_4

Spinel cobalt oxide: Co_3O_4

- (2) Oxides are present at ambient temperatures less than 200 C but are not detected by the X-ray Diffraction technique.

This may be true for the worn surfaces, but is not so for the wear debris analyses by X-ray diffraction. Table 1 relates to wear debris analyses. If any oxide was present on the metallic wear debris, it would have a much better chance of detection than the same thickness of oxide on the metal surface. The authors agree that the critical factor is the quantity and composition of the oxide in the contact zone and they think that X-ray diffraction of the wear debris is sufficiently sensitive to show amounts which could significantly affect the wear mechanisms.

- (3) It would have been interesting had the author conducted a preliminary study to see if the spinel oxides of cobalt and chromium really had a beneficial effect on the wear.

The authors agree and are planning to carry out a study in the near future.

Do the authors have an explanation for the expected behavior of fresh versus the previously-treated specimens?

The authors would prefer not to speculate on this behavior. However, they do *not* agree with Mr. Buckley's contention that, because the oxide film would be greater on the previously-heated specimens, then mild wear would occur more readily on these specimens. Mild wear occurs by the breaking-up of an oxide film when it reaches a critical thickness of about 4×10^{-6} m (7). Hence, the amount of previously formed oxide is only important in the very early stages of wear. It is

possible that the amount and the temperatures of previous heat treatments have an effect on the type and/or amount of oxide formed on the metal substrate in any particular experiment and hence affects the wear rate *indirectly* (rather than in the direct way envisaged by Mr. Buckley).

- (5) The authors agree with Mr. Buckley's final paragraph about the terms "mild" and "severe" wear, when applied to particular situations. However, the terms were intended to indicate different *types* of wear rather than different *magnitudes* of wear. The "mild" and "severe" classifications have proved most useful in general wear studies of metals, and the authors recommend their use when dealing with all wear studies in which one of the specimens is a metal or alloy.